Body-machine interfaces for non-homologous human-machine interactions

Thèse N° 9411

Présentée le 18 avril 2019

à la Faculté des sciences et techniques de l'ingénieur
Laboratoire d'ingénierie neurale translationnelle
Programme doctoral en génie électrique

pour l'obtention du grade de Docteur ès Sciences

par

Jenifer Cléa MIEHLBRADT

Acceptée sur proposition du jury

Prof. D. N. A. Van De Ville, président du jury
Prof. S. Micera, directeur de thèse
Prof. D. Bavelier, rapporteuse
Prof. K. Kuchenbecker, rapporteuse
Dr G. Rognini, rapporteur

2019

ÉCOLE POLYTECHNIQUE
FÉDÉRALE DE LAUSANNE

“Begin at the beginning," the King said gravely, “and go on till you come to the end: then stop."

— Lewis Carroll, *Alice in Wonderland*

“The important thing is not to stop questioning. Curiosity has its own reason for existence. One cannot help but be in awe when he contemplates the mysteries of eternity, of life, of the marvelous structure of reality. It is enough if one tries merely to comprehend a little of this mystery each day."

— Albert Einstein

Abstract

Virtual reality (VR), the interactive experience of being immersed in a simulated environment, has seen a tremendous development in the last years. Numerous applications came into being, ranging from flight simulators through a virtual ascent of Mount Everest, through surgery simulators or scenarios to treat acrophobia. These applications serve different purposes and are not designed for the same populations. To enhance the VR experience, the specifics of the targeted audience must be taken into account during the development of virtual environments.

The intensity of a virtual experience depends on three main factors: the quality and rendering of the virtual environment, the interaction opportunities and aspects inherent to the user such as physical abilities or previous VR experiences. This thesis addresses the latter two aspects.

Part I describes the development of a body-machine interface for the immersive steering of simulated or real drones. Chapter 2 describes a systematic analysis of spontaneous gestural strategies selected by untrained participants asked to interact with a drone. I show the existence of patterns common to the considered population. In chapter 3, I use these patterns to define gestural control strategies to pilot a drone. In particular, I demonstrate that using a set of torso movements leads to better steering performances and faster learning than with a joystick commonly used for this kind of task.

In Part II, I focused on multisensory integration, which is necessary to interact with such a system, and the development thereof along childhood. In chapter 4, I evaluated the steering abilities of 6-10 year-old children on the flight simulator developed earlier. These experiments revealed that the selection of the appropriate head-trunk coordination strategy is immature in children until the age of 8, even if these strategies are already part of the postural repertoire. Eventually, in chapter 5, a virtual archery game highlighted the development of visuomotor integration during childhood.

These studies emphasized the benefits of user-driven interaction interfaces over pre-existing devices and brought up age-related interaction differences which should be considered when

designing virtual environments.
Keywords: *Virtual reality, human-machine interaction, body-machine interface, teleoperation, motor control, motor coordination, motor development, multisensory integration, children*

Résumé

La réalité virtuelle (VR), c'est-à-dire l'expérience interactive d'être immergé dans un environnement simulé par ordinateur, a connu un développement fulgurant au cours des dernières années. De nombreuses applications ont ainsi vu le jour allant des simulateurs de vol à une escalade virtuelle de l'Everest, en passant par des systèmes d'entraînement à la chirurgie ou des scénarios pour traiter le vertige. Ces applications ont des buts différents et ne s'adressent pas aux mêmes publics. Pour que l'expérience de l'utilisateur soit optimale, il est donc indispensable de prendre en compte les spécificités de chaque population cible lors du développement d'un environnement virtuel.

L'intensité de l'expérience virtuelle dépend de trois facteurs principaux : la qualité et la présentation de l'environnement, les possibilités d'interactions et des qualités intrinsèques à l'utilisateur, telles que ses capacités physiques ou de précédentes interactions avec la VR. Dans cette thèse, je traite de ces deux derniers aspects.

La première partie présente le développement d'une interface corps-machine permettant à un utilisateur de piloter de manière immersive un drone virtuel ou bien réel. Le chapitre 2 décrit une analyse systématique des stratégies gestuelles choisies spontanément par des participants sans expérience préalable pour interagir avec un drone. Je montre que des motifs communs apparaissent dans la population étudiée. Dans le chapitre 3, ces motifs sont utilisés pour définir des stratégies de contrôle gestuelles pour piloter un drone. Je démontre en particulier que l'utilisation de mouvements du torse permet un meilleur contrôle et un apprentissage plus rapide qu'avec un joystick communément utilisé pour ce type de tâche.

Dans deuxième partie, je me suis intéressée à l'intégration multisensorielle nécessaire pour interagir avec ce type de système et le développement de celle-ci au cours de l'enfance. Dans le chapitre 4, j'ai évalué la capacité d'enfants âgés de 6 à 10 ans à piloter le simulateur de vol développé ci-dessus. Ces expériences ont montré que la sélection de la stratégie de coordination tête-tronc optimale n'était pas mature avant l'âge de 8 ans, bien que cette stratégie fasse déjà partie du répertoire postural. Enfin, dans le chapitre 5,un jeu de tir à l'arc virtuel à permis de mettre en lumière le développement de l'intégration visuo-motrice au cours de l'enfance.

Ces études soulignent les bénéfices d'interfaces d'interactions centrées sur l'utilisateur en comparaison avec des dispositifs pré-existants et mettent en avant des différences d'interaction liées à l'âge, qui doivent être prises en considération lors du développement d'environnements virtuels.

Mots-clés : *Réalité virtuelle, interface homme-machine, interface corps-machine, téléopération, control moteur, coordination motrice, développement moteur, intégration multisensorielle, enfants*

Zusammenfassung

Virtuelle Realität (VR), das interaktive Erlebnis, in einer simulierten Umgebung eingetaucht zu sein, hat sich in den letzten Jahren enorm entwickelt. Zahlreiche Anwendungen kamen zu Stande, von Flugsimulatoren, über Trainingssysteme für Chirurgen oder zur Behandlung von Höhenangst, bis zur virtuellen Besteigung des Mount Everest. Diese Anwendungen dienen unterschiedlichen Zwecken und richten sich an verschiedene Zielgruppen. Um die Benutzererfahrung zu steigern, sollten die Eigenschaften jeder Zielgruppe bei der Entwicklung einer virtuellen Umgebung berücksichtigt werden.

Die Intensität einer virtuellen Erfahrung hängt von drei Hauptfaktoren ab: der Qualität und der Wiedergabe der virtuellen Umgebung, den Interaktionsmöglichkeiten sowie den Aspekten, die dem Benutzer inhärent sind, wie z. B. körperliche Fähigkeiten oder frühere VR-Erfahrungen. Die vorliegende Arbeit beschäftigt sich mit den letzten beiden Aspekten.

Teil I beschreibt die Entwicklung einer Körper-Maschine-Schnittstelle zur immersiven Steuerung simulierter oder echter Drohnen. Kapitel 2 präsentiert eine systematische Analyse von spontaner Bewegungsstrategien, die von Teilnehmern ohne vorheriger Erfahrung ausgewählt wurden, und die zur Interaktion mit einer Drohne aufgefordert wurden. Ich zeige die Existenz von Mustern, die der untersuchten Bevölkerung gemeinsam sind. In Kapitel 3 verwende ich diese Muster, um gestische Steuerungsstrategien zum Lenken einer Drohne zu definieren. Ich zeige insbesondere, dass die Verwendung einer Reihe von Rumpfbewegungen zu besseren Lenkleistungen und schnellerem Lernen führt als mit einem Joystick, der üblicherweise für diese Art von Aufgaben verwendet wird.

In Teil II habe ich mich auf die multisensorische Integration konzentriert, die notwendig ist, um mit solch einem System zu interagieren, und auf derer Entwicklung während der Kindheit. In Kapitel 4 habe ich die Lenkfähigkeiten von 6- bis 10-jährigen Kindern auf dem Flugsimulator untersucht, der zuvor entwickelt wurde. Diese Experimente zeigten, dass die Auswahl der geeigneten Kopf-Rumpf-Koordinationsstrategie bei Kindern bis zum Alter von 8 Jahren noch nicht ausgereift ist, selbst wenn diese Strategien bereits Teil des Haltungsrepertoires sind. In Kapitel 5 zeigte ein virtuelles Bogenschießspiel schließlich die Entwicklung der visuomotori-

schen Integration in der Kindheit auf.

Schlüsselwörter: Virtuelle Realität, Mensch-Maschine-Schnittstelle, Körper-Maschine-Schnittstelle, Fernsteuerung, Bewegungskontrolle, Bewegungskoordination, motorische Entwicklung, sensorische Integration, Kinder

Acknowledgments

First, I wish to express my infinite gratitude to Silvestro Micera for giving me the opportunity to carry out my PhD in his laboratory. Thank you for your trust, for giving me the freedom to explore and pursue my own ideas and above all, for being such a humane advisor.
I am extremely thankful to Martina for accompanying me during the first years, being always available for my questions on statistics and most importantly for cheering me up during all the scientific downs I encountered.

I would like to acknowledge the work of Prof. Dario Floreano, Alex and Stefano from the LIS for all the drone-related developments and experiments, and Prof. Monica Gori, Luigi, Davide, Stefania and Elisa from Genoa for the organization and the insightful discussions about the studies on children.

A special thanks to Carine for designing this amazing (and portable!) FlyJacket. The demos we got to do together make some of the best memories I have of these four years.

A great thanks to all the past and present TNE members for being there all along this journey.

I would also like to thank the members of my jury, Prof. Dimitri van de Ville, Prof. Daphné Bavelier, Prof. Katherine Kuchenbecker and Dr. Giulio Rognini who accepted to review this work, and provided highly valuable comments.

I am eternally thankful to my parents and my grand-parents, who not only passed down their useful engineering genes, but also taught me to always be curious about the world surrounding me. Finally, I would like to express my gratefulness to Pascal, who unfailingly supported and encouraged me throughout this adventure.

Geneva, March 31, 2019 J. M.

Contents

1 Introduction: Fundamentals of virtual reality

Virtual reality (VR) describes an interactive experience in which a user is immersed into computer-generated environment, designed to be accepted as real, through the stimulation of one or several sensory modalities. The virtual environment (VE) can be a realistic representation of an existing scene or represent a completely fictitious world. VR is a powerful and versatile tool to elicit realistic perceptions of a plethora of scenarios. Well-designed environments allow for very intuitive and user-friendly interaction, with remarkably short adaptation times. Yet, the sensory integration necessary for a lifelike perception of such simulated environments relies on elaborate and well-coordinated neural processes which develop along childhood and into early adulthood.

User experience

The sensations a user may experience when immersed in a virtual environment can be described at different levels. *Immersion* is an objective measure of the extent to which a system presents a scenario perceived as realistic, and depends on the fidelity and diversity of stimulated modalities [1, 2, 3, 4]. *Presence* is defined as a user's feeling of 'being there' in a simulated environment and is therefore a subjective quantification [1, 3, 5, 4, 6]. The intensity of the experience is influenced by personal factors such as spatial orientation or cognitive involvement [7], and by technological aspects including the level of user-tracking, the use of stereoscopic visuals, and wider fields of view. On the contrary, improving the quality of visual and auditory content had only a minor influence [4]. Finally, *the sense of agency* refers to the feeling of controlling one's actions and by extension events in the external or virtual world [8, 9, 10]. Agency has been proposed to arise when the sensory consequences of one's actions resemble a prediction thereof [11, 12], and therefore requires some degree of volition [9]. Additionally, the congruent stimulation of different sensory modalities has also been shown to enhance agency [13]. On the contrary, discrepancies such as time delays, response inconsistency or movement

inaccuracy between an action and its associated feedback interfere with this feeling [14, 15], as do asynchronous cross-modal stimulations [13]. Interestingly, displaying body-specific visuals did not improve the experienced agency when compared to abstract shapes [15].

The user experience is shaped by three major factors: the rendering of the VE, which includes the quality and complexity of the display and the realism of the simulated physics; the user interface, and finally the users themselves, as intrinsic factors such as previous exposition, physical and cognitive abilities or emotional state affect the perception of the simulated scenario [16, 17, 18]. The interaction of these aspects is graphically represented in Figure 1.1.

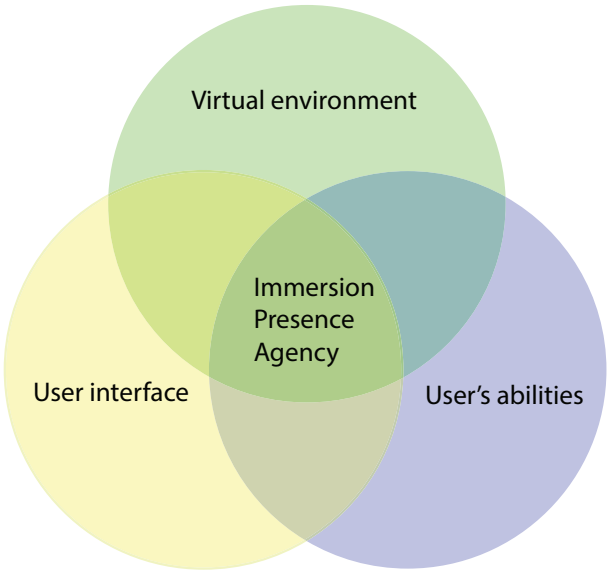

Figure 1.1 – Elements of a Virtual Experience. The propensity to experience a simulated environment as realistic relies on multiple factors: the rendering of the virtual world, the straightforwardness of the interaction interface, and the user's abilities. *(Adapted from [18])*

Sensory modalities to render virtual environments

The immersion of a user in a virtual world requires the creation and display of sensory representations of the environment, usually through visual, auditory and haptic stimuli.

Vision

Most VR systems use some visual representations to immerse the user in the simulated environment, as the sole stimulation of this sense appears to be sufficient to elicit a respectable degree of presence [19]. The simplest manner to display a VE is through a common computer monitor or television screen. Yet, however large this screen may be, the provided immersion is limited by the 2-dimensional projection of the VE and the remaining perception of the real

world. The low level of immersion provided by this approach leaves it on the edge of VR.

Cave automatic virtual environments (CAVEs) provide a higher level of immersion. A CAVE is a cubic room, in which the walls and often also the ceiling and floor serve as projection surface for the virtual environment [20]. Users will often wear 3-dimensional (3D) glasses, to get a stereoscopic perception of the displayed object. They can freely move within the room, while their real-time position is monitored to continuously adapt the projected images. Multiple users may be present in the CAVE, but in this case the perspective adapts only to one person. As the users still see their own body, the visual interface cannot alter its representation.

The highest level of visual immersion is provided by Head-Mounted Devices (HMDs), which completely mask the real world. A HMD contains two small displays, placed in front of each eye and each displaying a slightly shifted image to elicit stereoscopic imagery. Current HMDs embed an inertial sensor, which tracks the rotations of the head and adjusts the rendering of the VE accordingly, allowing the user to *look around*. Technical aspects including the resolution, the field of view and the latency strongly affect the perception of the simulated environment, and if sufficient standards are not met, may cause users to experience VR sickness, which induces symptoms similar to motion sickness [21]. Additionally, the short distance between the eyes and the displays recurrently causes eye strain and extended use may temporarily affect visual acuity [22].

Sound

Sound can be used to enhance the immersion in a virtual environment by providing additional and complementary information to vision, thanks to different spatio-temporal characteristics, thus deepening the immersion. In VR, audio elements have been used in combination with visual displays to attract the users' attention to an invisible object or to direct their awareness toward such an object, to notify events, to set an ambiance (see [18] for a review), or as cues in a navigation task [23].

Haptics

Haptic renderings provide tactile feedback the form of pressure, force or vibration. Haptic feedback increases the feeling of presence [24], and are essential when the virtual scenario involves contact with objects or surfaces, as it improves the realism of these interactions [25]. Interestingly, the addition of haptic information is described as beneficial, even if it is not realistic [26]. Similarly, haptic information proved to be a helpful alternative or addition when the users were not able to accurately integrate the information provided through other modalities, as may be the case for neurological patients [27, 28].

Haptic devices can take the form of handheld devices, particularly when the VE involves virtual tools [29, 30, 31], gloves [32, 33] (see also [34] for an overview of commercially available systems), or garments covering the upper or the entire body [24, 28].

1.1 Interaction interfaces

The richness of VR user experience does not only rely on the quality of the simulated environment, but also largely on the user-friendliness of the system's interaction possibilities. An ideal interface should be completely transparent to the users who should not perceive the existence of the intermediary medium [35, 36], and its use should be intuitive, meaning that only limited training is necessary for proficiency and its use does not require an extensive cognitive load [37]. In this respect, the requirements for VR user interfaces are comparable to the criteria for efficient teleoperation. Examples of user interfaces will thus be considered interchangeably from these domains.

In some cases, the interfaces are bidirectional as they provide sensory feedback while acquiring data to support the user's interaction with the VE. HMDs with embedded IMUs are an example of bidirectional interface.

Handheld devices

Joysticks or game pads are typically used for navigation simulators. The popularity of these devices derives from their conceptual simplicity and their long-term prevalence in the video gaming community. The major drawback of these systems lies in the relationship between the small hand or finger movements executed by the users and the corresponding actions of the controlled object. Encoding the underlying transformation between these spaces can thus become cognitively demanding, particularly when both categories of actions differ from each other to a large extent.

Recent controllers, often developed along with HMDs, combine functionalities of the old-fashioned devices such as buttons and analog sticks, or trackpads with spatial monitoring of the hands' position (see [38] for an overview). These controllers thus allow a (quasi-)transparent control of continuous motions, while discrete actions are executed through interaction with the devices' predefined features, which possibly once more requires a certain level of cognitive adaptation. Moreover,these systems restrain the interactions to gross hand movements, which limits the number and the diversity of the available command input.

Body tracking

Body tracking refers to the real-time acquisition of parameters defining the orientation and/or the position of body segments in space. Hardware classes include motion capture systems, vision-based systems and inertial sensors. Motion capture systems consisting of infrared cameras which track reflective markers placed on the monitored subject's body are highly reliable and able to precisely discern small movements. Yet, as these systems are often expensive and require a large, dedicated space, their use is often limited to research institutes, and restrained to a defined location. Instead, vision-based systems are often available at affordable range and have require less spacious areas. however, simple devices may only detect planar movements and are sensitive to occlusions. More importantly, their performance is affected by poor lighting conditions, thus once more constraining the compatible locations. An alternative portable solution is provided by inertial sensors (inertial measurement units, IMUs), which combine information from accelerometers, gyroscopes and magnetometers to provide robust estimates of angles or positions. While lightweight and usable in a large variety of combinations, IMUs have the flaw of being sensitive to external magnetic fields.

In the particular case of hand tracking, gloves can additionally be used, possibly also as bidirectional interfaces. By providing haptic information while tracking the hands' position, interactions with virtual objects such as grasping or holding reach a new level of realism [39, 33].

The direct translation of body movements into controlling commands for virtual objects or for teleoperation has been encapsulated under the term Body-Machine Interface (BoMI) [40]. BoMIs have the advantage of being extremely versatile and adaptable to a plethora of interactions and diverse populations.

Non-gestural interfaces

Non-gestural interfaces are of particular interest for users with physical limitations or disabilities, which would prevent them from using hand-held devices or to execute precise and differentiable control gestures, and include among others speech control and Brain-Machine or Brain-Computer Interfaces (BMI, BCI).

Interacting with a virtual system through speech appears as a straightforward approach, as this is our main way of communicating. The applications related to VR systems remain, however, rather anecdotal [41, 42], but the example provided by other electronic systems reveals the readiness of the necessary technology [43, 44]. Besides technical aspects of speech recognition, the main limitation of voice control lies in its ability to transmit only discrete commands. This restrains the modularity of the control and limits the levels of presence the users can

experience. Additionally, interactions with a third party, such as a therapist providing guidance during a treatment, is likely to interfere with the vocal commands . Using speech to interact with a VE may thus be worthwhile for precise, predefined actions, where gestural control would require a larger effort, and may need to be complemented by other interaction modalities.

BCIs directly acquire and process cortical activity, thus bypassing the motor system, and are therefore targeted at end-users with limited physical abilities. These interfaces use non-invasive electrodes to record different signals from the brain activity, which are translated in real-time into commands. BCI control has been used in VR for navigation [45], object control [46] or as in neurofeedback implementations [47]. BCIs have been also widely been developed for teleoperation, for instance to control telepresence systems [48], wheelchairs [49] or drones [50].

To be successfully operated, BCIs require the users to "encode" the commands in the extracted signals. The controlled modulation of such signals necessitates practice, but even then, may be challenging for some individuals and therefore become a cognitively demanding task[51]. Additionally, the low signal-to noise ratio of the acquired brain activity constrains the environments and situations in which such interfaces can be used.

1.2 Applications of virtual reality

Thanks to its wide potential and to the development of affordable and lightweight hardware, VR has been applied in very diverse fields and with different populations. The examples provided below aim at highlighting the large diversity of these applications, which advocates for the development of versatile and adaptable interaction interfaces.

Leisure and entertainment

The most prominent application field for VR is the leisure and gaming industry, where immersive systems have been used as supplementary features for computer games or as a risk-free way to provide one-of-a-kind experiences such as swimming with whales [52], exploring the top of the Everest [53] or riding a spaceship [54].

Training simulators

Besides entertainment, training simulators represent a prominent field of application for VR, as it provides learners a safe framework to practice and develop their skills without the real-life repercussions following errors or failure. These virtual training stations can also generate emergency-like, complex or situations, which could not be repeatedly practiced otherwise.

Moreover, the simulators can collect quantitative data on the task execution and provide feedback to the assessors. Fields of application include flight and pilot training, space training [55], and military training [56, 57].

Healthcare and medicine

Similarly to flight simulators, medical VEs allow the repeated and risk-free practice of diverse scenarios, and permit the generation of complex or rare situations with otherwise limited opportunities for practice. Existing simulators allowing medical students to practice among others diagnostic manipulations [29, 30], life-saving actions [58] or surgeries [59, 31, 26, 60]. Other systems have been designed for medical education, helping prospective physicians to spatially visualize organs or systems [61, 62].

Patient-oriented approaches mostly focus on rehabilitation after injuries to the nervous system and address motor function[63, 64, 65], balance [66, 67], or spatial disorientation [68].

Due to the playful nature of VR-based treatments, numerous systems have been developed specifically for pediatric conditions, including cerebral palsy[69, 70, 71], autism [72], attention disorders (see [73] for a review) or for pain alleviation during medical procedures [74, 75].

Sociology and psychology

In psychology, VR scenarios have been successfully implemented for the treatment and assessment of different disorders, including acrophobia [76], anxiety disorders [77], as well as schizophrenia, eating disorders, or diverse phobias (see [78, 79] for reviews). One major advantage of VR-based therapies is that patients can individually adapt the strength of the fearful stimulus, therefore actively influencing the evolution of their treatment. It is however worth noting that VR-based treatments do not outperform other therapeutic approaches [78, 79].

1.3 Ethical considerations

The increasing availability of highly realistic simulations has raised justified questions about the ethical implications of using such technology, in particular with vulnerable populations such as children or psychological patients, be it for research or with a therapeutic aim [80, 81]. State-of-the-art hardware allows the creation and rendering of largely immersive environments, causing the frontier between real and virtual worlds to thin down [4]. As mentioned above, VR has been successfully implemented for brief treatments of diverse phobias or traumatic disorders through gradual expositions to the fearful stimuli. However, while healthy

individuals are likely to recognize simulated elements, psychological patients with an altered awareness or sense of reality may react with unexpectedly strong negative behavioral and psychophysical responses [82].

Likewise, children and teenagers, whose perception of the reality is still under development, also present higher risks to hybridize virtual experiences with real events [83, 84]. In a recent study, Segovia and Bailenson demonstrated that immersive VR induced false memories in young children after a single exposition to an unknown scenario [85]. More generally, children have been shown to perceive virtual environments as more realistic than adults [74]. The stronger feeling of presence may be due to the absence of prefrontal cortical activity in children, which appeared to regulate this sensation in adults [86, 87].

1.4 Multisensory integration

Adults integrate multisensory information in a statistically optimal way

The gestural interaction with a virtual system requires the joint processing of different sensory modalities including visual, somatosensory and vestibular inputs, which influence and are influenced by motor output. The coordinated integration of different sensory inputs is described as multisensory integration (MSI) [88]. The fusion of congruent signals has been shown to yield estimates about surrounding elements with precision levels exceeding what could be achieved by a single modality, in terms of speed and accuracy of target detection and localization, or reduce detection thresholds [89, 88].

The successful handling of multiple sensory stimuli requires the brain to solve two computational problems. First the integration of informative signals provided by different modalities, to yield a common estimate. The main challenge of this step is caused by the fact that each sense provides signals corrupted by an unknown level of noise and may be biased [90] (see Figure 1.2A). In adults, the accepted model of multisensory integration relies on Bayesian causal inference, a general principle which minimizes the variance of the final estimate by weighting the incoming stimuli using maximum-likelihood estimations [91, 90] (see Figure 1.2B).

Additionally, the brain must distinguish between sensory inputs which originate from a single source and must therefore be fused to improve the precision of the estimate, and signals arising from separate source which are to be processed separately. The underlying decision-making process is an extension of the Bayesian approach described above, in which both hypotheses are weighed by the probability of the respective causal structure [90] (see Figure 1.2C).

The integration of apparently congruent stimuli may also lead to erroneous interpretations. As

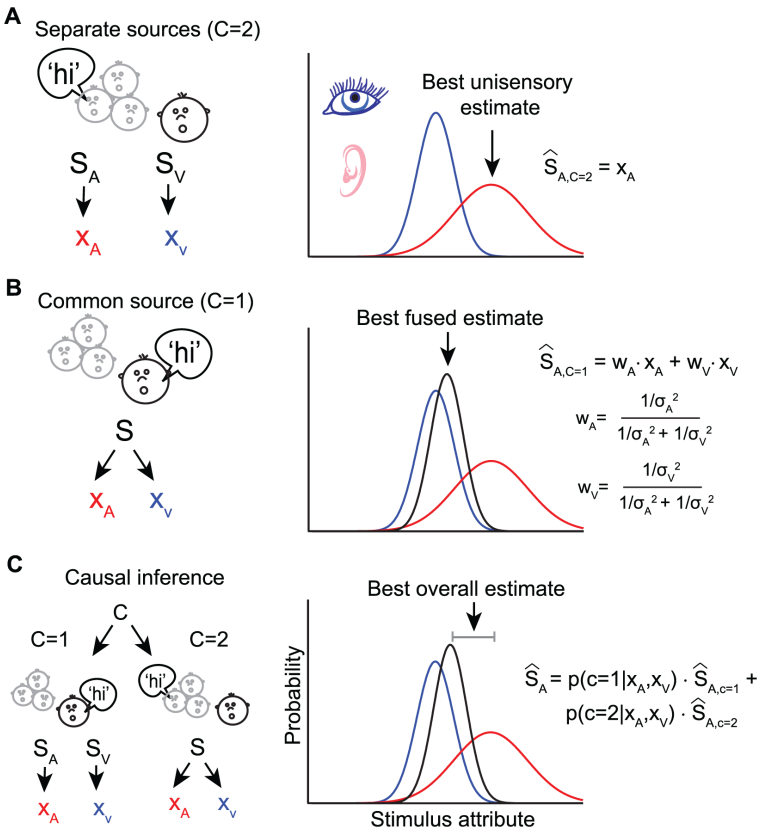

Figure 1.2 – Bayesian models of multisensory integration. **A** When the sources are separate, the optimal value matches the most probable unisensory location. **B** In case of a common souce, the visual and auditory stimuli are integrated, each weighted by its relative reliability. **C** The Bayesian approach can be extended to conflicting situations (e.g. one versus two sources), by weighing the two different hypotheses by their respective inferred probability [90]

an example, the rubber hand illusion [92] is a scenario in which participants observe a rubber hand being stroked with a paintbrush, while their own hand receives the same stimulus and is hidden below the dummy hand. Due to congruent multisensory stimuli (vision, touch and proprioception), participants begin to perceive the rubber hand as their own.

Visuo-vestibulo-proprioceptive integration for postural control

The integration of multiple sensory stimuli is not only beneficial to optimize the perception of the surrounding environment, but also to obtain reliable estimates about the body's current state. Such estimate is necessary to drive appropriate postural reflexes including head-eye coordination, the alignment of different body segments, or the generation of compensatory muscle activities during steady standing or sitting, or during voluntary locomotion [93]. First, a representation of the current body position and orientation is obtained by the integration of visual, proprioceptive and vestibular information, which occurs at the level of the cerebellum

and the cerebral cortex [94, 95] (see Figure 1.3). This allows the construction of internal bodily models representing (body schema) in the temporoparietal cortex including the vestibular cortex and posteroparietal cortex. This information is then transmitted to the supplementary motor area and the premotor area, where it is used as substrate for adequate motor behavior [95, 93].

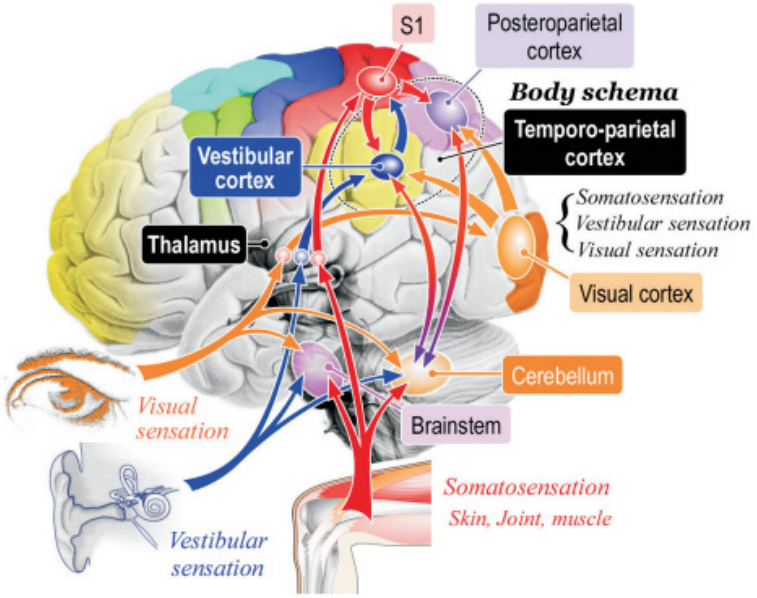

Figure 1.3 – Neural pathways of visuo-vestibulo-proprioceptive integration for postural control [95]

Development of multisensory integration

While early occurrences of MSI have been reported as early as one week after birth in situations, suggesting innate abilities for hand-eye coordination, or a sensitivity to audio-visual, visuo-tactile, or audio-tactile properties (see [89] for a review), there is evidence that the ability to meaningfully integrate the information from multiple sensory modalities matures along childhood [96, 97, 89]. When asked to discriminate objects based on size of orientation using visual and tactile cues, children younger than 8 do not show make an optimal use of the provided multimodal sensory information [98]; instead, one modality appears to dominate for such a decision task. Interestingly, while vision was used more reliably to discriminate orientation, tactile information was predominantly used in trials requiring a decision based on size. This suggests that during the maturation of these integration processes, there is not one absolutely superior modality, but rather that the most reliable source of information depends on the constraints of the task. Similarly, a study evaluating the use of multisensory cues during navigation found that only adults were able to efficiently integrate self-motion with the aid provided by visual aids, while children aged 8 and younger displayed only little improvement

when provided with both sensory signals [99]. However, a recent study showed that, when provided with a supplementary feedback on the reliability of the individual cues which additionally helped to resolve inter-cue biases, young children were able to advantageously integrate bimodal information in a virtual audio-visual hide-and-seek task [100]. Thus, the acquisition of efficient multimodal sensory processing may be delayed by the maturation of the precision and hence the reliability of the individual senses.

The late development of efficient MSI has also been observed in the framework of postural control. The contribution of the different sensory modalities on maintaining a steady posture can be assessed by measuring the displacement of the center of pressure of standing participants asked to keep their eyes open, closed or under optocinetic stimulation while standing on a fixed or a sway-referenced platform, the latter canceling the influx of proprioceptive information originating from the ankle joints. Unsurprisingly, a general trend shows an improvement of postural stability with age until early adulthood [101]. Replacing a sway-referenced platform by a fixed support allowed adults to reduce their postural sway by 90% when watching a sinusoidal visual stimulus, whereas children aged 7-12 only improved their stability by 50%, thus revealing the stronger reliance on vision over somatosensory inputs in this age range [102].

Interestingly, the postural stability was found to vary as a function of task demands [103]: higher postural sway was observed when sitting children were asked to manually aim at a distant object than when they were tracing a complex shape, a task requiring less postural adjustments. Other authors similarly found that young children display mature coordination and stability patterns during low-complexity tasks, but that adult-like behavior develops until the second decade of life for actions deemed as more difficult (see [104] for a review).

Outline of the thesis

This thesis focuses on two fundamental elements of affecting the interaction with a virtual system: the user interface and the user's abilities. **Part I** addresses the necessity for transparent interaction interfaces and describes a methodology for the development of such an interface for the particular of drone steering. **Chapter 2** presents a neurophysiological analysis of the spontaneous gestural behaviors observed in naive subjects asked to interact with a simulated drone. **Chapter 3** builds on this analysis and presents the development and evaluation of two gestural control strategies for the steering of simulated and real drones, and shows that an efficient gestural strategy is easier mastered by untrained participants than the use of a state-of-the-art remote controller. **Part II** focuses on the development of the postural and multisensory skills necessary to successfully use an interface as described in **Part I**. **Chapter 4** shows the age-related maturation of head-torso coordination in the context of VR interactions. **Chapter**

5 presents a simpler experiment, which demonstrates the development of the integration of vision with head and trunk movements and of spatial orientation. Finally, **Chapter 6** summarizes the results of this work and provides an outlook of their implications on various application domains.

Part I

Gestural strategies for non-homologous human-machine interactions

Abstract

The accurate teleoperation of robotic devices requires simple, yet intuitive and reliable control interfaces. However, current human-machine interfaces (HMIs) often fail to fulfill these characteristics, leading to systems requiring an intensive practice to reach a sufficient operation expertise. Here, we present a systematic methodology to identify the spontaneous gesture-based interaction strategies of naive individuals with a distant device, and to exploit this information to develop a data-driven body-to-machine interface (BoMI) to efficiently control this device. We applied this approach to the specific case of drone steering and derived a simple control method relying on upper-body motion. The identified BoMI allowed participants with no prior experience to rapidly master the control of both simulated and real drones, outperforming joystick users, and comparing with the control ability reached by participants using the bird-like flight simulator Birdly®.

The contents of Chapters 2 and 3 were published under:

Data-driven Body-Machine Interface for the accurate control of drones
Miehlbradt J., Cherpillod A., Mintchev S., Coscia M., Artoni F., Floreano D.*, Micera S.*
(PNAS, 2018)

Contributions as first author: design of the experiments, data collection, data processing and analysis, preparation of the figures and redaction of the manuscript. The flight simulators, the drone and its control were designed by A. Cherpillod.

Introduction

Teleoperation, a subfield of human-machine interaction (HMI), describes the control at a distance of an actuated device [105]. Typical applications include deployments in environments where it is not desirable or possible to send a human operator, such as nuclear plants [106, 107], scenes of natural hazards or more generally in search and rescue missions [108, 109, 110]. The use of teleoperated systems can augment human dexterity and precision, which are fundamental abilities in those and other fields of application, such as minimally invasive surgery [60] or microfabrication [111]. Patients suffering from neurological disorders may as well benefit from teleoperated systems to substitute for lost body functions by controlling wheelchairs [49, 112] , telepresence systems [113, 48] or robotic manipulators [114]. Successful teleoperation requires robust and reliable control interfaces. A well-defined interaction should be transparent [35, 36], rely on intuitive command inputs to ensure rapid proficiency and minimize the task-associated workload [37], and provide appropriate feedback (visual, auditory, haptic) to strengthen the awareness of the operator [115]. A number of existing interfaces already allow interactions with robotic devices. However, simple third-party devices such as a joystick show limited performance even with systems with few degrees of freedom (DOFs). The development of intuitive commands becomes yet more challenging in "non-homologous" interactions, that is when the operator's command behaviors significantly differ from the machine's realizable behavior, or when their physical abilities are restricted.

A possible approach to address this issue comes from brain-computer interfaces (BCIs), which bypass behavioral output by directly retrieving the desired information from the cerebral activity patterns, often relying on mental imagery. Successful examples include the control of humanoids [116], unmanned aerial vehicles (UAVs) [50, 117, 118], wheelchairs and telepresence systems for motion-impaired individuals [49, 112, 113, 48]. BCIs do nonetheless come with certain limitations, which may prevent their widespread utilization. Firstly, the non-invasive signal acquisition is associated with a low signal-to-noise ratio and thus a high sensitivity to perturbations. The use of these systems is therefore limited to relatively controlled environments and may not be suited to everyday activities. Another limitation of this approach comes from the execution of motor imagery tasks, which strongly constrains the user's focus on the completion of the control task. The system is therefore prone to errors in case of unpredicted and undesired stimuli and a long-term operation is likely to be cognitively demanding.

Recent and promising developments suggest that Body-to-Machine Interfaces (BoMIs) are a valuable alternative to BCIs for able-bodied or partially impaired persons. Instead of neural activity patterns, these systems retrieve information from body motion or from the underlying muscular activities [40]. The broad spectrum of applications ranges from the control of

assistive devices by neurological patients [119, 120, 121] to the control of UAVs [122, 123, 39, 124]. BoMIs present one unambiguous advantage over BCIs: they exploit the fine control the operators can have over their body, while operating a BCI requires to actively modulate the activity of designed cerebral areas, a task for which humans have no pre-existing ability [120]. BoMIs have therefore the potential to be more robust to external sensory perturbations and more straightforward to master.

Among the various types of mobile robots, drones have the potential to extend human perception in unprecedented ways for several civilian applications and disaster mitigation scenarios [125], but proficient teleoperation of drones with a standard joystick may require extensive training sessions. Therefore, the identification of more intuitive BoMIs between humans and drones could reduce training time, improve flight efficiency, and allow the operators to shift their focus from the control task to the evaluation of the information provided by the drone.

Over the last decade, gesture-based interfaces for the control of flying robots have gained increasing interest, including approaches using commands from the head [126, 127], the hand [122, 128, 129], the upper body [109, 123, 130, 131, 132, 133, 134] , or even the entire body [135]. Systems using head gestures involve a first-person view (FPV) visual feedback presented to the user through a head-mounted display (HMD) and are thus highly intuitive, yet this approach prevents the user from visually exploring the environment without affecting the flight trajectory. Relying on other body parts for the control decouples the steering from the visual exploration. However, aside from one exception [131] these implementations only offer a visual feedback in third-person view with the drone flying in the user's field of view, thus restricting the level of immersion offered to the operator. Another important limitation comes from the implementation of discrete commands instead of a continuous mapping of the user's movements to the drone's actions. This characteristic also reduces the immersion experienced by the user, as modulations of the control input have no effect on the trajectory of the drone [136] . Only one approach interfaced Microsoft's Kinect with a quadcopter, with a direct translation of the user's gestures into velocity commands for the drone [137]. Lastly, the majority of the HMIs for the control of drones make use of pre-selected movements, that the participants have to reproduce. The definition of the control strategy may thus be biased by the designers' preferences and fail to encounter patterns that are intuitive to potential operators. Recent works addressed this issue through Wizard-of-Oz sessions [130, 132, 134] or interviews [138] to develop more intuitive interfaces, yet still with a focus on discrete commands.

Outline

Chapter 2 presents a structured methodology to identify intuitive communication strategies for non-homologous continuous human-machine interactions, and we detail this approach in

the case of immersive gesture-based drone control. Briefly, we first recorded the upper-body kinematics and muscle activities during the generation of movements that would imitate the behavior of a flying drone and identified two main interaction strategies used by the participants. In chapter 3 we assessed the capacity of potential users to actively steer the path of the virtual drone employing these two strategies. Eventually, we evaluated the transferability of the skills acquired during simulation training to the control of a real drone. (See Figure 1.4 for an overview)

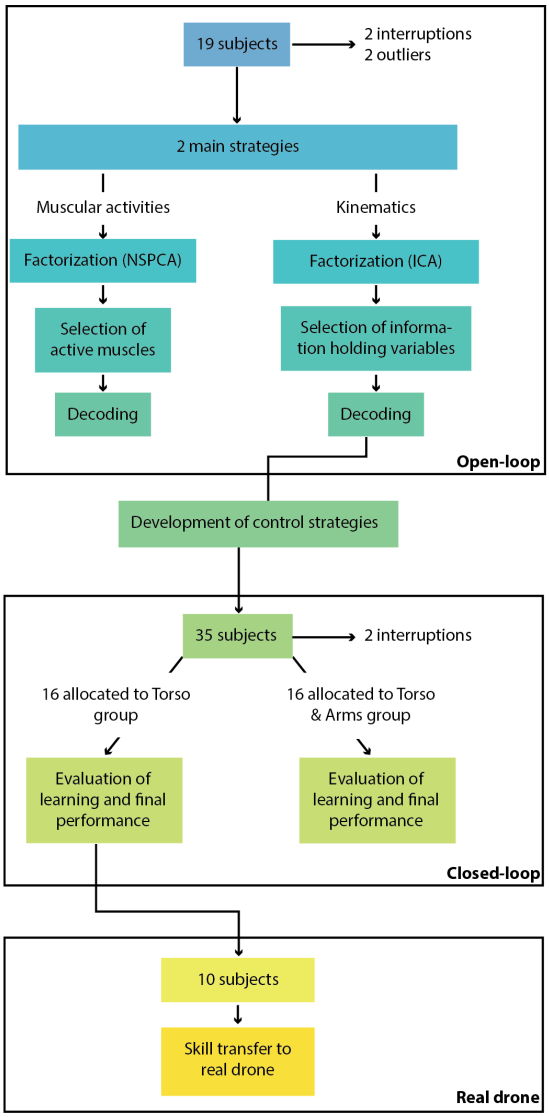

Figure 1.4 – Study overview

2 Identification of spontaneous gestural strategies during human-drone interactions

2.1 Methods

Participants

We recruited 19 young healthy participants for Experiment 1, 17 of which completed the experiment (23.7 ± 1.1 years old, one woman). In all the experiments, the participants who decided to interrupt the experiment suffered from virtual reality sickness. Their data was excluded from the analyses. All participants gave their written consent for their participation in the study and for the use of their data including pictures and videos. All experiments were approved by the local ethical committee.

Experimental conditions

Pilot experiments revealed that neither the flight dynamics (simulated fixed-wing drone or quadcopter), nor the participant's position (sitting, standing or lying face down) affected the movement strategy, or the subjective levels of comfort and immersion (Figure 2.1). To facilitate the translation towards the control of a real drone, we selected the sitting position, which requires only light equipment, yet is safer for the operator than standing upright. For the same reason, we decided to simulate the dynamics of a fixed-wing drone, as these aircrafts typically display a longer flight autonomy and thus allow the exploration of wider territories [125].

Experimental paradigm

The participants were shown an automatically controlled flight sequence in FPV through a HMD (Oculus Rift, Development Kit 2, Oculus VR, LLC), and were instructed to follow the movements of the simulated aircraft using self-selected, flight-like upper-body movements.

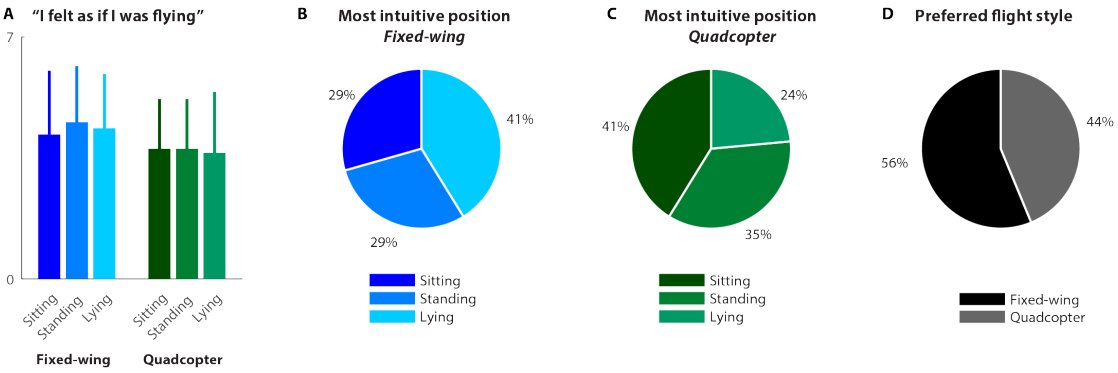

Figure 2.1 – (A) Reported sensation of flying on a 7-point scale (0: strongly disagree, 7: strongly agree). (B) Body postures reported as the most intuitive with the fixed-wing flight style. (C) Body postures reported as the most intuitive with the quadcopter flight style. (D) Overall preferred flight style

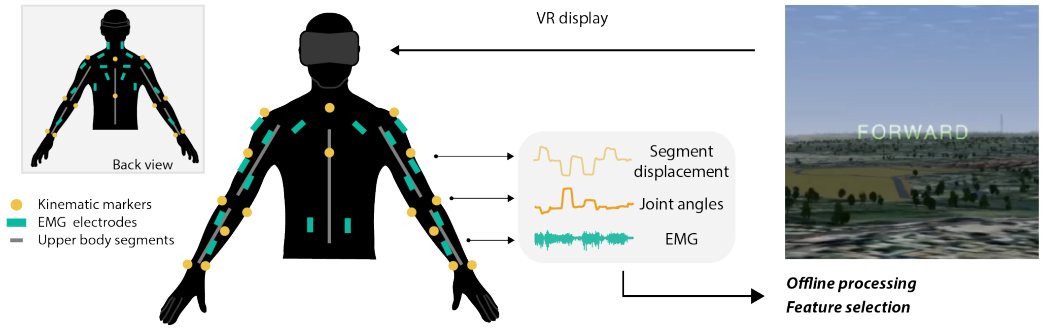

Figure 2.2 – Setup for experiment 1

The sequence consisted of alternations of a 6-second baseline (constant forward motion, speed 12 m/s) and 7-second randomized directional maneuvers (Right banked turn, Left banked turn, Upward pitch, and Downward pitch). Each new action was notified by a text indication one second prior to movement initiation. In total, we recorded ten repetitions of each maneuver. (See Figure 2.2 for a representation of the setup)

Flight simulator

We created a FPV flight simulator using FlightGear with the YASim dynamics model. Low-level controls, such as propeller thrust and flap inclination were regulated through PID controllers implemented in a C++ software running in parallel and communicating with the simulator through UDP/IP. This software also generated a randomized maneuver list before each flight sequence, and synchronization voltage pulses sent to the motion capture system through an Arduino board at the beginning of each maneuver.

Motion capture

We acquired the participants' three-dimensional (3D) kinematics using an eight-camera motion capture system (Vicon Bonita, Vicon Motion Systems, Oxford, UK) and reflexive markers placed on their upper body following Vicon's Plug-in Gait model [139]. Missing data points were estimated offline using pattern fill interpolations provided by the motion capture software (Vicon Nexus 1.7.4, Vicon Motion Systems Ltd., UK). All marker trajectories were low-pass filtered at 6 Hz using a zero-lag fourth-order Butterworth filter and were resampled at 100 Hz.

Recording of muscle activities

The EMG signals from 32 upper limb and torso muscles (sternocleidomastoid, STER, trapezius superior, TRAP, infraspinatus, INF, latissimus dorsi, LAT, rhomboid major, RHO, pectoralis major, PEC, rectus abdominis, ABD, deltoid anterior, DANT, medialis, DMED, and posterior, DPOST, biceps brachii long head, BIC, triceps brachii long head, TRI, brachialis, BRA, pronator teres, PRO, extensor digitorum communis, EXT, flexor carpi radialis, FLEX; see Figure 2.3 for a representation of the electrode placement) were recorded bilaterally using superficial Ag-AgCl electrodes (Kendall H124SG, ECG electrodes, 30x24 mm) and two wireless transmission systems (Desktop DTS, Noraxon Inc., USA). The skin was cleaned with medical ethanol and the electrodes were placed according to the standard procedure for surface electromyography for non-invasive assessment of muscles (SENIAM) guidelines [140]. Apparatus failures during the recording sessions rendered the EMG data of 6 participants unsuitable for analysis.

Extraction of the kinematic variables

Using the raw 3D positions of the markers, we computed the trajectories of the center of mass (COM) of the torso, and right and left upper and lower arms using de Leva's landmarks and inertia parameters [141, 142], as well as the bilateral shoulder and elbow joint angles, and the torso rotations relative to the laboratory framework explained by sequences of Cardan angles [143, 144]. The torso was modeled as a ball-and-socket joint and its rotation angles were computed using the 'Z-X-Y' sequence (i.e. lateral flexion – flexion/extension – rotation). The shoulder was also modeled as a ball-and-socket joint. Here, we used the 'X-Z-Y' sequence (flexion/extension – abduction – internal/external rotation) to minimize the occurrence of gimbal lock. The elbow was modeled as a hinge and pivot joint and the corresponding angles were obtained through the 'Z-X-Y' rotation sequence, where the second value was not considered (flexion – pronation/supination)[143, 144].

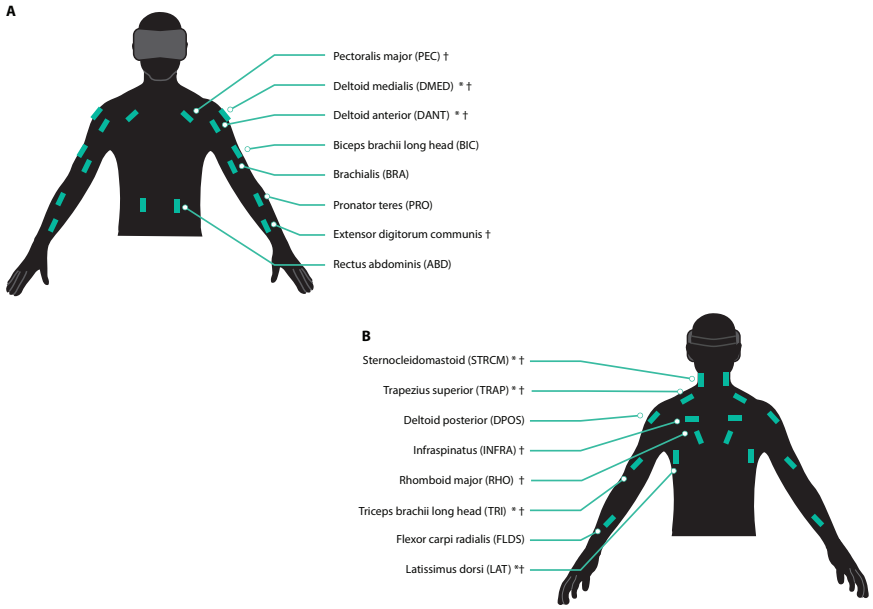

Figure 2.3 – (A) Front view. (B) Back view. * muscles selected for the subjects using only their torso, † muscles selected for the subjects using both their torso and their arms

EMG pre-processing

The raw EMG data were first resampled at 500 Hz and detrended. The signals were then low-pass filtered at 250 Hz, high-pass filtered at 50 Hz, rectified, and low-pass filtered at 5 Hz to remove noise using seventh-order Butterworth filters [145]. Eventually, each channel was normalized to its overall maximum.

Strategy clustering

We derived the angular velocities for the bilateral elbow and shoulder angles using the central differences formula, computed the root mean square (RMS) velocity for each joint and the norm of the vector containing the RMS values for all four joints. A two-class k-means clustering applied on the latter value clustered the subjects according to their upper-limb use.

Informativeness of the kinematic variables

The Reliable Independent Component Analysis (RELICA)[146, 147] method was used to parse the kinematic variables into maximally-independent components (ICs). RELICA enables to select the components, which are the most stable to data resampling and therefore more likely to carry significant information [148, 149]. For each subject, ICA was run twenty-five times, each time after performing a resampling of the original data, and yielded a couple of optimal

mixing and unmixing matrices of reliable ICs. Next, the absolute value of the weight that each input variable has on each extracted IC (variable weight) was computed. The Segment Weight was then defined as the sum of the variable weights corresponding respectively to the 3-dimensional COMs or rotation angles. The cumulative segment weight (CSW) was defined as the sum of the segment weights for all the retained ICs, and values were then normalized so that the sum of all the CSWs equaled 100 %. Finally, the Total Segment Weight (TSW) of each segment and its standard deviation were estimated as the average of the CSW across all the subjects within each group.

Variability of the muscular activities

We used non-negative sparse principal component analysis (NSPCA) to identify the muscles with the highest contribution to the overall variability of the dataset. NSPCA sorts out the components with the highest variance, while enforcing a non-negative constraint on their activation coefficients. This excludes the muscles, which were continuously active during the trials, and are therefore non-discriminant features [150, 151]. The new projection is computed iteratively from an initial estimation until convergence at a local optimum. For each participant, the principal components explaining on average 85% of the dataset's variance were used as initial values for the iterative scheme. Remaining (small) negative weights after convergence were set to zero. The non-negative components were normalized with respect to their norms. The weights were summed over all non-negative components, yielding coefficients, which represent the positive contribution of each muscle to the overall variability. Eventually, these coefficients were averaged across each group of subjects, and the muscles with a final weight above 0.45 were considered as significantly active.

Linear decoding of kinematic and muscular datasets

For each repetition of each maneuver, we discarded the first and last second of each sequence, which corresponded to the transitions between poses. We fitted linear discriminant (LDA) classifiers independently to the kinematic variable and the mean absolute values (MAV) of the muscular activities (100 ms non-overlapping windows) using leave-one-out cross-validation. In the subject-by-subject classification, one execution of one maneuver was used as test set. In the generalization step, we trained the classifier on the data of all-but-one subjects and evaluated its performance on the data of the remaining subject. The performance of the classifiers is reported as the percentage of correctly classified samples for each class.

Statistical analyses

For all experiments, the statistical analyses were performed using custom routines written in Matlab. Unless otherwise specified, the comparisons between the experimental conditions were computed with a Kruskal-Wallis test ($\alpha = 0.05$) and Bonferroni-corrected for multiple comparisons. The comparison between the variances was computed using Levene's test.

2.2 Results

Simulated human flight gives rise to two major distinct movement strategies

Out of the 17 participants who completed the experiment, 15 selected similar strategies which resembled gliding flight, and symmetrically involved both limbs (Figure 2.4D). The two outliers, which were excluded from subsequent analyses, performed very distinctive movements: one participant employed solely the arms, pointing towards the direction of change, and the second one impersonated a form of active, powered flight (Figure 2.4C). We categorized the participants according to their upper-limb usage, with a k-means classification on the norm of the root mean square (RMS) angular velocities of the different joints and found that 10 subjects used predominantly their torso but did not actively involve their arms (i.e., their arms were either rested on their thighs or extended sideward like wings, see Figure 2.4A), while 5 subjects combined torso and arm movements (Figure 2.4B). To account for these different patterns, we further analyzed both groups separately (hereafter "Torso" and "Torso & Arms" groups).

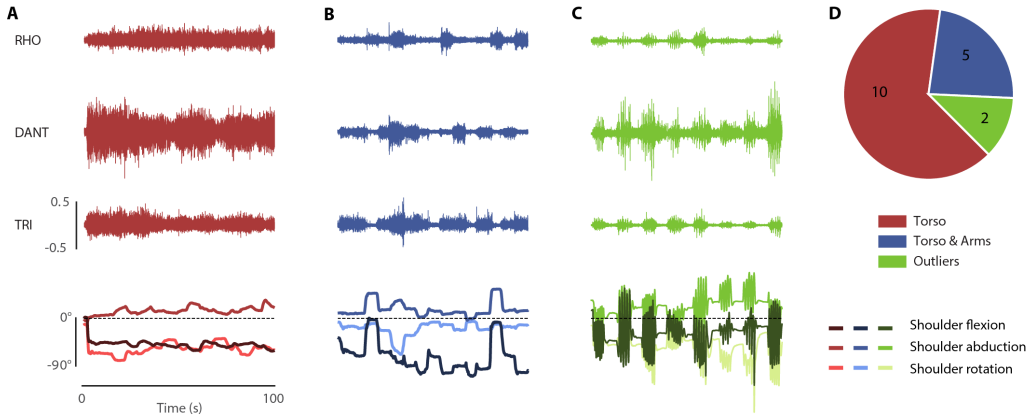

Figure 2.4 – Representative traces of the muscle activities and shoulder abduction angles during the execution of the open-loop task. (A) Participant using only the torso. (B) Participant actively using both the torso and the upper limbs. (C) Participant categorized as outlier. (D) Participant clustering according to the selected movement strategies.(top: rhomboid major, middle: deltoid anterior, bottom: triceps brachii lateral head)

Muscle activity patterns confirm the presence of two movement strategies

We assessed the activity of major upper body muscles groups during the imitation task and compared their contribution to the overall data variability across subgroups using NSPCA. The Torso group displayed a sparse pattern, with six pairs of muscles located on the superior back (sternocleidomastoid, trapezius superior, latissimus dorsi) and on the upper arm (deltoid anterior, deltoid medialis, triceps brachii, see Figure 2.5A) found to significantly contribute to the overall variability. The Torso & Arms group in turn showed a more uniform pattern, with ten pairs of muscles out of sixteen considered as carrying the relevant variability. All the contributors for the Torso group were also selected here. The additional muscles were located on the forearm (extensor digitorum communis) and in the upper trunk (infraspinatus, rhomboid major, pectoralis major, see Figure 2.5B). These results confirm the existence of two distinct motion strategies, one involving only the torso, the other one including both torso and arm movements.

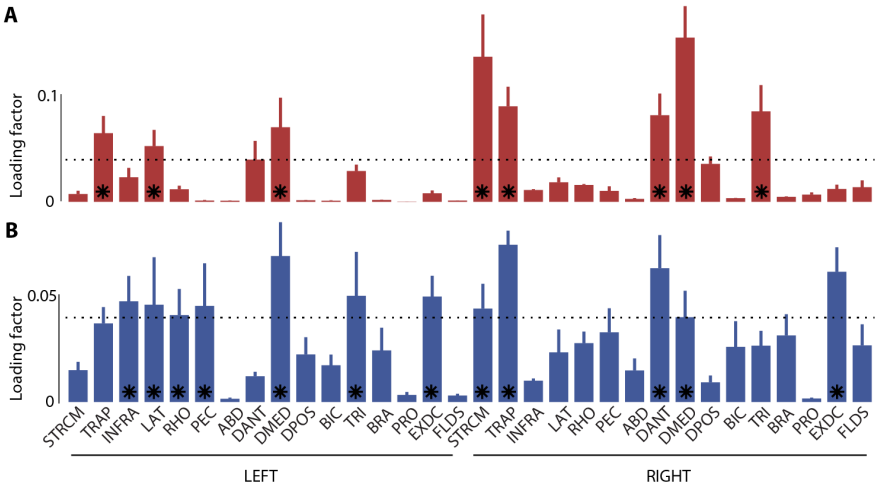

Figure 2.5 – Cumulated factor loadings showing the contribution of each muscle to the overall variance in the EMG dataset. (A) Participants using only their torso. (B) Participants using their torso and their arms. The retained muscles (indicated by the black stars) are STRCM, TRAP, LAT, DANT, DMED and TRI for the Torso group; STRCM, TRAP, INFRA, LAT, RHO, PEC, DANT, DMED, TRI and EXDC for the Torso & Arms group. The bar graphs represent the means + standard error of the mean over 4 (Torso group), respectively 5 subjects (Torso & Arms group).

Kinematic variables show uniform levels of discriminant information

We evaluated and compared the amount of discriminant information provided by all considered upper-body segments, that is the torso, both upper arms, and both forearms, as defined by the three-dimensional position of their COM, as well as the absolute orientation angles for the torso and the shoulder and elbow angles. We used the RELICA method to parse the multivariate dataset into independent components, and to identify the variables carrying

the relevant information. The averaged segment scores for the Torso group show that the information is uniformly distributed across all variables. In particular, we found no significant difference between the amount of information held by the torso COM and torso angles ($I_{TorsoCOM}$ = 9.25 ± 1.00, $I_{TorsoAngles}$ = 10.16 ± 0.65, p = 0.098), which indicates that the positional and angular variables are of equal interest for decoding the movements of this strategy (Figure 2.6A). Similarly, the level of information was nearly uniformly distributed across the individual segments for the Torso & Arms group. We also assessed the difference between the cumulated informativeness carried by all COMs and all joint angles. Once more, we found that the two subsets of variables held equivalent levels of information ($I_{allCOMs}$ = 51.93 ± 1.33, $I_{allAngles}$ = 48.07 ± 1.98, p = 0.062, Figure 2.6B). The discriminant information thus appeared to be equally distributed across all kinematic variables. In view of future applications, we decided to restrict the subsequent steps of our analysis to the angular data, which can be more robustly extracted with wearable sensors [152].

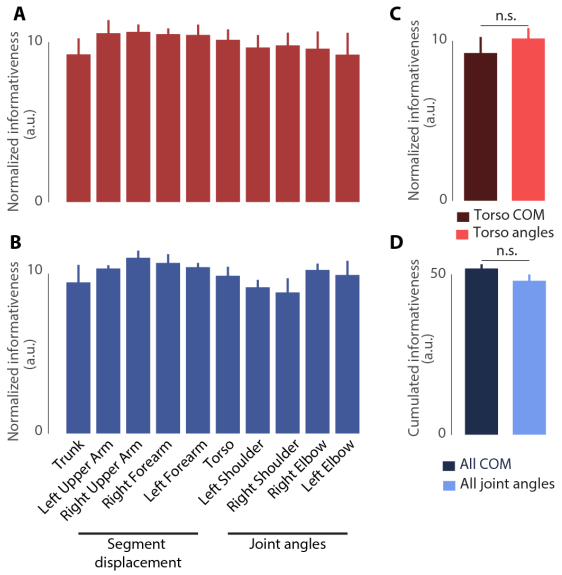

Figure 2.6 – Information levels held by the upper body segments in terms of 3-dimensional position or joint angles. (A) Participants using only the torso. The 3-dimensional displacement and the angles of the torso appear to hold equivalent levels of information (B) Participants using the torso and the arms. The informativeness is equally shared between the positional and angular data of all segments and joints. The bar graphs represent the means + standard deviation over 10 (Torso group) and 5 (Torso & Arms group) subjects.

Selected kinematic variables lead to higher decoding performances than selected muscles

Next, we assessed the decoding power held by the full sets of kinematic variables and the muscular activities, and by the reduced (selected) sets of both types of signals as identified

in the previous section. For each subject, we implemented LDA classifiers employing one set of variables with leave-one-out cross-validation. Eventually, we performed a generalized classification, using the data of all-but-one subjects to build the classifier, which was then tested on the data of the remaining subjects (Figure 2.7). The EMG-based classification for the Torso group yielded low accuracies, with similar results for the entire dataset ($A_{Torso,\ allEMG}$ = 37.65 ± 26.42%), and the selected variables ($A_{Torso,\ selectedEMG}$ = 34.87 ± 27.29%, p = 0.6).

In particular, the "Forward" and "Up" commands were poorly recognized, with scores in the range of chance level. In contrast, the data of the Torso & Arms group led to satisfying performances, again with similar results for the entire dataset ($A_{TorsoArms,\ allEMG}$ = 76.11 ± 6.23%), and the selected variables ($A_{TorsoArms,\ selectedEMG}$ = 72.15 ± 10.70%, p = 0.77); with all movements equivalently well decoded.

The kinematics-based classification yielded outcomes comparable with the EMG-based decoders. The accuracy obtained for the Torso group was similar when using the full dataset ($A_{Torso,\ allKin}$ = 55.90 ± 8.51%) and the selected variables ($A_{Torso,\ selectedKin}$ = 60.13 ± 17.16%, p = 0.93). Likewise, the decoding power for the Torso & Arms group was in the same range for the full dataset ($A_{TorsoArms,\ allKin}$ = 76.13 ± 14.43%) and for the selected variables ($A_{TorsoArms,\ selectedKin}$ = 75.08 ± 16.11%, p = 0.12). The generalized classification led to lower, yet not significantly different accuracies, for the Torso group ($A_{Torso,\ gen}$= 53.02 ± 14.88 %, p = 0.175) and Torso & Arms group ($A_{TorsoArms,\ gen}$= 40.69 ± 8.78%, p = 0.021, not significant at the corrected Bonferroni level).

These results confirm the good decoding power of the selected datasets as we observed only minor changes in the decoding performance when the full sets of variables were reduced to the selected subsets, indicating that the retained factors carried the discriminant information. In general, we obtained higher decoding accuracies for the Torso & Arms group than for the Torso group. This reflects the higher inter-movement variability displayed by the Torso & Arms group, due to the higher number of degrees of freedom. Overall, the selected kinematic variables, i.e. the joint angles, yielded the best decoding ability. Therefore, we used the joint angles (torso angles for the Torso group; torso, shoulder and elbow angles for the Torso & Arms group) as inputs for a closed-loop implementation.

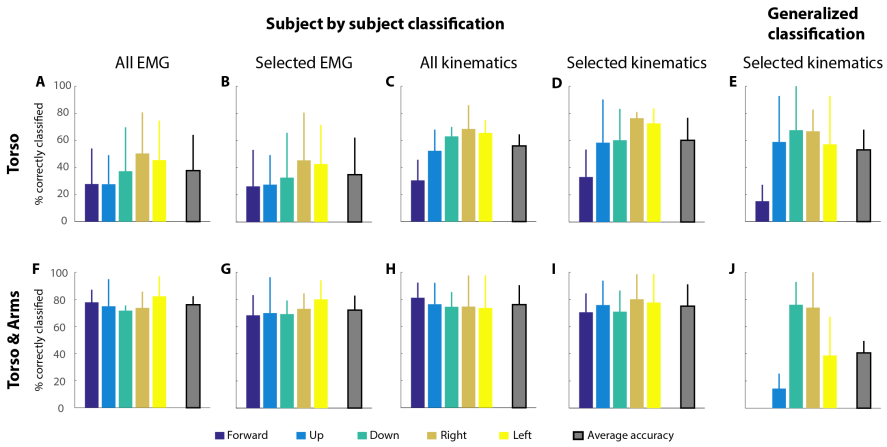

Figure 2.7 – Classification accuracy as percentage of correctly classified samples. (A-D) Subject by subject and (E) generalized classification for the Torso group. (F-I) Subject by subject and (J) generalized classification for the Torso & Arms group. The selected EMG were STRCM, TRAP, LAT, DANT, DMED, TRI for the Torso group and STRCM, TRAP, INFRA, LAT, RHO, PEC, DANT, DMED, TRI, EXDC for the Torso & Arms group. The selected kinematic variables consisted of the (absolute) torso rotation angles for the Torso group and the torso, and bilateral shoulder and elbow angles for the Torso & Arms group. The bar graphs represent the means + standard deviation over 4 (Torso group) and 5 (Torso & Arms group) subjects.

3 A Body-Machine Interface for the control of simulated and real drones

3.1 Methods

Experiment 1 - BoMI control of a simulated drone

Participants

We recruited 48 new, young healthy participants, 44 for of which completed the experiment (26.9 ± 5.9 years, seven women in the Torso group; 22.2 ± 4.1 years, six women in the Torso and Arms group). 6 subjects, randomly selected in each group, repeated the experimental protocol on three consecutive days (25.5 ± 2.1 years, three women in the Torso group; 28.3 ± 4.8 years, three women in the Torso and Arms group). The participants were assigned to the groups using covariate adaptive randomization with the gender as covariate [153]. 7 additional participants performed the 3-day experiment using the joystick (24.8 ± 4.2 years, 2 women)

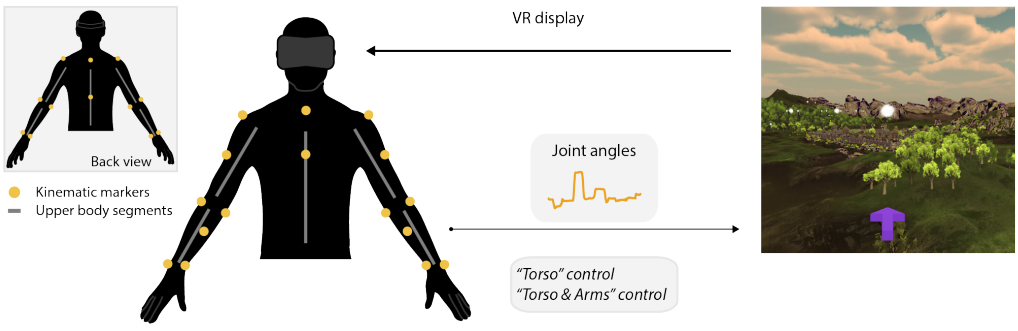

Figure 3.1 – Setup for experiment 2

Experimental paradigm

The participants were shown a virtual environment in FPV through a HMD. The experimental session consisted of three distinct parts. The subjects were first shown a one-minute demonstration sequence during which the simulated aircraft was flying autonomously through waypoints, while an avatar displayed the control movements corresponding to the motion of the aircraft. The participants were then asked to fly along a waypoint path alternating simple forward motion (baseline) and one of four directional maneuvers (Right banked turn, Left banked turn, Upward pitch, and Downward pitch), until they reached nine minutes of training. Eventually, we evaluated the participants' final ability to steer the virtual drone on two sequences of forty-two waypoints, corresponding to ten repetitions of each maneuver. For the overnight retention, the participants repeated the training and the evaluation on 3 consecutive days. (See Figure 3.1 for a representation of the setup).

Flight simulator

We developed a virtual environment using the game engine Unity3D, in which we embedded a simulated fixed-wing drone flying with a constant speed of 12 m/s. Cloud-shaped waypoints (diameter 0.6 m, inter-waypoint distance 40 m [154]) represented a path to follow, alternating simple forward motion (baseline) and one of four directional maneuvers (Right banked turn, Left banked turn, Upward pitch, and Downward pitch). A waypoint was validated when the simulated aircraft crossed its supporting vertical plane, defined as the plane passing through the waypoint and perpendicular to the vector connecting the previous and the current waypoint (Figure 3.2). The distance between the drone was computed at the position at which the drone crossed the supporting plane.

Closed-loop control of the flight simulator

The participants' 3D upper-body kinematics were recorded and streamed to the control routine in soft real-time using an eight-camera motion capture system as described above. The raw marker positions were imported into a custom Matlab routine using Vicon's DataStream SDK. The routine extracted the angular excursions for the torso, shoulders and elbows as described previously, and computed the corresponding pitch and roll angles for the virtual drone, and transmitted the latter values to the simulator via Ethernet after applying a moving average filter with a window of 10 frames to prevent instabilities, which could arise form the brief disappearance of the markers used for motion capture.

Definition of the Torso and Torso and Arms control strategies

We implemented two distinct control modes, corresponding to the two main movement strategies derived from the previous experiment. In the Torso mode, the flexion/extension of the trunk was directly transmitted as pitch angle, whereas the roll was computed as a linear combination of lateral flexion and axial rotation. The Torso and Arms strategy was implemented using a previously trained linear regression. The training set for the regression algorithm was derived from the data gathered from the participants using their torso and upper limbs during the strategy identification experiment. We extracted the joint angles corresponding to the stable phase of each maneuver and computed the average poses for each subject. The postures were then averaged across all participants of this group, and the resulting values were centered and rendered symmetric (i.e. the forward, up and down maneuvers were centered vertically, and the amplitude of the right and left movements was averaged). In order to enhance the inter-maneuver differentiation, we augmented the amplitude of each directional maneuver along the direction of displacement. Eventually, the computed joint angles were used as input for an avatar and were displayed as guideline to four participants familiar with the experimental setup during a repetition of the open-loop experiment. The recorded kinematics, and the pitch and roll values of the virtual aircraft served as training data for the linear regressor.

Performance

A performance metric was computed for each waypoint as a function of the distance d between its center and the virtual drone, when the drone crossed the vertical plane supporting the waypoint (Figure 3.2):

$$perf(d) = 100 \cdot e^{-(\frac{d}{\sigma})^2} \tag{3.1}$$

The decay factor σ was computed as the value yielding a performance of 1% when a waypoint was validated at a distance equal to the overall mean distance and 2.5 standard deviations. This value was computed from pilot data and corresponded to 21 m.

Learning

For each subject, we computed a learning curve using a moving average over a window of five waypoints. The individual curves were linearly interpolated between the query points to obtain a continuous representation of the performance in time and averaged across the subjects of each group. The resultant average curves were modeled by exponential functions

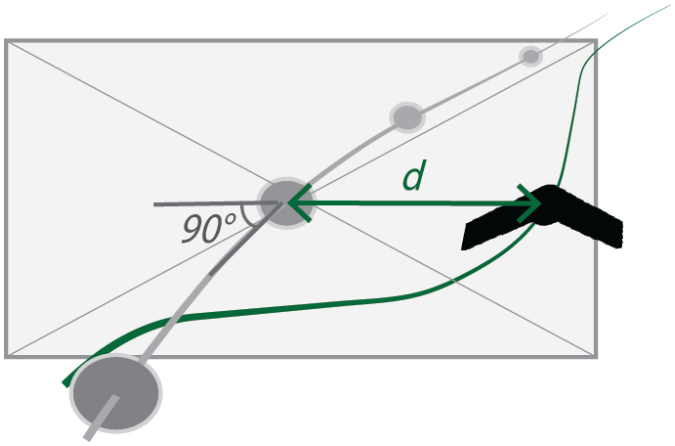

Figure 3.2 – Each waypoint was supported by a vertical plane, positioned perpendicularly to the trajectory from the previous waypoint. The distance d between the drone and the waypoint was computed at the instant at which the drone crossed the supporting plane.

of the following form [155]:

$$Perf(t) = a \cdot (1 - e^{-bt}) \tag{3.2}$$

Experiment 2 - BoMI control of a real drone

Participants

12 new, young healthy subjects were recruited to participate in Experiment 3, 10 of which completed the experiment (23.9 ± 1.2 years, one woman).

Experimental paradigm

The experimental session began with a training in simulation, consisting of a one-minute passive sequence teaching the control movements, followed by nine minutes of active waypoint navigation of the simulated aircraft, as in Experiment 2. After completion of the training, the participants were given the control of a real drone with FPV video streaming, which they could fly freely in the flight environment during two minutes to get used to its dynamics. Eventually, the subjects were asked to steer the drone through 6 circular gates forming an eight-shaped path comprising right and left turns as well as one ascent and one descent (Figure 3.4), for a total of ten loops.

(a) Pilot wearing the HMD providing visual feedback from the camera embedded on the drone.

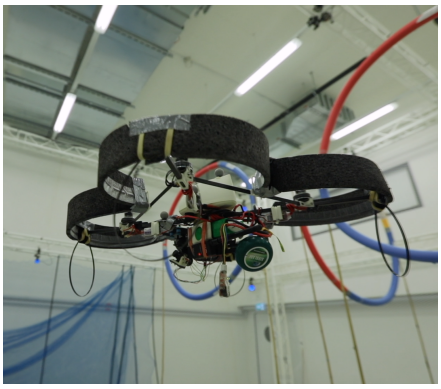

(b) Custom-made quadcopter and circular gates to be crossed during the piloting task

Figure 3.3 – Setup for the BoMI steering of a real quadcopter

Quadcopter and flight environment

We used a quadcopter (weight 0.7 kg, diagonal motor-to-motor distance 32 cm) with an embedded gimbal camera controlled by the operators' head movements to provide them a visual feedback through an HMD (Fatshark Dominator HD2). The control of the quadcopter reproduced the flight dynamics of a fixed-wing drone[154], as in the simulator. After an automated take off, the drone had a constant forward speed of 0.5 m/s.

The participants' raw, 3D trunk kinematics were acquired using an eight-camera motion capture system, and streamed in (soft) real-time to the control routine, as described above. Torso extension and flexion were translated into upward and downward commands to the quadcopter. Torso lateral flexion and axial rotation were linearly combined and translated into left or right turns. Backward and lateral displacements of the quadcopter were constrained. The roll and pitch angles computed from the operator's posture were transmitted to the drone's ground computer as previously described for the simulated aircraft. The ground computer sent commands to the drone through a wireless communication established thanks to two 3DR 915 MHz transmitter modules (3D Robotics, Inc.) connected respectively to the computer and to the drone. A motion capture system (Optitrack, Natural Point Inc.) monitored the position and orientation of the drone. This information was transmitted at 20 Hz to the ground computer and redirected to the drone through the same wireless communication as for the commands. These attitude data were used by the autopilot to actively stabilize the quadcopter through a stability control loop running at 250 Hz.

Using six circular gates, we set up a path shaped as a figure of eight comprising the four maneuvers evaluated in the simulation (right and left banked turns, upward and downward pitch). The gates had a diameter of 1.52 m. The three lower gates had a height of 1.5 m, while the higher three reached a height of 2.8 m. The length of the descending and ascending paths,

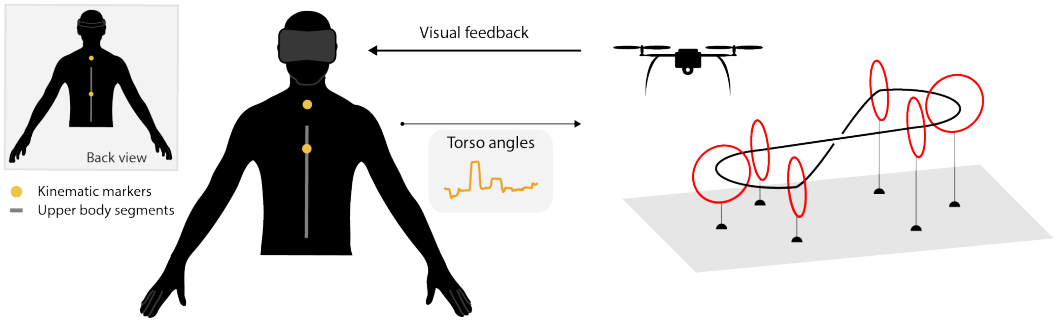

Figure 3.4 – Setup for experiment 3

as well as the diameter of the semicircular curves spanned 3 m (Figure 3.4). A virtual repulsive fence was present to restrict the flying space of the drone and to avoid collision with the walls, ground and ceiling. A safety pilot who could take over control the drone when necessary was present in the flight arena.

Performance

The participants' performance and learning during the VR training were assessed as described above. We evaluated the ability of the participants to steer the drone along the predefined path using the percentage of validly crossed gates (PVC) [50], defined as:

$$PVC = \frac{N_{ValidGates}}{N_{ValidGates} + N_{Collisions} + N_{SafetyPilotInterventions}} \tag{3.3}$$

An attempt was considered valid when the drone crossed the gate without any collision with the gate itself or its supports, or any intervention of the safety pilot.

3.2 Results

Experiment 2 - BoMI control of a simulated drone

Participants steering the aircraft using only their torso outperformed those using their torso and arms

Over a single practice session, all participants displayed a continuous performance improvement. The final performance, evaluated at the end of the session, was significantly higher for the group using only the torso ($Perf_{Torso}$ = 84.58 ± 17.79%) than for the group using the Torso

& Arms strategy ($Perf_{TorsoArms}$ = 62.59 ± 25.88%, p = 0.004) or the joystick ($Perf_{Joystick}$ = 59.42 ± 31.35%, p = 0.029). The performance of the Torso group was however comparable to the results obtained by the participants using Birdly® ($Perf_{Birdly}$ = 93.01 ± 5.87, p =, 0.43 Figure 3.5).

Three-day training leads to a homogeneous performance for the Torso strategy

After three training sessions, the participants using only their torso showed lower variability in their final performances than those using the Torso & Arms strategy ($F_{5,5}$ = 10.96, p = 0.02) and the joystick ($F_{6,5}$ = 19.88, p = 0.005). This was observed even if, with this reduced number of participants, there were no differences in terms of performances across the three strategies (p=0.25).

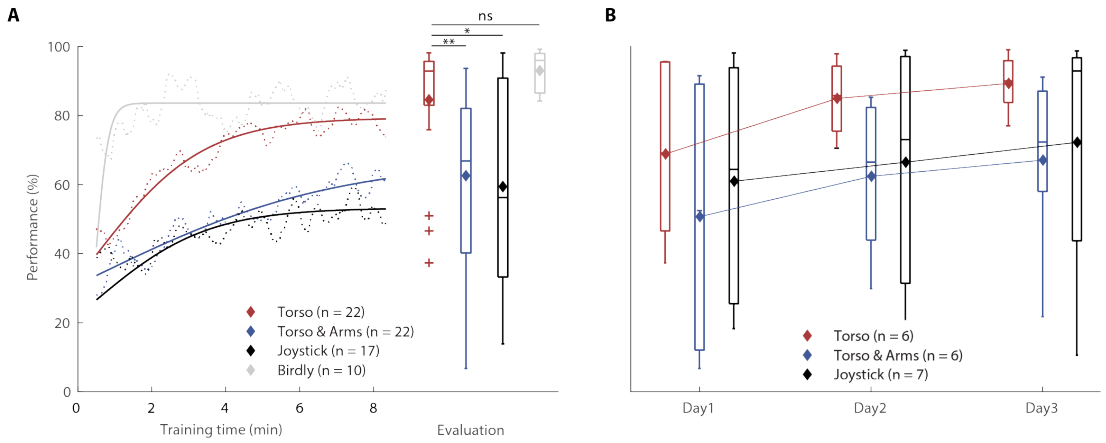

Figure 3.5 – Control of the simulated drone. (A) Performance evolution during the training phase and final evaluation after one session. The dotted lines represent the performance averaged across participants, the full lines the modeled learning curves, and the diamonds indicate the mean performance (* $p < 0.05$, ** $p < 0.01$). (B) Final evaluation on three training sessions on consecutive days. The diamonds indicate the mean performance.

Experiment 3 - BoMI control of a real drone

We evaluated the transferability of the skills acquired during the VR training to the control of an actual drone using the Torso strategy, as this approach proved to be superior for the control of a virtual aircraft. The participants began with a nine-minute VR training as described previously. Afterwards, they were given the control of a real quadcopter with FPV video feedback, which they could freely fly for two minutes to get used to its dynamics. Eventually, they were asked to steer the drone through six gates arranged along a trajectory shaped as a figure of eight (Figure 3.4)

Kinematic-based control skills transfer from simulation to real environment

After completing the VR training and the free flight, the participants were able to steer the quadcopter along the defined path with an average PVC of 87.67 ± 9.88%. This result suggests a transfer of the control skills acquired in simulation and confirms the usability of the Torso strategy for the steering of a real drone.

3.3 Discussion

We proposed a systematic selection process to identify effective body movement patterns in non-homologous HMIs and to reduce the sensor coverage necessary for the acquisition of the discriminant information. We applied the described method to the specific case of flight and derived a simple body-machine interface for drone control. We found that, despite the non-innate nature of flying, two common motives emerged during the spontaneous selection of congruent movements during a virtual imitation task. These two major patterns proved to be valid command inputs for the control of a virtual drone, with the simpler strategy involving only movements of the torso leading to higher performances than the strategy employing both the torso and the arms. Eventually, we demonstrated that a real quadcopter could be controlled with the first, simpler strategy.

When using only their torso to steer the trajectory of the simulated drone in the virtual environment, inexperienced participants needed less than 7 minutes of practice to reach a performance of 84.58% (Figure 6A). By comparison, users performing the same task with a joystick typically used for piloting drones only reached an average score of 59.42% (Figure 6A). Furthermore, the performance level obtained using the identified BoMI is comparable to the performance of subjects using the bird-flight simulator Birdly ® to steer the virtual drone [154](Fig. 5) However, the participants using this platform displayed higher initial performance and a steeper improvement. Yet, the Birdly ® platform provides haptic and vestibular feedback in addition to the visual information used in this study, factors known to improve the execution of teleoperated tasks [152]. The lying position imposed by Birdly ® may also have affected the rapid proficiency, since this platform allows the entire body to move as a whole, and this posture may be more closely associated to the idea of flying. Nonetheless, the comparable final steering performance suggests that the identification of intuitive BoMIs can compensate to a certain extent the absence of additional sources of feedback, while requiring only minimal recording apparatus. Moreover, the Torso control method led to 87.7% of gates crossed without collisions during the steering of a real drone along a complex trajectory following a 9-minute training in simulation.

On a single session, the two implemented gestural strategies led to significantly different

performance levels, with the participants using the Torso strategy outperforming those using the Torso & Arms approach (Figure 6A). This difference was expected, since the Torso & Arms strategy was derived from the movement patterns displayed by 5 out of 15 participants of Experiment 1, being therefore less representative of the population. Additionally, while the Torso strategy mapped 3 body DOFs (torso rotations) to 2 drone DOFs, the participants using their torso and arms had to correctly coordinate 13 DOFs to control the 2 rotations of the aircraft. Such an approach may however be of interest in the perspective of an extension of this work including additional commands or behaviors. All the subjects who practiced for three consecutive days improved their performance confirming the importance of practice. However, the intra-group variability significantly differed across the control methods after the third training session, as the steering ability displayed by some participants using either the joystick or the Torso and Arms strategy remained low (Figure 6B). Instead, all the subjects using the Torso strategy displayed a final performance above 77% and the overall performance variability significantly decreased over time. Therefore, the Torso strategy was the only approach which all participants managed to master following the three-day training, suggesting that this method may be suited to a broader range of users.

Surveying the spontaneous interaction strategies selected by non-trained users is a concept that has already been applied for the development of intuitive controllers for UAVs, either by means of interviews [138] or through Wizard-of-Oz experimentations [132, 134]. However, these systems focus on the identification of discrete commands and have the user interact with the drone from an external perspective. Conversely, our work presents the first case of a data-driven, gesture-based interface for the continuous and immersive control of drones using an immersive visual feedback. Our present approach could easily be translated into a wearable implementation using an inertial measurement unit (IMU) to acquire the 3-dimensional torso angles. This would provide a substantial benefit over HMIs using video-based motion tracking, which imposes constraints on lighting conditions in the operating environment and on the users' freedom of displacement, and thus limit the applicability of such a controller in natural environments.

A possible limitation of this study could be found in the mapping (scaling and offset constants) used to translate upper-body movements into commands of the simulated and real drones. The chosen mapping has shown to be sufficiently sensitive to steer the drone along the relatively smooth waypoint paths used in the experiments described here. However, we cannot exclude that sinuous trajectories involving sharp changes of directions may require different or even adaptive mapping values. Indeed, it is known that humans make directional errors when relying only on proprioception to estimate the spatial location of their limbs, and that these errors are proportional to the distance to the body centerline [156, 157] . Building on this knowledge, previous studies showed that non-linear transformations of the users' arm

movements led to faster and more precise control of a robotic arm than a simple scaling [35, 158]. Further studies will be needed to understand the role of more complex mappings to extend the results of this work.

Another limitation comes from the small diversity of our study population, which consisted mainly of young, male university students. It is unknown to which extent experience and observation shape the human representation of non-innate behaviors such as flight. We can therefore not exclude that factors such as age, gender, physical condition or familiarity with technology could lead to the identification of different body motion patterns. However, such discrepancies may highlight interesting causes in motor learning and representation rather than invalidating the proposed identification method.

3.4 Conclusion

The results of this study have a significant importance for the field of teleoperation and more generally HMIs. Often, control strategies are predefined and selected to comply with existing interfaces rather than derived from spontaneous representations of the interaction. The implementation of a methodology to identify body-machine patterns for specific applications could lead to the development of more intuitive and effective interfaces, which could in turn reduce the training time required to reach proficiency, limit the workload associated with the operation of the system and eventually improve the reliability of teleoperated missions. Moreover, the method described in this chapter could be extended to different populations, machines, and operations, including individuals with limited or impaired body functions.

Part II

On the use of virtual reality to expose developmental coordination patterns along childhood

Introduction

Coordinated motor behavior and efficient integration of stimuli from different sensory modalities are essential steps for successful interactions with the surrounding environment [159]. The development of these abilities follows a long-lasting and elaborate process, starting long before birth and extending into early adulthood. At the level of motor development, the skills are usually grouped into two categories. First, gross motor skills comprise postural control, locomotion and require the use of axial and proximal muscles. The maturation of these abilities shows a steep increase until the age of 2, and continues to refine until later during childhood [160, 161, 162, 163]. Conversely, fine motor skills include precise actions including functional hand movements, but also require multisensory integration such as hand-eye coordination. The time course of fine motor development typically extends over a longer time period and adult patterns are generally not observed before late childhood [164, 165].

The acquisition of a steady posture is a prerequisite for goal-directed behaviors such as reaching from a sitting position or locomotion [159, 164]. According to the ontogenetic model of postural development during childhood described by Assaiante et al., two main principles guide the selection of a given balance strategy: the choice of a stable reference, which shifts from the pelvis to the head [166, 159], and the gradual mastery of the involved degrees of freedom (DOF) [167, 168, 159].The coordination strategy evolves from an "en-block" behavior, which minimizes the number of DOF to be controlled [169, 170] to a fully articulated strategy, where each DOF is controlled individually. Mature, multi-jointed patterns are acquired at different ages, depending on the involved joint and the task characteristics. During locomotion, the "en-block" stabilization has been observed from the acquisition of upright stance until 6 years, while children aged 7 and more started to display a segmental control [168]. Similarly, rigid forearm-trunk coupling was observed until 6 years in seated both during voluntary trunk movements and in response to trunk perturbations [171]. Instead, in a reaching task, adult head-trunk-arm coordination patterns were observed in children as young as 2-3 years old for movements in the pitch plane and from 4 years onwards in the roll and yaw planes[172]. Yet, the activity and temporal recruitment of postural muscles appears to reach mature levels only after the age of 11 [166]. The ability to decouple head and trunk movements proves to be particularly useful when having to avoid or circumvent an obstacle while walking, where anticipatory head movements were observed from 5.5 years onwards, while younger children displayed a rigid head-trunk connection [173]. Children thus first build a repertoire of postural strategies, before learning how and when to adequately implement them. It is worth mentioning that the development of postural control is not a linear process. Periods with rapid morphological changes such as early adolescence destabilize the recently acquired patterns and require a recalibration of the sensory-motor strategies [174].

Notwithstanding, successful postural stabilization does not only involve appropriate multi-jointed coordination, but often also requires the integration of the information provided by different sensory modalities. The Bayesian model of multisensory integration (MSI) suggests that adults fuse redundant sensory inputs in a statistically optimal way by weighting the sources according to their uncertainty [91, 175]. The ability to combine different cues to obtain more precise estimates of one's surroundings appears late in childhood development [98, 176], that is after the individual modalities have matured [177, 97], unless additional feedback on the reliability of each cue is provided [100]. Younger children will thus favor the information provided by the most modality with the highest reliability, in a given context [98, 178]. In the context of postural control, children and adolescents until 15 years standing on an oscillating platform displayed better stabilization with open than with closed eyes, thus indicating a strong reliance on vision [174, 162]. The display of an optic flow to elicit automatic postural movements led to stronger responses in children and adolescents when compared to adults, and the ability to stabilize these movements improved with age until late adolescence [179]. This effect was further enhanced when the participants were standing on a sway-referenced platform [102, 101]. When standing on the unstable platform, which attenuates the proprioceptive feedback, adults use primarily vestibular information to stabilize their posture, and this ability matures only during late adolescence [101]. Interestingly, children aged 7–10 years have been shown to display similar spatiotemporal muscle activation patterns than adults in response to platform oscillations [180], revealing an earlier development of automatic postural responses. Similarly, the predominance of visual cues over self-motion has been shown in children up to 11 years in a navigation task [99, 181]. The late maturation of visuo-vestibular and visuo-proprioceptive integration has been correlated with the individual development of these modalities when put in conflict: while adult levels were observed from 3 years for proprioception and from 14 years for vision, vestibular function in 15 year-old still displayed lower levels of vestibular function than adults [182].

The subjective straight-ahead (SSA), which defines the perception of the antero-posterior orientation of the body, is a suitable candidate to act as a common reference during the calibration of visuomotor integration. As a by-product of MSI, the SSA can be altered by acting on vision through prismatic goggles[183], on vestibular information through subthreshold rotations [184, 185], or through stimulation of the neck muscles [94]. Neck muscles have been shown to contribute to the integration of proprioceptive and visuo-vestibular cues in the absence of vision [184].This yielded a hierarchical model in which the head orientation in space is defined by the trunk orientation in space and the orientation of the head relative to the trunk. These results have, however, all be obtained on adult populations, and the maturation pattern of the SSA is still poorly understood.

The reliance on visual cues can be further challenged by the use of experimental setups

involving immersive virtual reality (VR) where the participants are immersed in a digital environment through a head-mounted display (HMD) or thanks to a specifically designed room with projections on the walls, floor and ceiling (Cave automatic virtual environment, CAVE [20]). Most VR systems use a visual rendering of the simulated environment, although other senses have been additionally involved to deepen the immersion [18]. Over the last years, and thanks to the development of lightweight HMDs [186], the use of VR is expanding to applications in education [187, 188, 189, 190] and research [85, 191, 181] with healthy children, and for neurorehabilitation [192, 71, 28, 193] or distraction from painful medical procedures [74, 75] for pediatric patients. Yet, the majority of these applications offer none or limited interactions with the virtual environment. Therefore, little is known about how children perceive the effect of their actions when immersed in VR. Recently, Adams et al. showed that children displayed stronger and longer-lasting responses than teenagers to prism adaptation in immersive VR [194].

We previously developed a body-machine interface (BoMI) for the immersive control of a first-person view (FPV) flight simulator, and showed that healthy adults reached a higher steering performance with this approach than with a standard joystick [195]. In chapter 4, we evaluated the ability of school-aged children to control this flight simulator using either their head or their torso, and we assessed the intersegmental coordination patterns which emerged during the execution of this task. In chapter 5, we present a different VR system which allows to specifically study the use of the SSA as a reference frame.

4 Development of head-trunk coordination for the gestural control of an immersive flight simulator

Abstract

The development of appropriate motor coordination patterns is essential for interacting with the surrounding world. This process relies on a balanced integration of inputs from different sensory modalities. This integration can be challenged under altered sensory feedback, as is the case for vision in immersive virtual reality. We have previously developed a Body-Machine Interface (BoMI) for the immersive control of simulated and real drones, which was rapidly mastered by adult users without prior piloting experience. Here, we assessed the development of the motor skills necessary to the control of the BoMI along childhood. We found that children younger than 9 years old fail to select the most efficient coordination strategy. In particular, when asked to steer the flight simulator with their upper body, the younger participants did not use the 'en-block' behavior displayed by older children and adults, albeit preferentially selecting this strategy in other tasks.

The contents of this chapter are part of the publication in preparation:

Immersive virtual reality interferes with the selection of postural strategies in young children
Miehlbradt J., Cuturi L., Gori M., Micera S.

Contributions as first author: design of the experiments, adaptation of the experimental setup, data collection, processing and analysis, preparation of the figures and redaction of the manuscript.

4.1 Methods

Participants

Thirty-six typically developing children aged 6-10 participated in the study. Two children asked to stop the experiment and two other ones did not comply with the instructions; their data was excluded from further analyses. The age groups were as follows: nine 6 year-olds (5 girls), eight 8 year-olds (2 girls), four 9 year-olds (1 girls) and eleven 10 year-olds (2 girls). Parental written consent was obtained for all underage participants and the study was approved by the ethics committee of the health service of the city of Genoa, Italy. In addition, 13 healthy adults participated to the study (3 women, 10 men, age 28.5 ±3.4 years). The adult participants gave their written consent for participating to the experiment and this part of the study was approved by the ethical commission of the Canton of Geneva, Switzerland.

Virtual environment

The virtual environment (VE) was developed using the game engine Unity3D and consisted of a FPV flight simulator, embedding the dynamics of a fixed-wing drone flying at a constant speed of 12 m/s, as previously described [154, 195]. A succession of coins to catch (distance between consecutive coins: 58 m) represented a path to follow, randomly alternating simple forward motion and one of four directional maneuvers (right turn, left turn, ascent, descent). The coins' initial diameter was 1 m and every time one coin was caught, the next one was enlarged to 2 m. To minimize possible effects of path planning abilities, we additionally displayed a colored line smoothly connecting the coins, computed as a Catmull-Rom spline [196]. During the training sequences (see below), a supplementary visual aid was rendered in the form of a dotted line connecting the participant's position in the VE to the upcoming coin. Similarly, to provide the participants a visual cue of their own position in space, an eagle was displayed below their visual horizon, rendering the impression to ride on the bird's back. Finally, to keep the experiment engaging, a tinkling sound was played when the coin was caught at a distance smaller than 10 m, which also added points to a total score for the trial, displayed at the top of the screen.

Control of the flight simulator

The participants were asked to control the flight simulator using either head or trunk movements. The ascent (upward pitch) and descent (downward pitch) were achieved by flexion and extension of the controlling body part. Gains of 2.5 and 1.5 were applied to the ascent and descent respectively. The right and left turns were computed as *lateral flexion + 2·axial rotation*. The head and torso rotations were reset to zero before each sequence, at the participants'

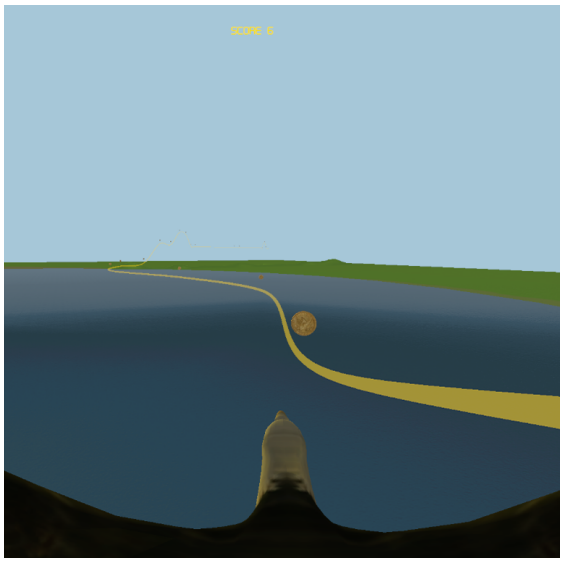

Figure 4.1 – Virtual environment, as seen by the participants, showing the coins to collect and the yellow line to aid in navigation.

self-selected neutral position corresponding to a straight, forward flight.

Experimental setup

The participants were equipped with a head-mounted display (HMD, Oculus Rift) through which they were shown the virtual environment, and an inertial measurement unit (IMU, X-sens MTw Awinda) placed in their back between the scapulae and maintained with a custom harness to acquire their trunk's 3-dimensional (3D) rotation (Figure 4.2). The IMU embedded within the HMD was used both to control the view in the VE and to acquire the head rotations. The kinematic data were acquired with a sampling period of 68 ms.

Experimental protocol

Upon arriving, the participants were shown the movements to control the simulator using the head or the torso. They were equipped with the HMD and the IMU, and were seated on a stool or on a chair and asked not to lean against backrest. The participants were randomly allocated to start the experiment using the head or the torso. For the torso-controlled trials, the participants were advised to keep their neck rigid as to move their entire upper body as a whole. Similarly, before starting the head-controlled trials, the experimenter made the participant aware that moving their trunk was unnecessary. The recording sessions took place on two consecutive days (see Figure 4.3). On day 1, the participants had to steer the simulator along four paths with each body part. The first sequence contained 26 coins and was an

Figure 4.2 – Experimental setup including the Oculus Rift and one IMU placed in the back

initial evaluation of the performance (hereafter: *Before*). The second and third sequences each contained 50 coins and included the supplementary visual feedback. These sequences were considered as training. The fourth sequence contained 18 coins and did not display the additional visual feedback anymore (hereafter: *After*) All the sequences controlled with a given body part were executed successively. On day 2, one sequence containing 26 coins had to be performed with each body part (hereafter: *Day After*). Breaks were allowed between the sequences, at the participants' demand.

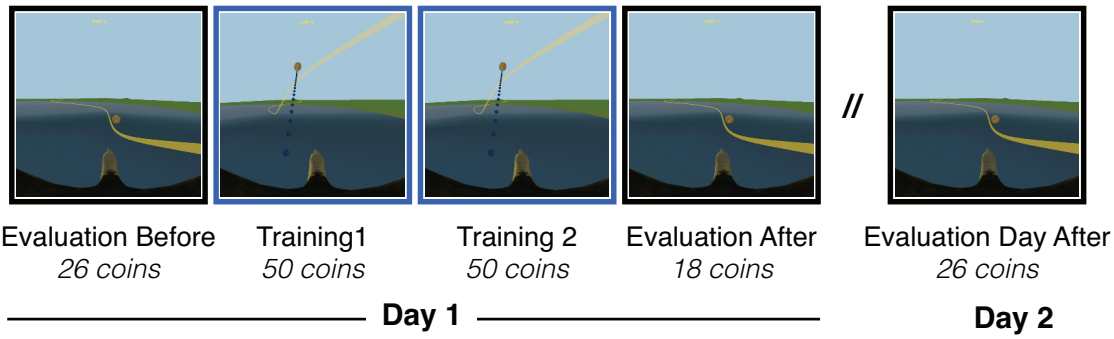

Figure 4.3 – Experimental protocol

Descriptive variables

The kinematic data was divided into segments corresponding to the intervals between consecutive coins. The descriptive variables were computed on these segments and averaged for each sequence (see also Appendix A).

Distance to coin center, horizontal and vertical error [m] For each coin, the unsigned distance to its center was computed when the participant crossed the vertical plane perpendicular to the trajectory supporting the coin (see Figure 3.2). The unidimensional errors were computed at the same location, taking into account only the distance in the corresponding plane. Lower values indicate a better precision in the task execution.

Path ratio [·] The path ratio was defined as the quotient of the traveled path and an ideal path computed by a Catmull-Rom interpolation between the coins (seesection 4.1). The path ratio was computed for the entirety of the sequence. High values indicate large deviations from the ideal path.

Time [s] The duration of the interval between two consecutive coins was extracted as an indirect indicator of path efficiency. Longer durations indicate large deviations from the ideal path.

Rotation amplitudes [°] For the head and torso rotations, the amplitudes in each direction were computed as the interquartile range of all the values recorded during the interval.

Torso speed [°/s] The mean and maximum torso angular velocities were extracted for each direction individually and normed. In addition, the ratio of the mean and maximum velocities were computed for the individual directions. A speed ratio close to 1 stands for a smooth velocity profile, while low values indicate jerky patterns [197, 198].

Head-torso correlation [·] The head-torso correlation assesses the stiffness of the segmental bond, and was computed in the sagittal, medial and axial planes, and between the latter two planes.

Anchoring index [·] The head anchoring index $\Delta\sigma$ describes whether the head stabilization occurs with respect to the torso or with respect to the external space and is defined as follows [167, 172]:

$$\Delta\sigma = \sigma_r - \sigma_a \tag{4.1}$$

where σ_a is the standard deviation of the absolute head angles and σ_r the standard deviation of the head angles relative to the torso. Positive $\Delta\sigma$ values indicate a preferred head stabilization to the external space and negative values a better head stabilization to the torso.

Cross-correlation peak time [s] The peak time of the head-torso cross-correlation indicates which is the leading body part. Negative delays indicate that the head is moving ahead of the body, while positive delays mean that the body is leading.

Dynamic time warping (DTW) distance [·] DTW is an algorithm measuring the similarity between two time series, which may vary in speed, by computing an optimal match between the sequences. A similarity metric is computed as the sum of the absolute differences between each pair of matched indices. Since this metric is affected by the number of data points present in the sequences, the segments to be compared were linearly interpolated to yield the same number of data points [199, 200].

Spectral arc length (SAL) [·] SAL is a dimensionless measure quantifying movement smoothness based on the arc length of the movement speed profile's normalized Fourier magnitude spectrum [201]. SAL values are negative values, where higher absolute values are related to jerkier movements.

Number of velocity peaks, normalized to the duration of the segment [peaks/s] The time-normalized number of velocity peaks was computed in each plane for head and torso rotations, as well as for the rotations of the simulator as a measure of movement smoothness. A lower number of peaks indicates smoother movements [202].

Principal Component Analysis

Principal component analysis (PCA) was computed on the dataset containing the kinematic variables extracted from all trials, or from the head- and torso-controlled trials respectively. Outliers were detected as data points whose euclidean distance to the centroid of the zscored dataset deviated from the average value by more than 4 standard deviations. These points were given a weight of 0.5 in the PCA computation. The variables with normalized loadings > 0.75 on the first (all trials, head-controlled trials) or the first two principal components were considered as significant and were regrouped into functional clusters.

Cluster separability

We assessed the separability among age-defined clusters in the space defined by the first two principal components using the Davis-Boulding index (DBI) between each pair of clusters [203].

Statistical analyses

Statistical evaluations were performed using paired t-tests or repeated-measures ANOVA, using the age as between-subjects factor and the control type and/or experimental phase as within-subjects factors. The p-values were corrected using the Greenhouse-Geisser correction, when Mauchly's test indicated a violation of sphericity. The p-values were adjusted to the false discovery rate when multiple ANOVAs were performed. Post hoc analyses were conducted using Tukey's honest significant differences test.

4.2 Results

Controlling body part and age affect steering performance

The participants' ability to steer the flight simulator was assessed by the average distance to the center of the coins during three phases (see Figure 4.5, higher values indicate lower performances): before and after the training (*Before* and *After*, see 4.1) and on the subsequent day (*Day After*). Figure 4.4 displays examples of navigation trajectories and the corresponding head and torso kinematics. A repeated measures ANOVA revealed a significant effect of Age ($F(4,35) = 7.45$, $p < 0.001$), Control ($F(1,35) = 29.52$, $p < 0.001$) and Phase ($F(2,70) = 15.44$, $p < 0.001$), as well as significant interactions for Age and Phase ($F(8,70) = 4.41$, $p = 0.003$), Age and Control ($F(4,35) = 5.97$, $p < 0.001$), Phase and Control ($F(2,70) = 11.94$, $p < 0.001$) and Age, Phase and Control ($F(8,70) = 4.21$, $p = 0.003$).

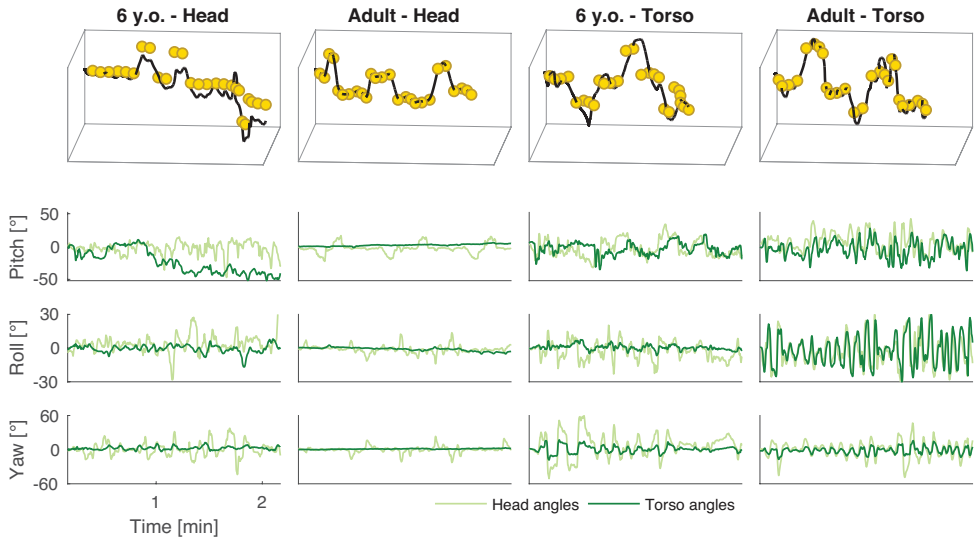

Figure 4.4 – Performance on the steering task

A post hoc Tukey test (see Table **??**) revealed that 6 year-olds performed better in the head-

than in the torso-controlled trials in all phases (Before: p = 0.002, After: p = 0.009, Day After: p < 0.001). This difference was also significant for the 8 year-old for the evaluation Before (p < 0.001), but not during the other phases. The 6 year-olds improved their steering between the evaluation before and after training (p = 0.013) and between before training and the second day (p = 0.014). Similarly, the average distance to the targets diminished in the 8 year-olds between the evaluation before and after training (p = 0.001) and between before training and the second day (p = 0.002). In the torso-controlled trials, the 6 year-olds showed significantly lower performance than the 10 year-olds before training (p = 0.023) and on the second day (p = 0.02) and than adults in all phases (Before: p = 0.06, After: p = 0.042, Day After: p = 0.001). Likewise, the 8 year-olds performed worse than the 10 years olds and the adults before training (p = 0.015 and p = 0.005 respectively). In the head-controlled trials, the 6 year-olds displayed higher distances than the adults after training (p = 0.001), and than the 10 year-olds and the adults on the second day (p = 0.013 and p = 0.002 respectively).

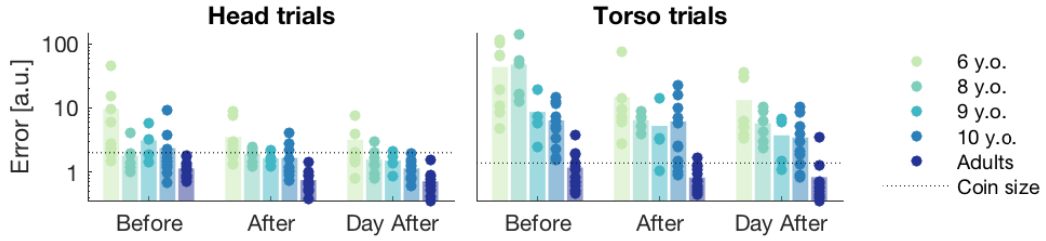

Figure 4.5 – Performance on the steering task

Age	Control - Phase1	Control - Phase2	Difference	*p*		Cohen's *d*
6	Head - Before	Torso - Before	-38.6	0.002	**	-1.17
	Head - After	Torso - After	-14.27	0.01	**	-0.83
	Head - Day After	Torso - After	-14.58	0.008	**	-0.85
	Torso - Before	Torso - After	30.43	0.013	*	0.85
	Torso - Before	Torso - Day After	32.15	0.014	*	0.97
8	Torso - Before	Torso - After	50.51	0.001	**	1.26
	Torso - Before	Torso - Day After	52.42	0.002	**	1.28

(a) Effect of experimental condition

Control - Phase	Age1	Age2	Difference	*p*		Cohen's *d*
Head - After	6	Adults	2.76	0.002	**	1.55
Head - DayAfter	6	10	2.05	0.013	*	1.13
	6	Adults	2.47	0.002	**	1.44
Torso - Before	6	10	40.01	0.023	*	1.34
	6	Adults	46.41	0.006	**	1.66
	8	10	50.63	0.015	*	1.45
	8	Adults	57.03	0.005	**	1.78
Torso - After	6	Adults	16.54	0.042	*	1.09
Torso - DayAfter	6	10	11.39	0.02	*	1.07
	6	Adults	14.8	0.001	**	1.52

(b) Effect of age

Table 4.1 – Significant simple effects for the steering performance, * $p < 0.05$, ** $p < 0.01$, *** $p < 0.001$

Additional visual feedback

To evaluate the potential benefits of an additional visual information, we compared the task performance before, at the beginning at the end and after the training. The introduction of the visual feedback (*Early training*) led to a mild improvement, except for the 8 year-olds who displayed a substantial drop in the distance to the targets in the torso controlled trials. Similarly, the suppression of the feedback line after the training did not worsen the performance, which instead remained at a stable level or further improved. Thus the observed progress in the steering abilities is most likely attributable to practice, and not the presence of the supplemental visual aid.

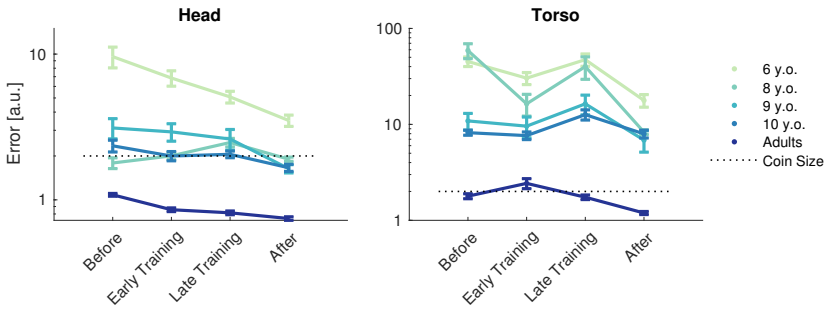

Figure 4.6 – Effect of the additional visual feedback on the task performance

Segmental coordination differs between torso and head trials

Principal Component Analysis (PCA) applied to all the recorded trials revealed that the first principal component (PC) accounted for 34% of the dataset's variability and separated the head-controlled from the torso-controlled trials ($p < 0.001$, see Figure 4.7). The kinematic variables displaying normalized loadings > 0.75 were regrouped into functional clusters: Cluster 1 encompassed variables describing the torso movements and Cluster 2 variables associated with the correlation of the head and the torso (see Figure 4.8).

We next assessed the effect of the controlling body segments and the possible interactions thereof with the participants' age and the experimental phase on the selected kinematic variables using repeated measure ANOVAs. The variables with significant effects of Control, or interactions of Control with Age and/or Phase are summarized in Table 4.2, and Figure 4.9 displays 8 representative variables by age and experimental phase.

Effect	**Variable**	F	**DOF1**	**DOF2**	***p***		η_p^2
Control	Torso Amplitude, roll	56.98	4	35	<0.001	***	0.62
	Torso Amplitude, pitch	128.91	4	35	<0.001	***	0.79
	Torso Amplitude, yaw	72.52	4	35	<0.001	***	0.67
	Mean Speed torso, roll	73.84	4	35	<0.001	***	0.68
	Mean Speed torso, pitch	119.41	4	35	<0.001	***	0.77
	Mean Speed torso, yaw	97.61	4	35	<0.001	***	0.74
	Max Speed torso, roll	76.45	4	35	<0.001	***	0.69
	Max Speed torso, pitch	111.96	4	35	<0.001	***	0.76
	Max Speed torso, yaw	85.77	4	35	<0.001	***	0.71
	Torso Speed norm, mean	131.52	4	35	<0.001	***	0.79
	Torso Speed norm, max	121.77	4	35	<0.001	***	0.78
	Head-torso correlation roll	283.23	4	35	<0.001	***	0.89
	Head-torso correlation roll-yaw	1792.71	4	35	<0.001	***	0.98
	Head-torso correlation yaw-roll	195.11	4	35	<0.001	***	0.85
	AI, roll-roll	83.59	4	35	<0.001	***	0.7
	AI, pitch-pitch	196.7	4	35	<0.001	***	0.85
	Cross-correlation peak time, pitch	313.97	4	35	<0.001	***	0.9
	Cross-correlation peak time, roll-yaw	115.65	4	35	<0.001	***	0.77
	Cross-correlation peak time, yaw-roll	208.79	4	35	<0.001	***	0.86
	DTW distance, roll	231.23	4	35	<0.001	***	0.87
	DTW distance, yaw	161.63	4	35	<0.001	***	0.82
Age:Control	Torso Amplitude, roll	4.31	8	70	0.017	*	0.33
	Head-torso correlation roll	6.49	8	70	0.002	**	0.43
	Head-torso correlation yaw-roll	5.37	8	70	0.005	**	0.38
	AI, pitch-pitch	8.97	8	70	<0.001	***	0.51
	Cross-correlation peak time, pitch	3.56	8	70	0.036	*	0.29
	Cross-correlation peak time, yaw-roll	13.37	8	70	<0.001	***	0.6
	DTW distance, roll	9.66	8	70	<0.001	***	0.52
	DTW distance, yaw	9.24	8	70	<0.001	***	0.51
Phase:Control	Mean Speed torso, pitch	5.99	4	35	0.012	*	0.15
	Mean Speed torso, yaw	5.29	4	35	0.021	*	0.13
	Max Speed torso, pitch	5.94	4	35	0.017	*	0.15
	Torso Speed norm, mean	4.75	4	35	0.029	*	0.12
	Torso Speed norm, max	4.72	4	35	0.037	*	0.12
	Head-torso correlation roll	4.38	4	35	0.037	*	0.11
	AI, pitch-pitch	4.68	4	35	0.031	*	0.12
Age:Phase:Control	Mean Speed torso, pitch	3.61	8	70	0.005	**	0.29
	Torso Speed norm, mean	3.32	8	70	0.009	**	0.27

Table 4.2 – Variables selected after PCA on all trials, with significant effect of Control, or interactions of Control with Age and Phase

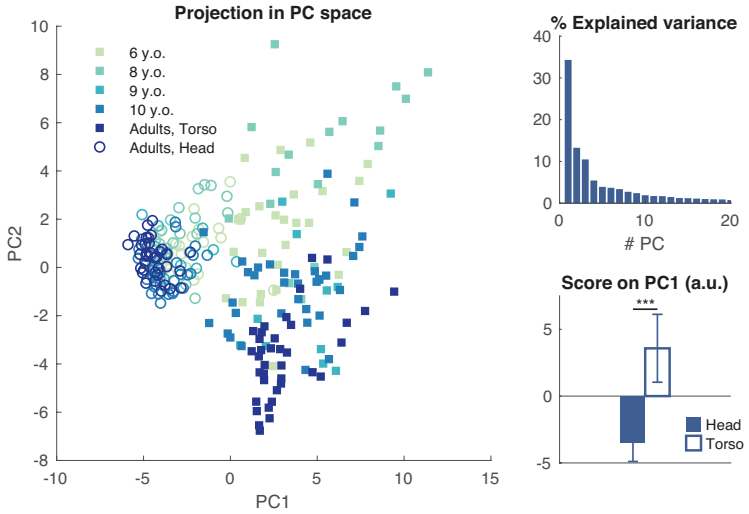

Figure 4.7 – Principal component analysis of all trials. Left: projection of the original data onto the space defined by the first two PCs. Circles represent head-controlled trials, full squares torso-controlled trials. Right, top: proportion of variance explained by each PC. Right, bottom: projected value on PC1, by controlling body part (bars indicate mean+standard deviation)

Efficient head-torso coordination develops with age

To extract the specific variability inherent to the torso steering, we repeated the procedure described above using only the data from the corresponding trials.

On this partial dataset, PCA revealed an age-based separation in the space spanned by the first two PCs, accounting respectively for 25.91% and 19.38% of the total variance (see Figure 4.10). Individually, both PC1 and PC2 showed a decreasing trend with age.

Considering the kinematic variables with normalized loadings on the first two PCs larger than 0.75 yielded five functional clusters (see Figure 4.11): Cluster 1 (PC1) and Cluster 2 (PC2) holding variables describing the torso movements, Cluster 2 (PC1) corresponding to head movements, Cluster 1 (PC1) characterizing head-torso correlation and finally Cluster 3 (PC2) containing only the error.

The effects of Age and the interaction of Age with Phase on the identified variables was assessed by repeated measures ANOVAs. The results of this analysis are displayed in Table 4.3, and Figure 4.12 shows 8 representative variables by age and experimental phase.

Torso involvement in head-controlled trials decreases with age

Eventually, we reiterated the same analytic process with the data corresponding to the head-controlled trials. The PCA revealed a soft age-based separation along the first principal

Effect	Variable	F	DOF1	DOF2	*p*		η_p^2
Age	Error	6.92	4	35	0.003	**	0.44
	Head Amplitude, pitch	6.32	4	35	0.004	**	0.42
	Head Amplitude, roll	5.92	4	35	0.004	**	0.4
	Torso Amplitude, roll	3.12	4	35	0.041	*	0.26
	Torso Amplitude, pitch	6.94	4	35	0.003	**	0.44
	Torso Amplitude, yaw	3.67	4	35	0.027	*	0.3
	Mean Speed Torso, roll	1.53	4	35	0.226		0.15
	Mean Speed Torso, pitch	3.31	4	35	0.037	*	0.27
	Mean Speed Torso, yaw	3.05	4	35	0.041	*	0.26
	Max Speed Torso, roll	0.75	4	35	0.563		0.08
	Max Speed Torso, pitch	3.29	4	35	0.037	*	0.27
	Max Speed Torso, yaw	4.15	4	35	0.016	*	0.32
	Torso Speed norm,mean	2.32	4	35	0.088		0.21
	Torso Speed norm,max	2.87	4	35	0.048	*	0.25
	Head-torso correlation, roll-roll	4.56	4	35	0.01	*	0.34
	Cross-correlation peak time, yaw-roll	9.57	4	35	<0.001	***	0.52
	DTW distance, roll-roll	5.7	4	35	0.005	**	0.39
	DTW distance, yaw-yaw	6.89	4	35	0.003	**	0.44
Age:Phase	Error	4.51	8	70	0.007	**	0.29
	Head Amplitude, pitch	3.45	8	70	0.007	**	0.1
	Head Amplitude, roll	3.81	8	70	0.005	**	0.11
	Torso Amplitude, roll	2.62	8	70	0.036	*	0
	Torso Amplitude, pitch	3.27	8	70	0.01	**	0.14
	Torso Amplitude, yaw	2.44	8	70	0.041	*	0.1
	Mean Speed torso, roll	3.27	8	70	0.01	*	0.02
	Mean Speed torso, pitch	4	8	70	0.004	**	0.19
	Mean Speed torso, yaw	3.36	8	70	0.009	**	0.21
	Max Speed torso, roll	2.51	8	70	0.038	*	0
	Max Speed torso, pitch	1.93	8	70	0.087		0.14
	Max Speed torso, yaw	2.29	8	70	0.045	*	0.14
	Torso Speed norm,mean	4.17	8	70	0.003	**	0.17
	Torso Speed norm,max	1.97	8	70	0.085		0.11
	Head-torso correlation, roll-roll	1.81	8	70	0.105		0.12
	Cross-correlation peak time, yaw-roll	2.38	8	70	0.041	*	0.07
	DTW distance, roll-roll	1.92	8	70	0.088		0.14
	DTW distance, yaw-yaw	1.3	8	70	0.263		0.11

Table 4.3 – Variables selected after PCA on torso-controlled trials, with significant effect of Age, or interactions of Age with Phase

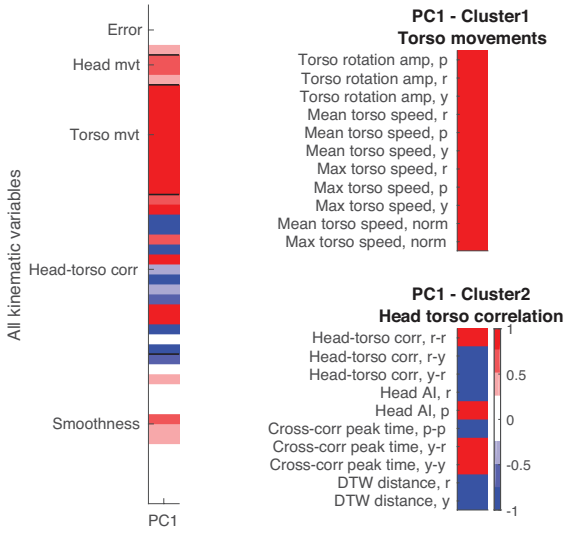

Figure 4.8 – Variable loadings (all trials). Left: Loadings of all kinematic variables on the first PC. Right: functional clusters of variables with loadings > 0.75

component, accounting for 25% of the total variance (see Figure 4.13). Clustering the variables with normalized loadings larger than 0.75 yielded one single cluster describing the movements of the torso.

We conducted repeated measures ANOVAs to identify the selected variables on which Age and the Age:Phase interaction had a significant effect; the results are summarized in Table 4.4. Figure 4.15 displays 4 representative variables by age and experimental phase.

Cluster separability exposed different patterns between head- and torso-controlled trials

The pairwise DBI confirmed the similarity of 6 and 8 year-olds in the head-controlled trials (DBI = 10.39) and reveals that the separability gradually increases with age from 9 years onwards. This analysis also reveals a persisting difference between 10 year-olds and adults. A different pattern is observed for the torso-controlled trials, where all the age groups appear to be well separable. Only 9 and 10 year-olds share higher similarities (DBI = 4.61).

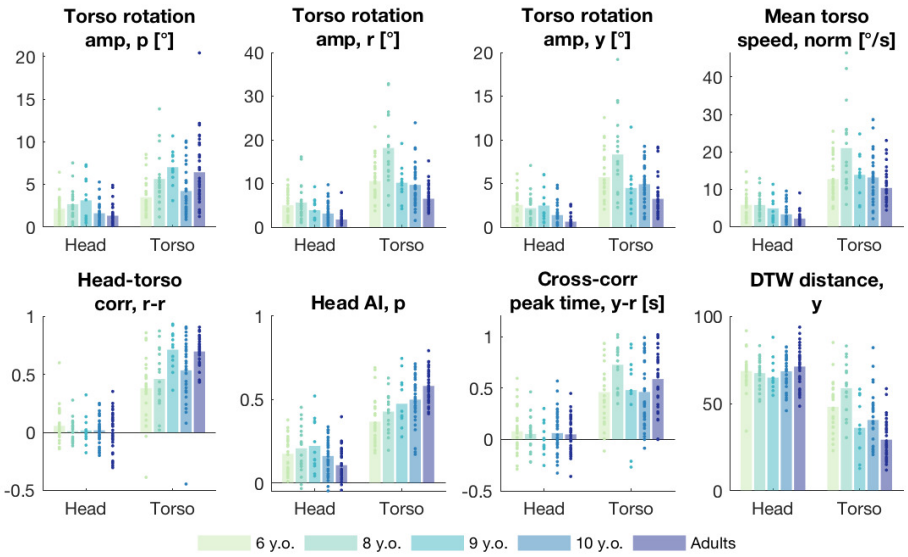

Figure 4.9 – Representative kinematic variables (all trials), showing a significant effect of control type or control:age interaction

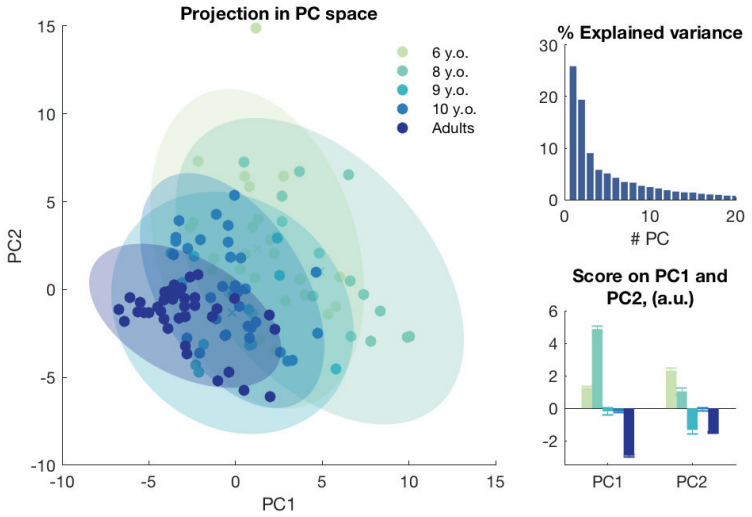

Figure 4.10 – Principal component analysis of torso-controlled trials. Left: projection of the original data onto the space defined by the first two PCs. Right, top: proportion of variance explained by each PC. Right, bottom: projected value on the first two PCs, by age and experimental phase (bars indicate mean+standard error of the mean)

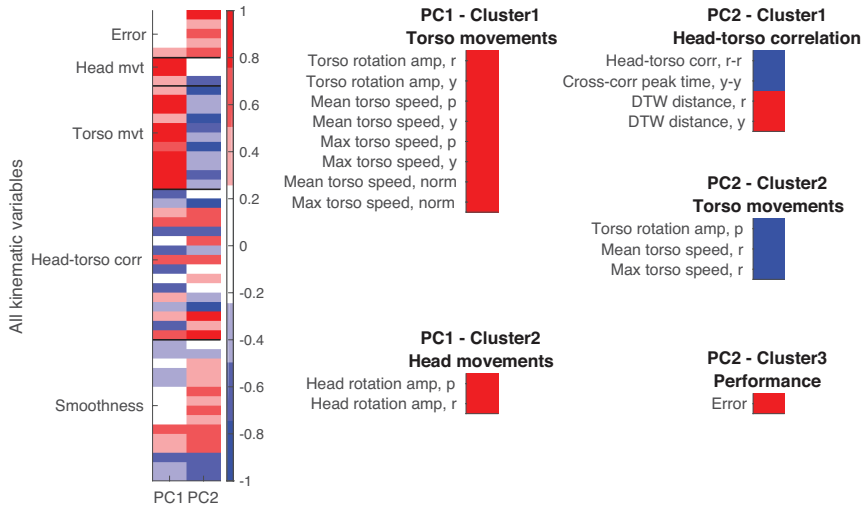

Figure 4.11 – Variable loadings (torso-controlled trials). Left: Loadings of all kinematic variables on the first PC. Right: functional clusters of variables with loadings > 0.75

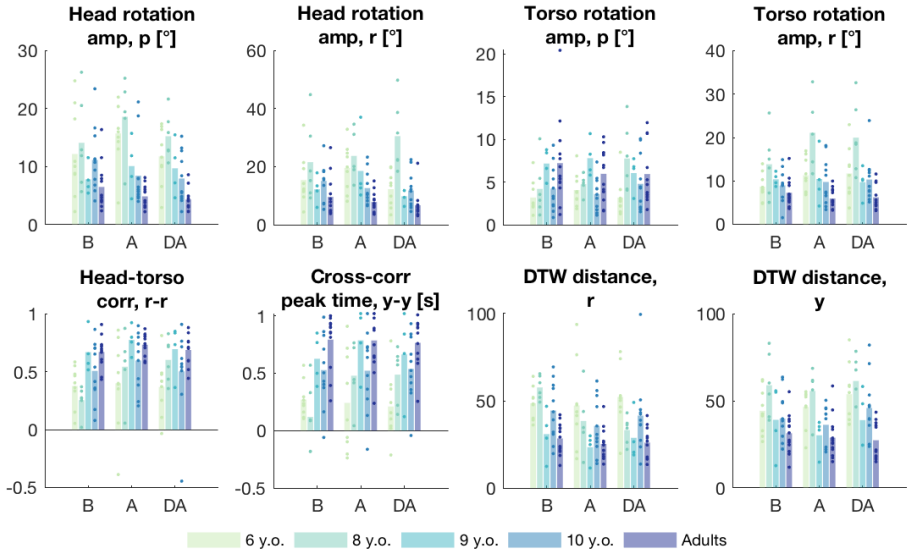

Figure 4.12 – Representative kinematic variables (torso-controlled trials), showing a significant effect of experimental phase or phase:age interaction

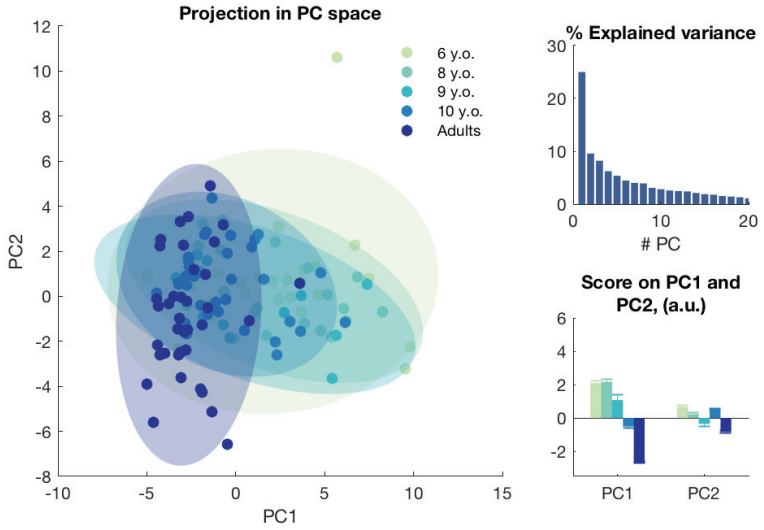

Figure 4.13 – Principal component analysis of head-controlled trials. Left: projection of the original data onto the space defined by the first two PCs. Right, top: proportion of variance explained by each PC. Right, bottom: projected value on the first PC, by age and experimental phase (bars indicate mean+standard error of the mean)

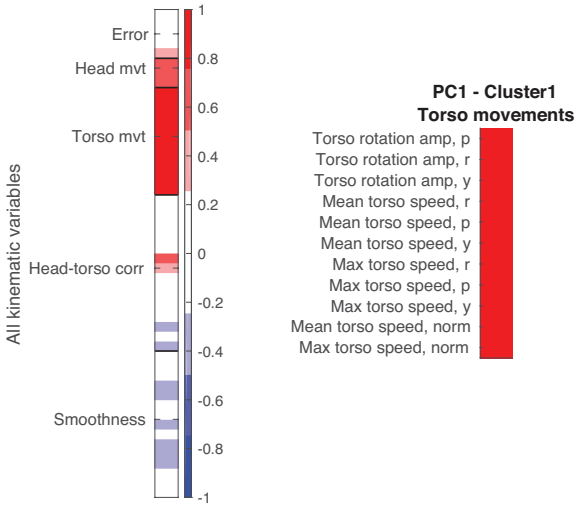

Figure 4.14 – Variable loadings (head-controlled trials). Left: Loadings of all kinematic variables on the first PC. Right: functional clusters of variables with loadings > 0.75

Effect	Variable	F	DOF1	DOF2	p		η_p^2
Age	Torso Amplitude, roll	1.98	4	35	0.13		0.18
	Torso Amplitude, pitch	4.09	4	35	0.016	*	0.31
	Torso Amplitude, yaw	4.3	4	35	0.015	*	0.32
	Mean Speed torso, roll	2.42	4	35	0.076		0.21
	Mean Speed torso, pitch	4.25	4	35	0.015	*	0.31
	Mean Speed torso, yaw	4.31	4	35	0.015	*	0.32
	Max Speed torso, roll	2.55	4	35	0.068		0.22
	Max Speed torso, pitch	4.45	4	35	0.015	*	0.32
	Max Speed torso, yaw	4.81	4	35	0.015	*	0.34
	Torso Speed norm, mean	3.99	4	35	0.016	*	0.3
	Torso Speed norm, max	4.34	4	35	0.015	*	0.32
Age:Phase	Torso Amplitude, roll	2.78	8	70	0.018	*	0.05
	Torso Amplitude, pitch	2.6	8	70	0.038	*	0.04
	Torso Amplitude, yaw	3.04	8	70	0.016	*	0.01
	Mean Speed torso, roll	3.21	8	70	0.015	*	0.11
	Mean Speed torso, pitch	2.92	8	70	0.021	*	0.07
	Mean Speed torso, yaw	3.26	8	70	0.015	*	0.11
	Max Speed torso, roll	2.29	8	70	0.054		0.12
	Max Speed torso, pitch	1.04	8	70	0.41		0.04
	Max Speed torso, yaw	2.7	8	70	0.02	*	0.1
	Torso Speed norm, mean	3.34	8	70	0.015	*	0.09
	Torso Speed norm, max	1.23	8	70	0.316		0.05

Table 4.4 – Variables selected after PCA on head-controlled trials, with significant effect of Age, or interactions of Age with Phase

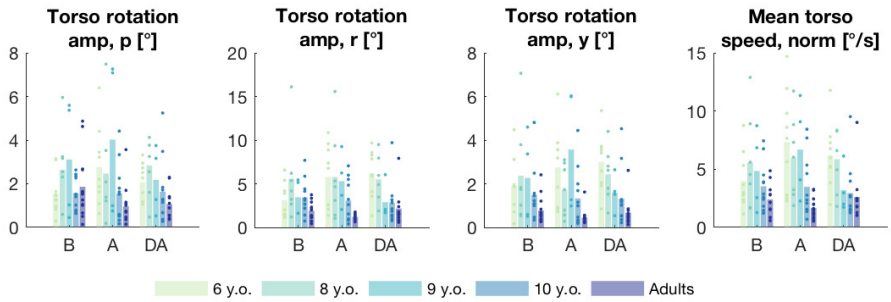

Figure 4.15 – Representative kinematic variables (head-controlled trials), showing a significant effect of experimental phase or phase:age interaction

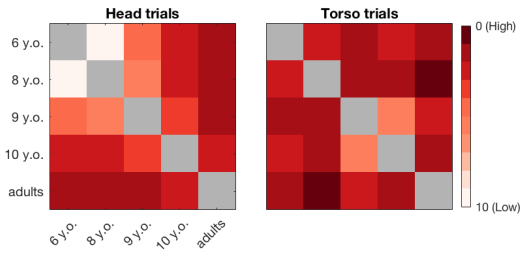

Figure 4.16 – Pairwise separability of the age-defined clusters assessed by the Davies-Bouldin index. Dark values indicate better separability

Discussion

We evaluated the ability of children aged 6-10 and young adults to perform an immersive piloting task in VR, using either their head or their torso as controlling body part. All the participants were able to steer the simulator using their head. However, the 6 year-olds showed significantly lower performances than the 10 year-olds and the adults, and this difference was even after practicing the task. On the contrary, 6 and 8 year-olds initially struggled to use the torso to control the simulator, but substantially improved their performance with training. Yet, their average error in the navigation task remained significantly higher than the 10 year-olds' and the adults'. Overall, the 6 year-olds performed worse with the torso than with the head. This difference also appeared when comparing the initial evaluations of the 8 year-olds. Kinematically, the major distinction between the head- and torso-controlled trials could be explained by variations in the movements of the torso, but also by modulations of the head-torso coordination. Age-related differences in the torso-controlled trials were attributable to a combination of variables describing head and torso movements, as well as the coordination of these segments. Conversely, the age-associated variation among the head-controlled trials could be explained by variables describing the torso kinematics.

Even though younger children performed significantly worse than 10 year-olds and adults, their scores in the head-controlled trials reached a range comparable with the results from other age groups, revealing that, in a simplified experimental environment, children as young as 6 are able to understand and perform an immersive virtual navigation task. This suggests that HMD-induced optical flow induces vection in young children in a way similar to adults, expanding results obtained with visual stimuli presented on screens [204, 205, 206]. The ability to navigate in a 3D environment also requires a sufficiently developed spatial perception. While 6 year-olds have been shown to perceive planar spaces similarly to adults [207], the visual integration of 3D spaces begins to develop at 6 years [208] and continues to mature until early adolescence [209]. The different developmental time courses for the head- and torso-based control of the simulator were confirmed when we evaluated the separability of the age-defined clusters. We observed a high similarity between 6 and 8 year-olds in the head-controlled trials, which decreased later on, which corroborates the pivotal changes occurring from 8 years onwards. Interestingly, this analysis also highlights a persisting difference between 10 year-olds and adults, which may be explained by the tight spread of the adult data along the first PC (low inter-cluster distance). Conversely, in the torso-controlled trials, all the clusters were highly separable, suggesting that the maturation of the underlying coordination processes happens over a longer time period.

When comparing the steering performance across sessions, we found that only 6 and 8 year-olds improved their skills in the torso-controlled trials, and that the improvement persisted

overnight. Yet, 6 year-olds performed significantly better using their head than their torso in all phases. 10 year-olds outdid 6 year-olds in the evaluations before training and on the second day when using the torso, and on the second day when using the head. Likewise, the adult group showed lower errors than the 6 year-olds at all phases when using the torso, and in the evaluations after training and on the second day when using the head. These differences were observed in 8 year-olds in the initial evaluations when comparing the head- and torso-controlled trials and with respect to 10 year-olds and adults in the torso-controlled trials. These results also reveal that the ability to steer the simulator is already mature at the age of 8, but only starts to evolve towards adult levels at this age. The earlier maturation of the head control is not surprising, as the joint control of vision and steering direction yields a task with lower complexity.

The kinematic analysis of the head-controlled trials showed that the major age-related difference could be attributed to differences in the torso movements, with rotation amplitudes, and mean and maximum rotation velocities decreasing with age. The ability to decouple head from torso movements thus develops along childhood, confirming previous results obtained during obstacle avoidance during locomotion [173, 159], where adults display anticipatory head movements [210]. However, mature coordination patterns appear later with our experimental setup when compared to simple locomotion. This is in line with observations revealing that developing children tend to increase their head-body stiffness with increasing task difficulty [167]. In our case, the increased difficulty can be imputed to the use of immersive VR, which provides altered visual information and requires higher cognitive processing abilities to appropriately interpret the displayed VE [86, 87].

In the torso-controlled trials, the age-related differences were explained by kinematic variations of both body segments and in their coordination. In general, movement amplitudes decreased with age. The higher head movement amplitudes in younger children reveal that these age groups had the tendency to erroneously involve this body part to control the simulator. Smaller amplitudes of the torso movements suggest an increase in torso positioning accuracy with age, as previously demonstrated [160]. Interestingly, the amplitude of the torso movements in the pitch plane uniquely increased with age, suggesting that younger children had more difficulties to properly engage their bodies for up- and downward movements of the simulator. Yet, larger torso movements may also be the result of larger deviations from the path to follow and not a consequence thereof: indeed, while the coins were placed on a trajectory necessitating only small directional changes, correcting one's direction from further distances required maneuvers of larger amplitude. More importantly, the differences in head-torso coordination indicate that adults and older children favorably selected an "en-block" strategy, with a stiff intersegmental link. This comes in opposition with previous studies, where such a behavior was preferentially observed in younger children [173, 159]. One study found a

similar behavior in adults, who displayed a head-to-torso stabilization in dimensions in which independent head were not beneficial [172]. This is concomitant with our results, as head movements in the torso-controlled trials tended to disturb the participants' spatial orientation. Younger children instead failed to use this simpler coordination pattern, suggesting that the increased difficulty provided by the VR setup prevented them from selecting the most adequate coordination strategy, thus corroborating the model of postural development as a two-step process in which children first acquire a repertoire of postural strategies and later on learn how and when to select the appropriate strategy [159].

Limitations of the study

The results of this study should be interpreted taking in consideration the unequal group sizes, particularly the small number of 9 year-old participants. The robust behavioral differences we found between 6 and 10 year-olds suggest the occurrence of developmental changes between this ages, for which we could not find any statistical evidence here. Likewise, the small proportion of female subjects did not allow us to evaluate any gender-associated effects, which have been previously observed for example in task execution [211, 174] and in the development of functional networks [212].

Other aspects to consider come from the design of the task and the virtual environment itself. First, in our experimental protocol, the participants were directly asked to steer the flight simulator along the path defined by the coins, without having some time to freely experience the dynamics and the sensitivity of the system. Having to focus simultaneously on the task and on the mapping of one's movements to the actions of the simulator likely let to an initially high cognitive load and delayed the appropriation of the control strategy. In sensitive participants, this initial period tended to induce some first symptoms of VR sickness. In addition, young children happened to be discouraged by this early hurdle, leading some of them to interrupt the experiment. Second, the gamification of the steering task which rewarded the successful collection of a coin by a tinkling sound and points added to a global score appeared to encourage the participants to aim at each coin individually, rather than to follow a smooth, long-ranging trajectory. This again increased the difficulty of the task, by requiring a multitude of small and rapid adjusting movements. Another issue resided in the continuous character of the task, particularly for the participants showing difficulties to remain close to the displayed path. While steering the simulator along the path required only maneuvers of small amplitude and a rudimentary understanding of the surroundings, returning to the trajectory after deviating thereof necessitated both a higher steering precision and a stronger spatial cognition. Validating a given waypoint with a large error therefore negatively influenced the possible score on the following ones, thus doubly penalizing less skilled participants. Finally, preventing the participants from adapting the speed may have

induced some variability in the level of perceived difficulty, particularly for younger children, who have been shown to experience stronger vection than adults in response to backward optical flows [204]. The consistency of this parameter does however allow a more formal comparison of the task execution performance across subjects.

Conclusion

We showed that young children are able to understand a body-machine interface to interact with immersive VR, but that 6 year-olds fail to successfully use such a system when a decoupling of vision and steering commands is required. In particular, the stronger reliance on vision than on vestibular or proprioceptive inputs may have prevented younger children from selecting the most efficient head-torso coordination strategy. The results of this study highlight the importance of the end user's abilities for successful interactions with VEs, and should be considered when designing HMIs for populations including children and/or patients with neuromotor conditions.

5 Development of visual-body coordination and perception of the straight-ahead direction

Abstract

The integration of visual information with head and trunk movements is essential to interact with the surrounding environment, and develops along childhood. The subjective straight-ahead (SSA), that is the perception of the antero-posterior orientation of the body, could be used as a common reference to calibrate this integration. Using an immersive virtual reality scenario, we investigated the use of the SSA as a spatial reference, the development of the vision-head-trunk integration during childhood, and the impact of motor coordination maturation on these aspects. We found that in 6 year-olds, the head is a necessary intermediate for the integration of vision with trunk movements. Instead, 10-11 year olds showed mature behavior in terms of multisensory integration and head-trunk coordination. These results expose a possible role of the SSA in the calibration of the vision-head-trunk integration during childhood and its age related development.

The contents of this chapter are part of the publication in preparation:

Get Out of the Body! Virtual Reality Displays Link Between Visual-Body Coordination and Egocentric Reference Developments
Esposito D., Miehlbradt J., Tonelli A., Mazzoni A., Gori M.,in preparation

Contributions as second author: design of the experiments, data collection, revision of the analysis and manuscript.

5.1 Methods

Experimental setup

Using the game engine Unity3D, we designed a VE representing an archery field, in which an arrow had to be guided towards a target by planar (yaw) rotations of the head or the trunk. The participants were immersed in the VE through a HMD (Oculus Rift. Targets appeared at a distance of 60 m from the starting position at three different positions: straight ahead and with lateral deviations of ± 30° (Figure 5.1, panels A and B). The participants' torso movements were acquired using an IMU (X-sens) maintained in their back by a custom harness and their head rotations were measured by the IMU embedded in the HMD (Figure 4.2). To reduce the risk of losing balance, the participants were seated on a chair which allowed the upper body to move freely.

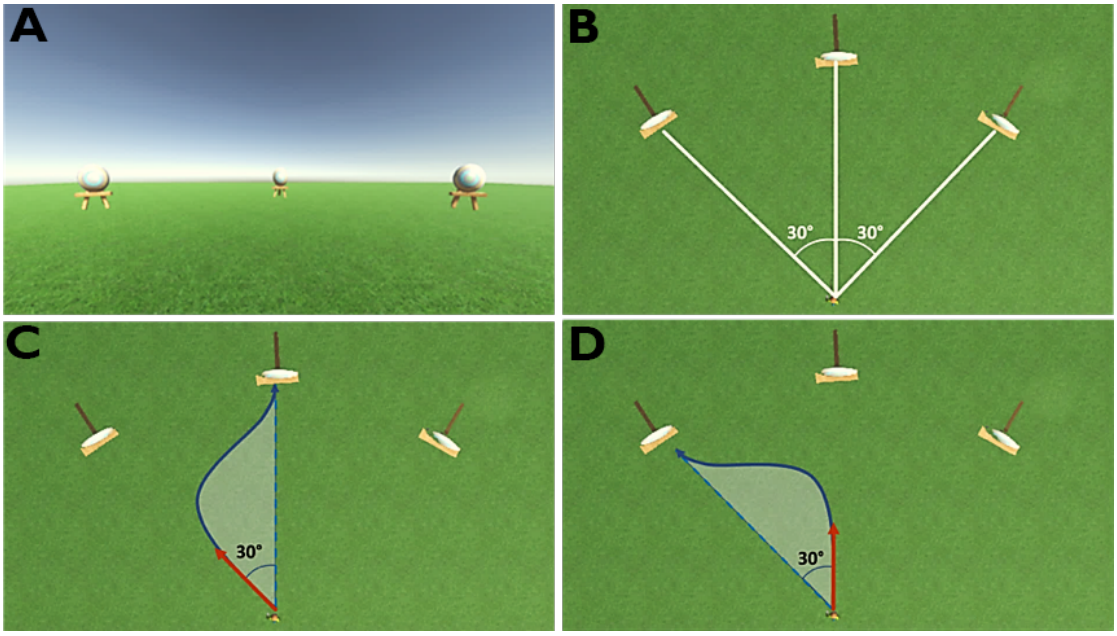

Figure 5.1 – Virtual environment for the archer game. A,B position of the targets, C trajectory for a *central* trial, D trajectory for a *lateral* trial

Experimental conditions and protocol

We implemented eight different experimental conditions, corresponding to the combinations of three 2-level factors:

- **Control** designates the body part used to guide the arrow, that is either the *head* or the *torso*. When the head was the guiding segment, it controlled both the vision and the direction of the arrow. Instead, in the trunk-controlled condition, the visual field was

moved according to the sum of the head and trunk rotation angles, while the arrow was guided only by the torso.

- **Direction** describes the position of the target and could take the value of *central* or straight ahead of the participant or *lateral*, meaning at 30° left- or rightwards away from the straight-ahead direction (see Figure 5.1, panels C and D);
- **Coordination** refers to the constraints put on the non-controlling body part: in the *free* condition, the angle of the arrow is equal to the angle of the controlling part and the movements of the non-controlling part have no influence. Instead, in the *conflict* condition, the orientation of the arrow is defined by the relative angle between the controlling and non-controlling body parts: $\theta_{arrow} = \theta_{controlling} - \theta_{non-controlling}$. In this case, the participants thus had to keep the non-controlling body part still.

The participants initialized the trial by aligning the controlling body part to the center for *lateral* trials or to the indicated lateral target during *central* trials. The conditions were tested in random order, and eight repetitions were performed blockwise for each condition. Before each block, the experimenter described the upcoming condition to the participant.

Participants

We recruited eleven 6 year-old children (5 females), twelve 10-11 year-old children (3 females, age = 10.1±0.8 years), and ten adults (5 women, age = 32.2±1.1 years). Informed consent was obtained from the adult participants and from the parents of the underage participants. The study was approved by the local ethics committee.

Analysis

We computed two metrics to describe the participants' task performance:

- The **score** is a value between 0 and 100, proportional to the distance to the center of the target and is computed as:

$$\text{score} = 100 \cdot \max\left(0, 1 - \frac{\text{distance to center}}{\text{target radius}}\right) \tag{5.1}$$

- The **sum of distances** is the sum of the frame-by-frame deviations from the straight path and is computed as the dot product between the position of the arrow and the position of the target:

$$\text{sum of distances} = \sum_i \overrightarrow{\text{arrow position}_i} \cdot \overrightarrow{\text{target position}} \tag{5.2}$$

The data from each condition were averaged and subjected to repeated measures ANOVA, with Age as between-subjects factor, and Control, Direction and Coordination as within-subjects factors. The Greenhouse-Geisser correction was applied, due to violations of the data sphericity. Post hoc analyses were computed using Tukey's HSD test.

5.2 Results

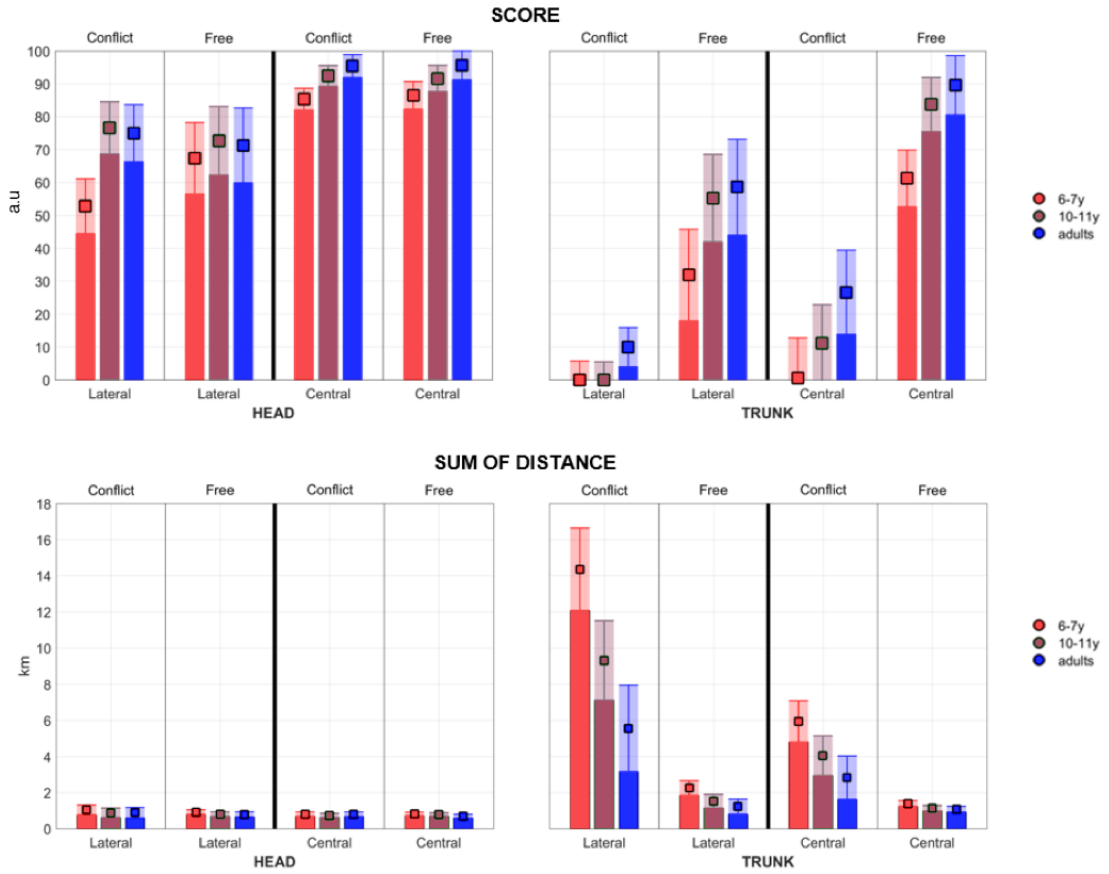

Figure 5.2 – Score (top) and sum of distances (bottom), grouped by controlling body segment and target direction.

Score

The repeated measures ANOVA revealed that all the main effects and the four-way interaction were significant for the score (see Table 5.1).

The overall differences due to age were significant between 6 and 10-11 year-olds ($p < 0.001$) and between 6 year-olds and adults ($p < 0.001$), with the younger children displaying lower scores in both cases.

Effect	Df	*F* value	*p* value	
Age	2,33	17.86	< 0.001	***
Control	1,33	562.54	< 0.001	***
Direction	1,33	256.19	< 0.001	***
Coordination	1,33	213.30	< 0.001	***
Age:Control:Direction:Coordination	2,33	3.62	0.04	*

Table 5.1 – ANOVA table for the score. * p < 0.05, ** p < 0.01, *** p < 0.001

The post hoc analysis of the effect age on the experimental conditions revealed a significant effect for all conditions except when the head was guiding towards lateral targets, freely from the trunk (see Table 5.2).

Condition	Age group 1	Age group 2	*p* value	
Trunk, central, free	6	10-11	0.002	**
Trunk, lateral, free	6	10-11	0.048	*
Head, central, conflict	6	10-11	0.010	**
Head, lateral, conflict	6	10-11	0.001	***
Trunk, central, conflict	6	Adults	0.014	*
Head, central, free	6	Adults	0.012	*
Trunk, lateral, conflict	10	Adults	0.046	*

Table 5.2 – Significant post hoc tests for the score, assessing the effect of age on the experimental conditions. Age group 1 indicates the group for which the score was lower. * p < 0.05, ** p < 0.01, *** p < 0.001

Sum of distances

The repeated measures ANOVA revealed that all the main effects and the four-way interaction were significant for the sum of distances (see Table 5.3).

Effect	Df	*F* value	*p* value	
Age	2,33	19.21	< 0.001	***
Control	1,33	231.13	< 0.001	***
Direction	1,33	142.43	< 0.001	***
Coordination	1,33	167.13	< 0.001	***
Age:Control:Direction:Coordination	2,33	5.08	0.013	*

Table 5.3 – ANOVA table for the sum of distances. * p < 0.05, ** p < 0.01, *** p < 0.001

The sum of distances were significantly higher for 6 than 10-11 year-olds (p = 0.001) and for 6 year-olds when compared to adults (p < 0.001).

The post hoc analysis on the sum of distances revealed significant effects of age for all the conditions in which the trunk was the guiding segment. None of the conditions involving the head were significant (see Table 5.4).

Condition	Age group 1	Age group 2	*p* value	
Trunk, lateral, free	6	10-11	0.020	*
Trunk, lateral, conflict	6	10-11	0.008	**
Trunk, central, free	6	Adults	0.022	*
Trunk, central, conflict	6	Adults	0.002	*

Table 5.4 – Significant post hoc tests for the sum of distances, assessing the effect of age on the experimental conditions. Age group 1 indicates the group for which the sum of distances was higher. * $p < 0.05$, ** $p < 0.01$, *** $p < 0.001$

5.3 Discussion

The overall difference between 6 year-olds and the older age groups, both on the score and the sum of distances reveals that visuomotor integration is immature at this age. No significant difference was observed between 10 year-olds and the other two age groups, but visual observations suggest a continuous developmental trend of these abilities. These outcomes are coherent with previous works on head-trunk coordination [173], and multisensory integration [98, 97].

The simplest experimental condition appeared to use the head as control segment, when guiding the arrow towards lateral targets, and without conflict, as in this case, the younger children showed no difference with the older age groups. The visuomotor integration involved only two agents (vision and head movement), and possible proprioceptive noise at the torso level had no impact on the task execution. This suggests a certain level of maturation of the visuomotor integration at the age of 6, which is however not robust to more complex situations. This also confirms the ability of our younger participants to adequately perceive the VE. Adding the coordination constraint between the head and the trunk led to differences in the score between 6 and 10-11 year-olds, which can be imputed to immature coordination patterns in the younger children [159] or higher proprioceptive noise at the torso level [160]. These differences were however not observed in the sum of distances, confirming that the maturation of gross motor control of the head is acquired at the age of 6 [161].

Conversely, when the trunk was used as controlling segment, 6 year-olds performed worse than older children or adults both in terms of score and of the sum of distances. As in the head-controlled trials, the condition showing the earliest development involved lateral targets and no conflict on the trunk movements, where 10-11 year-olds and adults displayed similar results by both metrics. When aiming at central targets, adult-level scores were reached at

10 years, but the sum of distances appeared to further improve during adolescence. Lastly, constraining the head affected both children groups, revealing that the adult-like patterns observed under other conditions are not yet robust to such a level of difficulty at 10-11 years. This corroborates previous results showing that refinement of motor control prevails until adolescence [173].

The overall effect of direction on the score and the sum of distances highlights the importance of the SSA for in the encoding of spatial information. The lower performance observed in younger children suggests however, that the precision of the SSA is not yet mature in early childhood and acquires robustness with age[213].

Conclusion

These results confirm a descending development of postural coordination, with an increase in interjoint modularity. Likewise, while younger children extensively rely on the head for visuomotor integration of trunk movements, 10 year-old children and adults display the ability to bypass this intermediate information. In addition, we highlighted the role of the SSA for spatial orientation, and showed that its precision and robustness also develops with age. Finally, 10-11 year-old children generally display adult like coordination and multisensory integration, but these patterns are not robust under the most complex condition, confirming a refinement in gross motor control until adolescence.

6 Conclusion and outlook

6.1 Summary

Virtual reality is a powerful and versatile tool which allows to create realistic perceptions of computer-simulated environments. The last decade saw a tremendous increase in the development of dedicated hardware, which in turn led to a multitude of applications in very diverse domains. Some of these implementations may influence the daily life of the users directly, as is the case for VR-based treatment of phobias, or indirectly as for flight or surgery training simulators. VR has also proven to be a valuable tool for research, providing advances in neuroscience on aspects including somatosensory processing or sensorimotor integration [214] and social phenomena such as interpersonal interactions [215].

The potential benefits which could arise form well-designed VR scenarios motivate the quest for smooth and flawless interactions. However, while the hardware to display such environments and provide the immersion is robust and easily available, the development of user-centered interaction interfaces is often left aside, favoring pre-existing devices. In addition, individual mental or physical abilities of VR users also contribute to the quality of the interaction with the virtual system. Yet, except for a small number of studies, the effect of a parameter as important as age on the ability to interact with a VE has rarely been studied [194, 83].

This thesis addressed two aspects, central for the successful interactions with VEs: the design of user-centered, application-specific interfaces and the age-related development of the sensorimotor patterns enabling these interactions.

Chapter 2 presents a systematic methodology to design a BoMI for the non-homologous control of a virtual drone, and by extension the teleoperation of a real quadcopter. We surveyed the kinematic and muscular patterns displayed by participants without previous experience

during simulated interactions with a virtual drone, using self-selected upper-body gestures. A clustering analysis revealed the existence of two major, common gestural patterns, within which we could identify discrete maneuvers using only the (relative) angles of the involved body segments. In **Chapter 3**, these two sets of gestures were implemented as control strategies first for a virtual drone and later on also for a real drone. We observed that the strategy using solely movements of the torso led to better steering performances in a waypoint navigation task than a joystick commonly used in this kind of applications, and that within 3 days of short practice, all the participants were able to master this interface. Conversely, in the group using the joystick, about half of the participants displayed only minimal improvement across sessions. The second strategy, which involved arm movements and trunk movements led to scores comparable to the joystick. This demonstrated the superiority of a user-centered, gestural approach for non-homologous interactions with virtual systems.

In **Chapter 4**, we evaluated the ability of young children to control an adapted version of the immersive flight simulator, when piloting with the trunk or with the head. We found that the selection of the appropriate head-trunk coordination strategy was not mature until the age of 8. Finally, **Chapter 5** used an alternate VE to expose the developmental pattern of visuomotor integration along the head-trunk axis and revealed that important maturation steps occur between the ages of 6 and 10, and continue to refine towards adolescence.

6.2 General discussion

The BoMI proposed in Part I despite being very simple, has proved to surpass the performances obtained with a well-known third-party device. There is however room for further improvements and developments, which can be organized around different axes. First, the current implementation only provides control over two DOF, the pitch and the roll. Controlling the velocity is an absolute necessity, both to provide adaptability to different environments or surroundings, and to accommodate personal preferences of the users. In the case of a fixed-wing drone, the yaw cannot be independently controlled, thus eliminating the need to implement additional directional command. However, should the BoMI be applied to the control of a quadcopter, a UAV with more DOF, several other maneuvers would be of interest including hovering and lateral displacements. Likewise, automated commands for takeoff and landing are required.

Moreover, in the implementation described in this work, the translation of the pilot's gesture into steering commands relies on basic linear transformations, in which the gains have been kept constant across participants. Yet this model is far from optimal, as demonstrated by previous studies, which relied on the non-linear distribution of directional reaching errors in the space surrounding the body to define a new, intuitive mapping [158]. The linear

approximation we used in our model was be suited for the application in which it was tested, presumably because the control of the simulator only required small-amplitude movements, centered around the neutral starting position. Conversely, modifications of the setup which would require larger movements may reveal the limits of the linear mapping.

The selection of the gestural strategies for the particular case of FPV flying has been done based on a screening study carried out in young healthy adults. It may be that different patterns would emerge if this study was repeated on a different demographic group. In particular, the young children who were asked to use the simulator may have spontaneously selected a different set of gestures. More interestingly, evaluating the distribution of precision errors in the space surrounding a body would not only provide the bases for a better adapted interaction interface for this age group, but also provide an insight onto the development of the spatial representation of this space.

Indeed, postural and coordination patterns have been shown to develop beyond childhood [173], a claim which is supported by evidence for maturation of the central nervous system until early adulthood both at the structural and functional level[216, 217, 163].

Another aspect worth investigating relies in the previous experience of the tested population or the expected final users of such a system. Even in the case of low-complexity control movements associated with a low cognitive load, intrinsic factors may affect the ability of any individual to learn and master a BoMI similar to the ones presented in this work. In particular, recent studies have shown that the regular playing of action video games provided substantial advantages in learning, including novel sensorimotor tasks [16, 17]. Thus far, it is unknown whether action video gaming affects the accuracy of the body scheme, and to which extent regular players may display a faster improvement in learning how to use such a BoMI.

6.3 Outlook

The results presented in this thesis have potential implications for several VR-related domains.

Firstly, the methodology developed in Chapter 2 to identify gestural interaction strategies and a suitable set of sensors to acquire the discriminant information is adaptable to any situation in which an object, real or simulated has to be controlled efficiently and intuitively. The application of this method could thus bring an evolution to the device-centered field of VR interfaces. Similarly, applying this method at the level of the individual, starting either from a global working solution or from a blank page could allow the design of individualized interfaces.

Moreover, the BoMi we developed allowed untrained users to master the control of a virtual

drone after a short period of training and these ability translated to the steering of a real quadcopter. Nowadays, drones are increasingly used to acquire rapid visual mappings over inaccessible scenes, but this service is too often delayed because no experienced drone pilot is available. Reducing the training time would enable any person present on such a scene to rapidly take over the drone-aided mapping, which could in turn save some precious time during rescue missions.

Next,we demonstrated that children aged 6 and above are able to perceive an adapted immersive VE, if not as adults, at sufficiently mature level to execute adequate interactions. Therefore, VR can be considered as a suitable tool to investigate the age-related development of visuomotor function and other aspects of multisensory integration during childhood, or as a therapeutic means.

Nonetheless, our results highlight the importance of considering the perception which will be experienced by the end users of a particular implementation. This is particularly crucial when these end users significantly differ from the developing team, as is the case for children or neurological patients. The risk is otherwise to develop systems which will fail to achieve their (therapeutic) goals.

To conclude, this work demonstrated the benefits of closely investigating user-related effects on VR experiences We showed that a data-driven interface significantly outperforms an existing controlling device, even though it is considered as the standard approach and well-mastered by experienced users. We also showed that children may perceive VEs similarly to adults, but lack the functional sensorimotor coordination to properly interact with these systems. These results can serve as a base for good practice guidelines for the development of new VR applications.

A Descriptive kinematic variables

	Variable description	**Group**
1.	Distance to coin center [m]	
2.	Horizontal distance to coin center [m]	
3.	Vertical distance to coin center [m]	Steering performance
4.	Path ratio [·]	
5.	Time [s]	
6.	Head rotation amplitude, *pitch* [°]	
7.	Head rotation amplitude, *roll* [°]	Head movements
8.	Head rotation amplitude, *yaw* [°]	
9.	Torso rotation amplitude, *pitch* [°]	
10.	Torso rotation amplitude, *roll* [°]	
11.	Torso rotation amplitude, *yaw* [°]	
12.	Mean torso speed, *roll* [°/s]	
13.	Mean torso speed, *pitch* [°/s]	
14.	Mean torso speed, *yaw* [°/s]	Torso movements
15.	Maximum torso speed, *roll* [°/s]	
16.	Maximum torso speed, *pitch* [°/s]	
17.	Maximum torso speed, *yaw* [°/s]	
18.	Mean torso speed, *norm* [°/s]	
19.	Maximum torso speed, *norm* [°/s]	

Table A.1 – Description and grouping of the kinematic variables - part I: Task performance, head and torso movements

	Variable description	**Group**
20.	Head-torso correlation, *pitch-pitch* [·]	Head-torso coordination
21.	Head-torso correlation, *roll-roll* [·]	
22.	Head-torso correlation, *roll-yaw* [·]	
23.	Head-torso correlation, *yaw-roll* [·]	
24.	Head-torso correlation, *yaw-yaw* [·]	
25.	Head anchoring index, *roll* [·]	
26.	Head anchoring index, *pitch* [·]	
27.	Head anchoring index, *yaw* [·]	
28.	Peak time of head-torso cross-correlation, *pitch-pitch* [s]	
29.	Peak time of head-torso cross-correlation, *roll-roll* [s]	
30.	Peak time of head-torso cross-correlation, *roll-yaw* [s]	
31.	Peak time of head-torso cross-correlation, *yaw-roll* [s]	
32.	Peak time of head-torso cross-correlation, *yaw-yaw* [s]	
33.	DTW distance, *roll* [·]	
34.	DTW distance, *pitch* [·]	
35.	DTW distance, *yaw* [·]	
36.	Torso SAL [·]	Movement smoothness
37.	Head SAL [·]	
38.	"Bird" SAL [·]	
39.	Number of peaks, head *pitch* [peaks/s]	
40.	Number of peaks, head *roll* [peaks/s]	
41.	Number of peaks, head *yaw* [peaks/s]	
42.	Number of peaks, torso *pitch* [peaks/s]	
43.	Number of peaks, torso *roll* [peaks/s]	
44.	Number of peaks, torso *yaw* [peaks/s]	
45.	Number of peaks, "bird" path *pitch* [peaks/s]	
46.	Number of peaks, "bird" path *roll* [peaks/s]	
47.	Number of peaks, "bird" path *yaw* [peaks/s]	
48.	Torso speed ratio, *roll* [·]	
49.	Torso speed ratio, *pitch* [·]	
50.	Torso speed ratio, *yaw* [·]	

Table A.2 – Description and grouping of the kinematic variables - part II: Coordination and smoothness

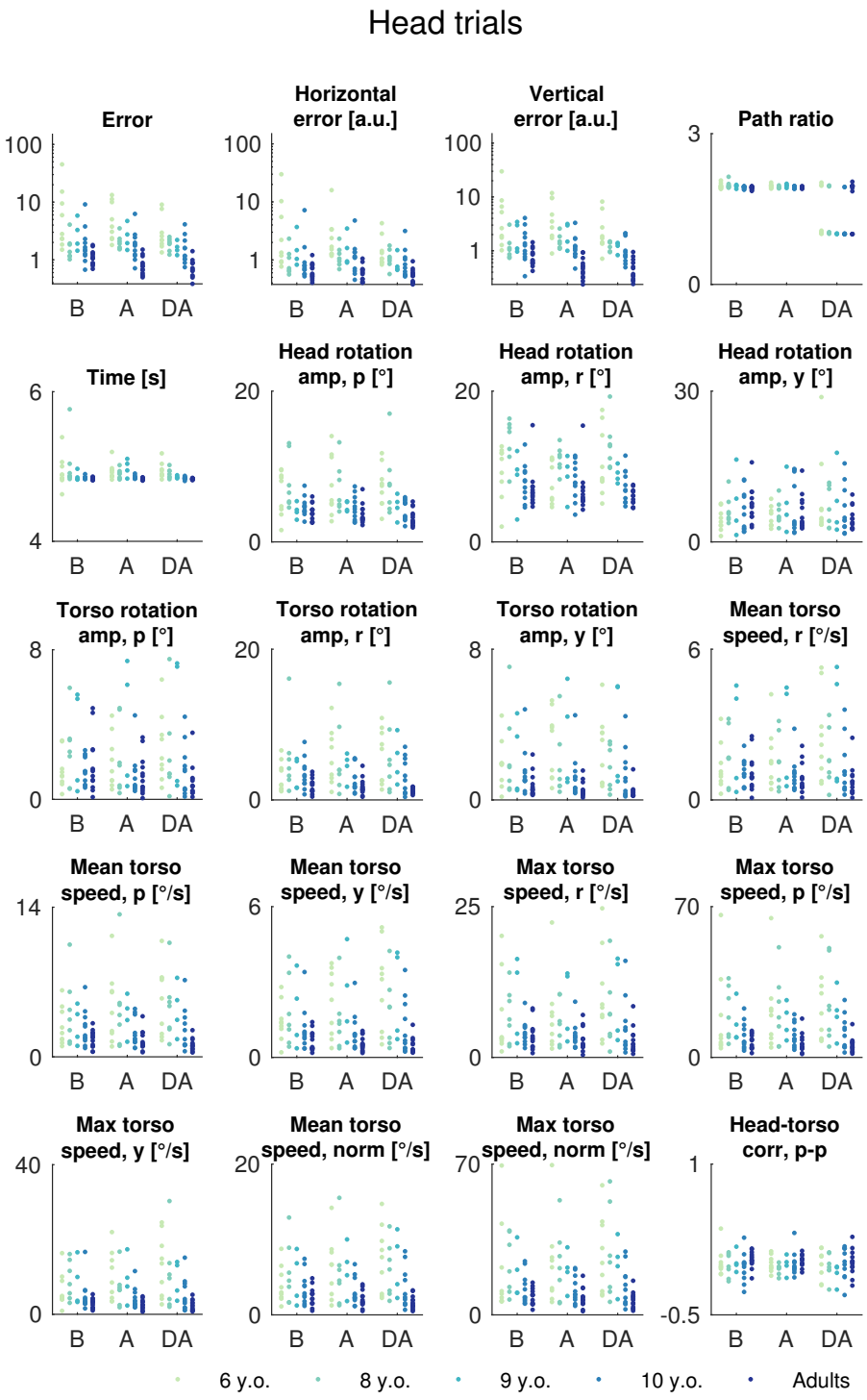

Figure A.1 – Kinematic variables, head controlled trials (I)

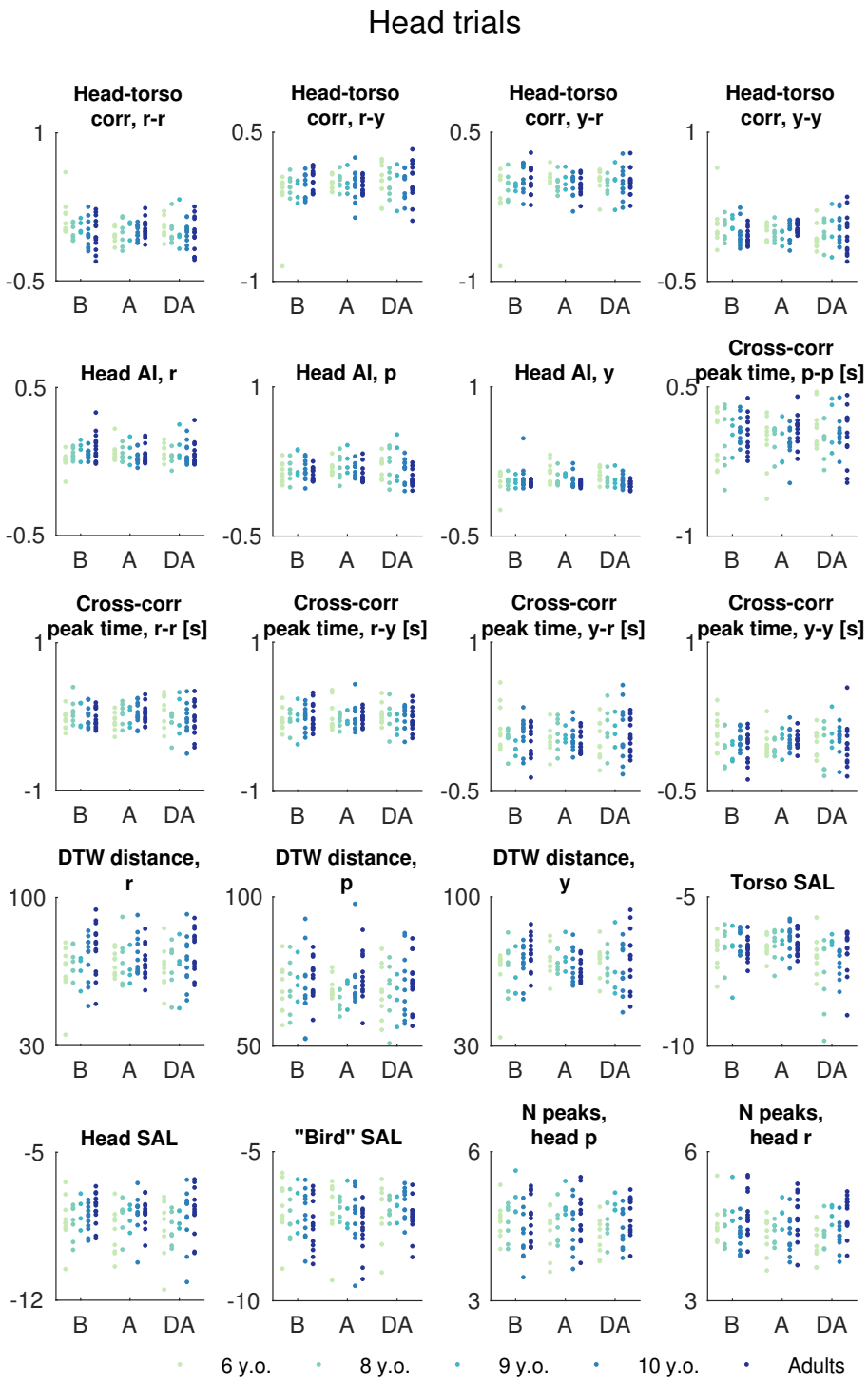

Figure A.2 – Kinematic variables, head controlled trials (II)

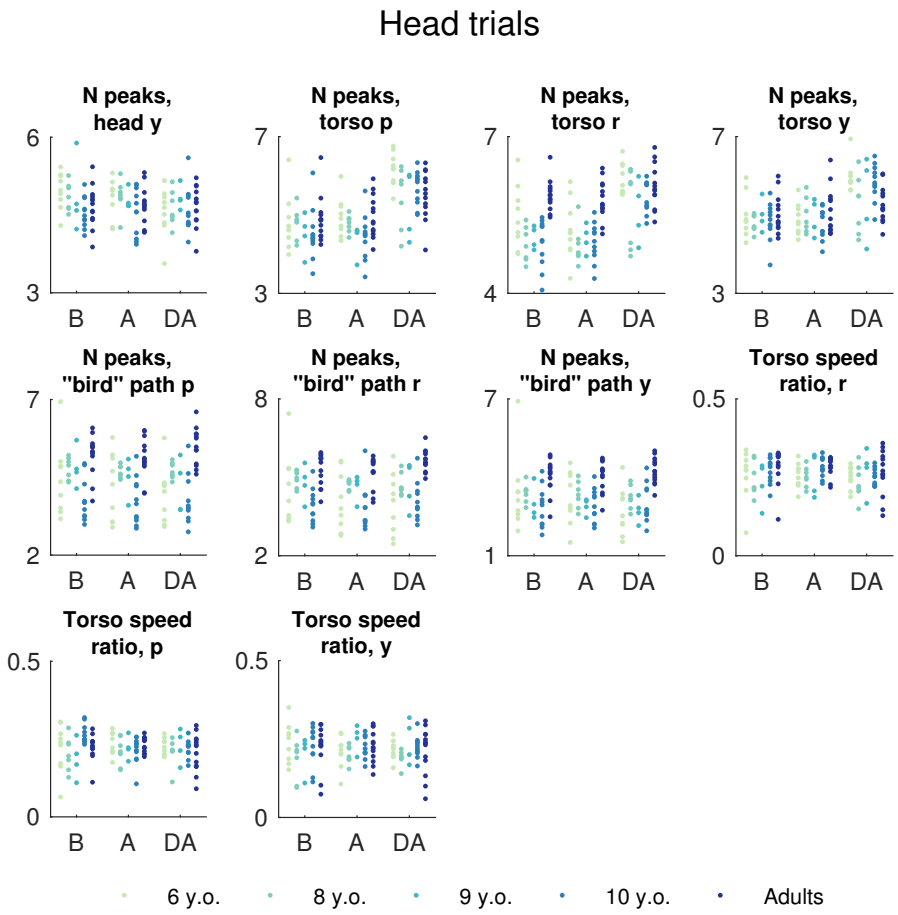

Figure A.3 – Kinematic variables, head controlled trials (III)

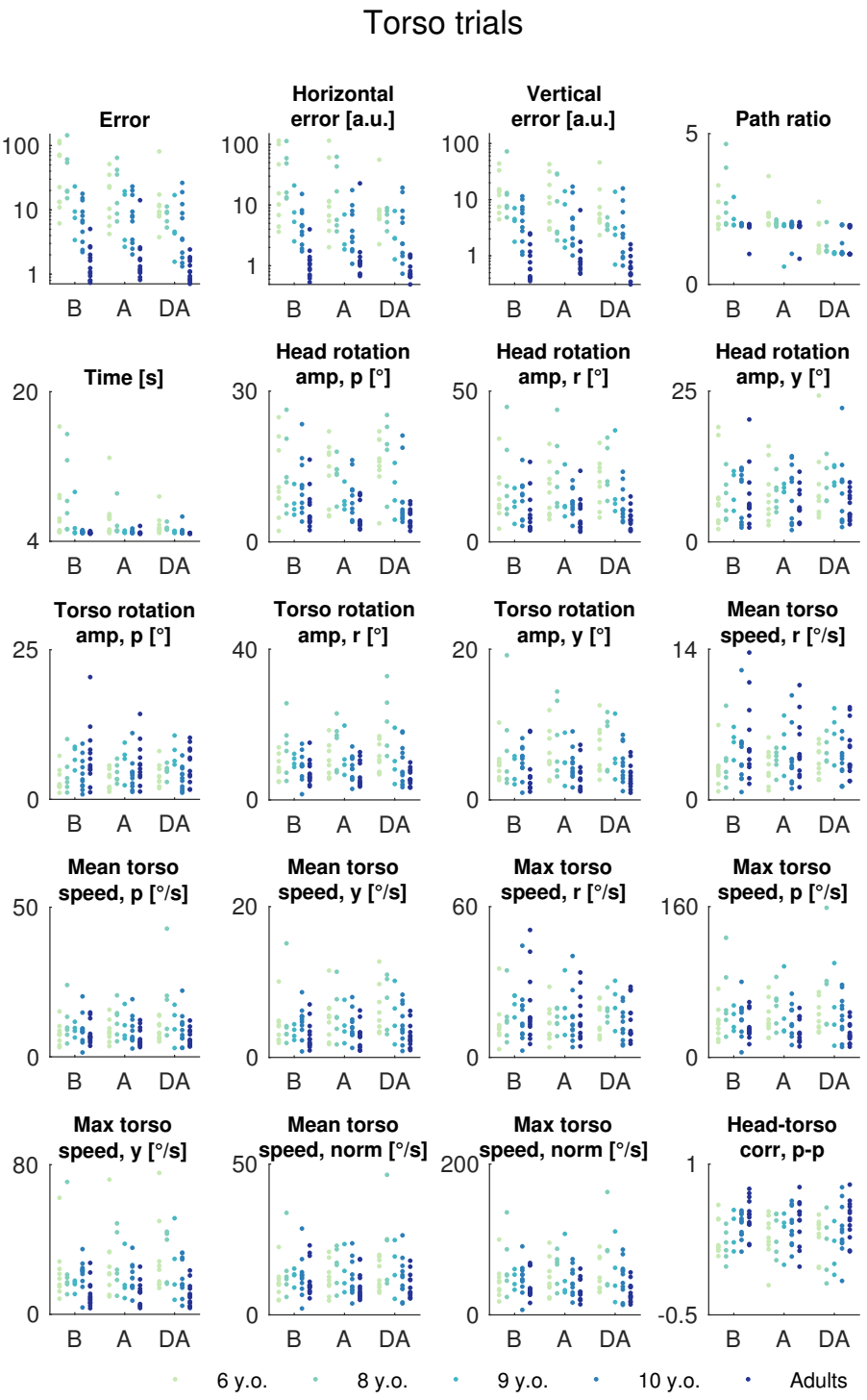

Figure A.4 – Kinematic variables, torso controlled trials (I)

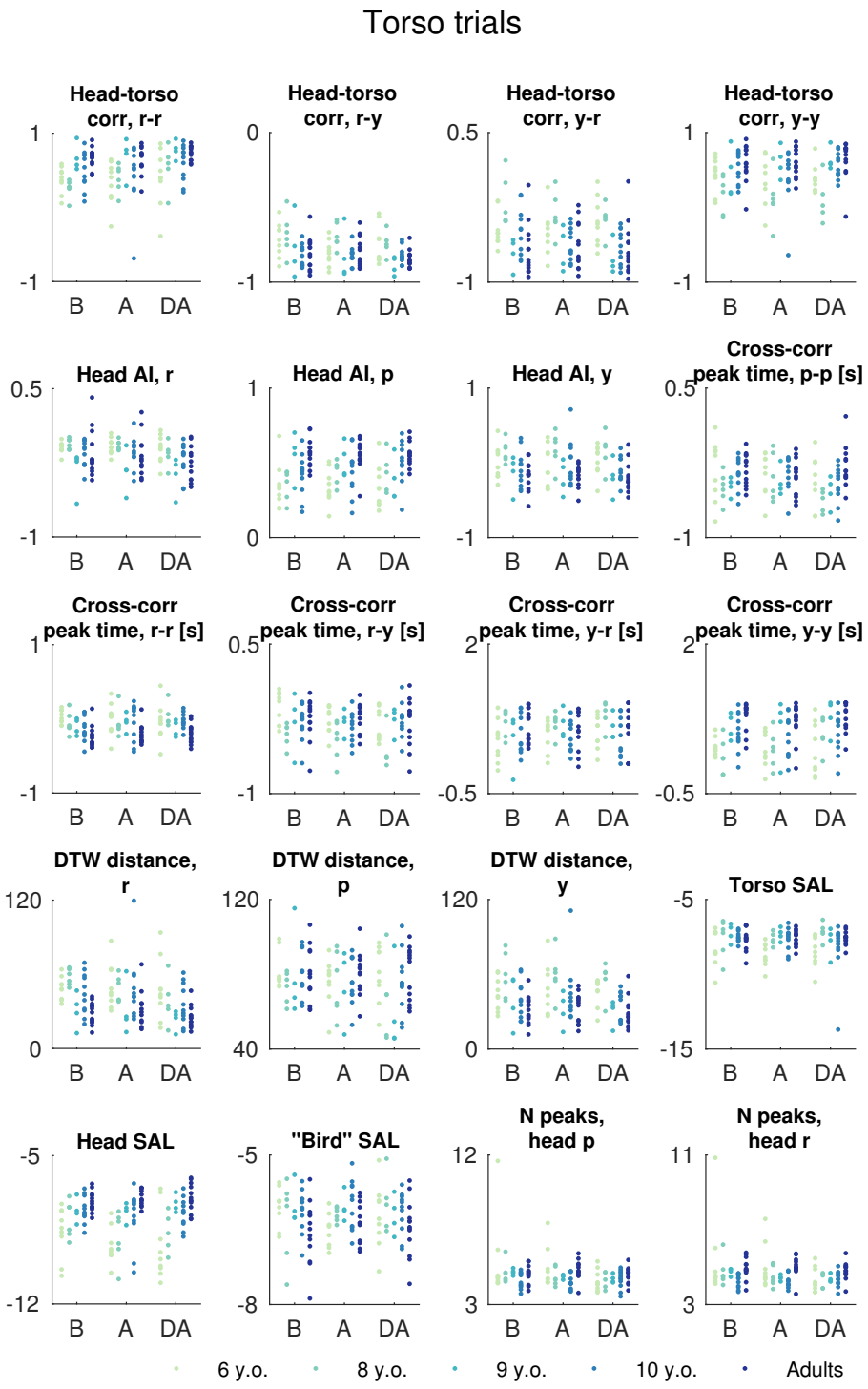

Figure A.5 – Kinematic variables, torso controlled trials (II)

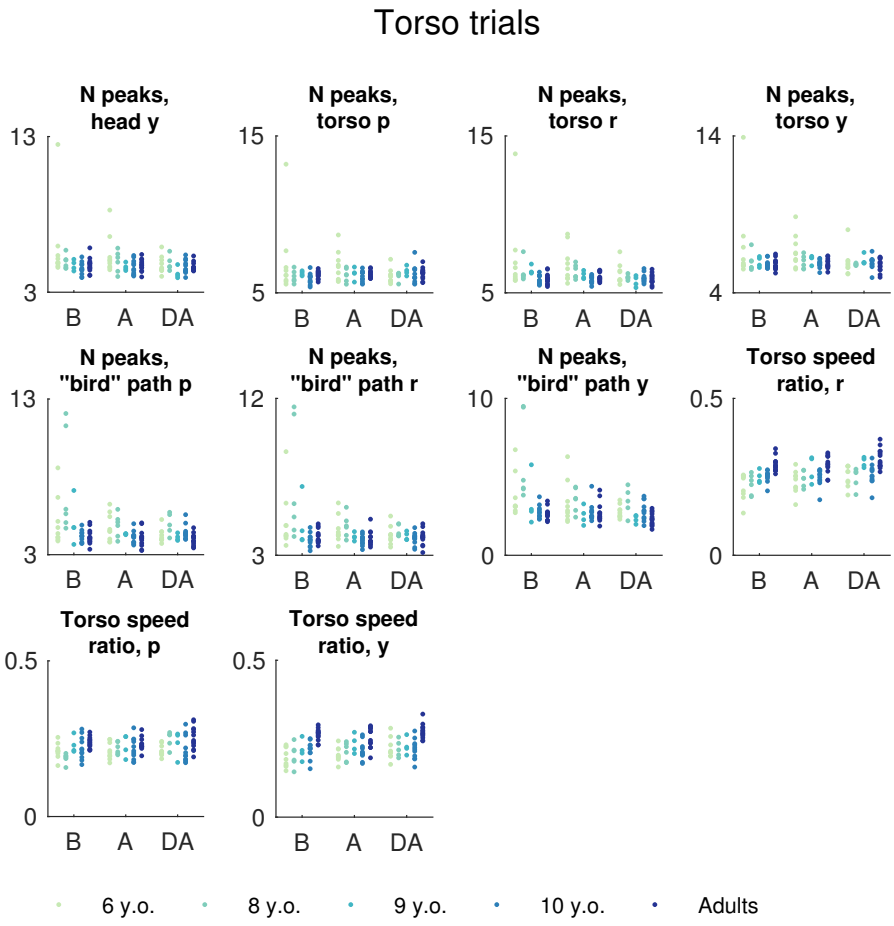

Figure A.6 – Kinematic variables, torso controlled trials (III)

B Statistical analyses

Age	Control - Phase1	Control - Phase2	Difference	*p*		Cohen's *d*
6	Head - Before	Head - After	6.1	0.113		0.6
	Head - Before	Head - DayAfter	6.42	0.072		0.63
	Head - Before	Torso - Before	-38.6	0.002	**	-1.17
	Head - Before	Torso - After	-8.17	0.518		-0.41
	Head - Before	Torso - Day After	-6.45	0.138		-0.44
	Head - After	Head - Day After	0.32	0.693		0.12
	Head - After	Torso - Before	-44.7	<0.001		-1.42
	Head - After	Torso - After	-14.27	0.01	**	-0.83
	Head - After	Torso - Day After	-12.55	<0.001		-1.14
	Head - Day After	Torso - Before	-45.01	<0.001		-1.43
	Head - Day After	Torso - After	-14.58	0.008	**	-0.85
	Head - Day After	Torso - Day After	-12.87	<0.001	***	-1.17
	Torso - Before	Torso - After	30.43	0.013	*	0.85
	Torso - Before	Torso - Day After	32.15	0.014	*	0.97
	Torso - After	Torso - Day After	1.72	0.997		0.09
8	Head - Before	Head - After	-0.07	1		-0.14
	Head - Before	Head - Day After	0.6	1		0.25
	Head - Before	Torso - Before	-56.89	<0.001		-1.45
	Head - Before	Torso - After	-6.37	0.911		-3.59
	Head - Before	Torso - Day After	-4.47	0.775		-2.03
	Head - After	Head - Day After	0.67	0.219		0.55
	Head - After	Torso - Before	-56.82	<0.001		-1.45
	Head - After	Torso - After	-6.3	0.83		-3.8
	Head - After	Torso - Day After	-4.4	0.78		-2.05
	Head - Day After	Torso - Before	-57.49	<0.001		-1.46

Age	Control - Phase1	Control - Phase2	Difference	*p*		Cohen's *d*
	Head - Day After	Torso - After	-6.97	0.763		-3.88
	Head - Day After	Torso - Day After	-5.07	0.652		-2.15
	Torso - Before	Torso - After	50.51	0.001	**	1.26
	Torso - Before	Torso - Day After	52.42	0.002	**	1.28
	Torso - After	Torso - Day After	1.9	0.999		0.27
9	Head - Before	Head - After	1.48	0.998		1.04
	Head - Before	Head - Day After	1.61	0.997		1.12
	Head - Before	Torso - Before	-7.75	0.992		-1.25
	Head - Before	Torso - After	-3.74	0.995		-0.74
	Head - Before	Torso - Day After	-1.9	0.996		-0.65
	Head - After	Head - Day After	0.13	0.998		0.28
	Head - After	Torso - Before	-9.23	0.984		-1.52
	Head - After	Torso - After	-5.22	0.945		-1.07
	Head - After	Torso - Day After	-3.38	0.945		-1.3
	Head - Day After	Torso - Before	-9.37	0.983		-1.54
	Head - Day After	Torso - After	-5.35	0.939		-1.1
	Head - Day After	Torso - Day After	-3.51	0.932		-1.34
	Torso - Before	Torso - After	4.01	1		0.52
	Torso - Before	Torso - Day After	5.85	0.998		0.89
	Torso - After	Torso - Day After	1.84	0.999		0.33
10	Head - Before	Head - After	0.69	0.999		0.37
	Head - Before	Head - Day After	1.21	0.991		0.7
	Head - Before	Torso - Before	-5.85	0.978		-1.4
	Head - Before	Torso - After	-5.61	0.773		-0.93
	Head - Before	Torso - Day After	-2.31	0.912		-0.7
	Head - After	Head - Day After	0.52	0.109		0.68
	Head - After	Torso - Before	-6.53	0.969		-1.68
	Head - After	Torso - After	-6.3	0.485		-1.08
	Head - After	Torso - Day After	-3	0.773		-1.03
	Head - Day After	Torso - Before	-7.06	0.956		-1.84
	Head - Day After	Torso - After	-6.82	0.397		-1.17
	Head - Day After	Torso - Day After	-3.52	0.625		-1.24
	Torso - Before	Torso - After	0.24	1		0.03
	Torso - Before	Torso - Day After	3.53	0.998		0.74
	Torso - After	Torso - Day After	3.3	0.91		0.51
Adults	Head - Before	Head - After	0.42	1		1.25
	Head - Before	Head - Day After	0.45	1		1.23

Age	Control - Phase1	Control - Phase2	Difference	*p*	Cohen's *d*
	Head - Before	Torso - Before	-0.63	1	-0.67
	Head - Before	Torso - After	-0.06	1	-0.23
	Head - Before	Torso - Day After	-0.09	1	-0.14
	Head - After	Head - Day After	0.03	1	0.11
	Head - After	Torso - Before	-1.05	1	-1.13
	Head - After	Torso - After	-0.48	1	-1.17
	Head - After	Torso - Day After	-0.51	1	-0.58
	Head - Day After	Torso - Before	-1.08	1	-1.15
	Head - Day After	Torso - After	-0.51	1	-1.18
	Head - Day After	Torso - Day After	-0.54	1	-0.6
	Torso - Before	Torso - After	0.57	1	0.53
	Torso - Before	Torso - Day After	0.54	1	0.39
	Torso - After	Torso - Day After	-0.03	1	-0.02

Table B.1 – Significant simple effects for the steering performance (I - Experimental Conditions), * $p < 0.05$, ** $p < 0.01$, *** $p < 0.001$

Control - Phase	Age1	Age2	Difference	*p*		Cohen's *d*
Head - Before	6	8	7.67	0.288		0.73
	6	9	6.49	0.526		0.54
	6	10	7.26	0.155		0.76
	6	Adults	8.44	0.07		0.95
	8	9	-1.18	0.999		-0.92
	8	10	-0.41	1		-0.28
	8	Adults	0.77	1		0.98
	9	10	0.77	1		0.33
	9	Adults	1.95	0.988		2.12
	10	Adults	1.19	0.994		0.74
Head - After	6	8	1.5	0.37		0.75
	6	9	1.87	0.235		0.78
	6	10	1.84	0.06		0.91
	6	Adults	2.76	0.002	**	1.55
	8	9	0.37	0.996		0.6
	8	10	0.34	0.992		0.28
	8	Adults	1.26	0.51		3.41
	9	10	-0.02	1		-0.03
	9	Adults	0.9	0.832		2.9
	10	Adults	0.92	0.587		1.29
Head - Day After	6	8	1.85	0.115		0.78
	6	9	1.69	0.241		0.73
	6	10	2.05	0.013	*	1.13
	6	Adults	2.47	0.002	**	1.44
	8	9	-0.17	1		0.09
	8	10	0.19	0.999		0.76
	8	Adults	0.62	0.908		1.67
	9	10	0.36	0.99		0.84
	9	Adults	0.79	0.847		2.07
	10	Adults	0.43	0.942		1.15
Torso - Before	6	8	-10.62	0.959		-0.09
	6	9	37.33	0.192		0.98
	6	10	40.01	0.023	*	1.34
	6	Adults	46.41	0.006	**	1.66
	8	9	47.95	0.099		1.02
	8	10	50.63	0.015	*	1.45
	8	Adults	57.03	0.005	**	1.78

Control - Phase	Age1	Age2	Difference	*p*	Cohen's *d*
	9	10	2.67	1	0.43
	9	Adults	9.08	0.98	2.3
	10	Adults	6.4	0.983	1.73
Torso - After	6	8	9.46	0.657	0.52
	6	9	10.91	0.598	0.52
	6	10	9.81	0.419	0.57
	6	Adults	16.54	0.042 *	1.09
	8	9	1.45	1	0.33
	8	10	0.35	1	0.05
	8	Adults	7.08	0.83	4.99
	9	10	-1.1	1	-0.14
	9	Adults	5.63	0.937	1.81
	10	Adults	6.73	0.714	1.21
Torso - Day After	6	8	9.65	0.197	0.73
	6	9	11.04	0.152	0.84
	6	10	11.39	0.02 *	1.07
	6	Adults	14.8	0.001 **	1.52
	8	9	1.39	0.999	0.65
	8	10	1.75	0.993	0.71
	8	Adults	5.15	0.737	2.57
	9	10	0.36	1	0.09
	9	Adults	3.76	0.921	1.91
	10	Adults	3.41	0.842	1.2

Table B.2 – Significant simple effects for the steering performance (II - Age), * $p < 0.05$, ** $p < 0.01$, *** $p < 0.001$

Appendix B. Statistical analyses

Effect	Variable	F	DOF1	DOF2	*p*		η_p^2
Control	Torso Amplitude, roll	56.98	4	35	<0.001	***	0.62
	Torso Amplitude, pitch	128.91	4	35	<0.001	***	0.79
	Torso Amplitude, yaw	72.52	4	35	<0.001	***	0.67
	Mean Speed Torso, roll	73.84	4	35	<0.001	***	0.68
	Mean Speed Torso, pitch	119.41	4	35	<0.001	***	0.77
	Mean Speed Torso, yaw	97.61	4	35	<0.001	***	0.74
	Max Speed Torso, roll	76.45	4	35	<0.001	***	0.69
	Max Speed Torso, pitch	111.96	4	35	<0.001	***	0.76
	Max Speed Torso, yaw	85.77	4	35	<0.001	***	0.71
	Torso Speed norm, mean	131.52	4	35	<0.001	***	0.79
	Torso Speed norm, max	121.77	4	35	<0.001	***	0.78
	Head-torso correlation, roll	283.23	4	35	<0.001	***	0.89
	Head-torso correlation, roll-yaw	1792.71	4	35	<0.001	***	0.98
	Head-torso correlation, yaw-roll	195.11	4	35	<0.001	***	0.85
	AI, roll	83.59	4	35	<0.001	***	0.70
	AI, pitch	196.70	4	35	<0.001	***	0.85
	Cross-corr peak time, pitch	313.97	4	35	<0.001	***	0.90
	Cross-corr peak time, roll-yaw	115.65	4	35	<0.001	***	0.77
	Cross-corr peak time, yaw-roll	208.79	4	35	<0.001	***	0.86
	DTW distance, roll	231.23	4	35	<0.001	***	0.87
	DTW distance, yaw	161.63	4	35	<0.001	***	0.82
Age:Control	Torso Amplitude, roll	4.31	8	70	0.017	*	0.33
	Torso Amplitude, pitch	3.12	8	70	0.057		0.26
	Torso Amplitude, yaw	1.35	8	70	0.321		0.13
	Mean Speed Torso, roll	2.67	8	70	0.086		0.23
	Mean Speed Torso, pitch	2.81	8	70	0.073		0.24
	Mean Speed Torso, yaw	1.29	8	70	0.342		0.13
	Max Speed Torso, roll	1.67	8	70	0.228		0.16
	Max Speed Torso, pitch	2.23	8	70	0.134		0.20
	Max Speed Torso, yaw	1.62	8	70	0.240		0.16
	Torso Speed norm, mean	1.79	8	70	0.208		0.17
	Torso Speed norm, max	1.68	8	70	0.227		0.16
	Head-torso correlation, roll	6.49	8	70	0.002	**	0.43
	Head-torso correlation, roll-yaw	2.88	8	70	0.068		0.25
	Head-torso correlation, yaw-roll	5.37	8	70	0.005	**	0.38
	AI, roll	2.92	8	70	0.068		0.25
	AI, pitch	8.97	8	70	<0.001	***	0.51

Effect	Variable	F	DOF1	DOF2	p		η_p^2
	Cross-corr peak time, pitch	3.56	8	70	0.036	*	0.29
	Cross-corr peak time, roll-yaw	1.40	8	70	0.305		0.14
	Cross-corr peak time, yaw-roll	13.37	8	70	<0.001	***	0.60
	DTW distance, roll	9.66	8	70	<0.001	***	0.52
	DTW distance, yaw	9.24	8	70	<0.001	***	0.51
Phase:Control	Torso Amplitude, roll	0.44	4	35	0.676		0.01
	Torso Amplitude, pitch	2.49	4	35	0.145		0.07
	Torso Amplitude, yaw	2.34	4	35	0.158		0.06
	Mean Speed Torso, roll	0.79	4	35	0.514		0.02
	Mean Speed Torso, pitch	5.99	4	35	0.012	*	0.15
	Mean Speed Torso, yaw	5.29	4	35	0.021	*	0.13
	Max Speed Torso, roll	1.13	4	35	0.374		0.03
	Max Speed Torso, pitch	5.94	4	35	0.017	*	0.15
	Max Speed Torso, yaw	4.04	4	35	0.056		0.10
	Torso Speed norm, mean	4.75	4	35	0.029	*	0.12
	Torso Speed norm, max	4.72	4	35	0.037	*	0.12
	Head-torso correlation, roll	4.38	4	35	0.037	*	0.11
	Head-torso correlation, roll-yaw	3.97	4	35	0.060		0.10
	Head-torso correlation, yaw-roll	3.16	4	35	0.086		0.08
	AI, roll	2.67	4	35	0.132		0.07
	AI, pitch	4.68	4	35	0.031	*	0.12
	Cross-corr peak time, pitch	1.14	4	35	0.373		0.03
	Cross-corr peak time, roll-yaw	0.19	4	35	0.853		0.01
	Cross-corr peak time, yaw-roll	1.42	4	35	0.303		0.04
	DTW distance, roll	2.44	4	35	0.143		0.07
	DTW distance, yaw	2.59	4	35	0.137		0.07
Age:Phase:Control	Torso Amplitude, roll	0.95	8	70	0.531		0.10
	Torso Amplitude, pitch	2.37	8	70	0.068		0.21
	Torso Amplitude, yaw	1.56	8	70	0.218		0.15
	Mean Speed Torso, roll	1.58	8	70	0.202		0.15
	Mean Speed Torso, pitch	3.61	8	70	0.005	**	0.29
	Mean Speed Torso, yaw	2.31	8	70	0.065		0.21
	Max Speed Torso, roll	1.77	8	70	0.144		0.17
	Max Speed Torso, pitch	1.94	8	70	0.129		0.18
	Max Speed Torso, yaw	2.10	8	70	0.093		0.19
	Torso Speed norm, mean	3.32	8	70	0.009	**	0.27
	Torso Speed norm, max	2.07	8	70	0.105		0.19

Effect	Variable	F	DOF1	DOF2	p	η_p^2
	Head-torso correlation, roll	1.52	8	70	0.219	0.15
	Head-torso correlation, roll-yaw	0.82	8	70	0.611	0.09
	Head-torso correlation, yaw-roll	1.61	8	70	0.195	0.16
	AI, roll	0.24	8	70	0.975	0.03
	AI, pitch	1.42	8	70	0.253	0.14
	Cross-corr peak time, pitch	0.50	8	70	0.858	0.05
	Cross-corr peak time, roll-yaw	0.83	8	70	0.611	0.09
	Cross-corr peak time, yaw-roll	2.02	8	70	0.116	0.19
	DTW distance, roll	0.94	8	70	0.533	0.10
	DTW distance, yaw	0.38	8	70	0.925	0.04

Table B.3 – ANOVA on the variables selected after PCA, on all trials

List of Figures

List of Tables

Glossary

3D	3-dimensional
ABD	Rectus abdominis
AI	Anchoring index
ANOVA	Analysis of variance
BIC	Biceps brachii long head
BMI	Brain-machine interface
BoMi	Body-machine interface
BRA	Brachialis
CAVE	CAVE automatic virtual environment
CNS	Central nervous system
COM	Center of mass
DANT	Deltoid anterior
DBI	Davies-Bouldin index
DMED	Deltoid medialis
DPOST	Deltoid posterior
DTW	Dynamic time warping
EEG	Electroencephalography
EMG	Electromyography
EXT	Extensor digitorum communis
FLEX	Flexor carpi radialis
FPV	First-person view
HMD	Head-mounted display
HMI	Human-machine interface
IC	Independent component
ICA	Independent component analysis
IMU	Inertial measurement unit
INF	Infraspinatus
MAV	Mean absolute value
MSI	Multisensory integration

NSPCA	Non-negative sparse PCA
NUTMEG	Neurodynamic Utility Toolbox for Magnetoencephalo- and Electroencephalography
PC	Principal component
PCA	Principal component analysis
PEC	Pectoralis major
PRO	Pronator teres
RELICA	Reliable ICA
RMS	Root mean square
RHO	Rhomboid major
SAL	Spectral arc length
SENIAM	Surface electromyography for non-invasive assessment of muscles
STER	Sternocleidomastoid
TRAP	Trapezius superior
TRI	Triceps brachii long head
UAV	Unmanned aerial vehicle
VE	Virtual environment
VR	Virtual reality

Bibliography

[1] M. Slater, "A note on presence terminology", *Presence-Connect*, vol. 3, Jan. 2003.

[2] M. V. Sanchez-Vives and M. Slater, "From presence to consciousness through virtual reality", *Nature Reviews Neuroscience*, vol. 6, no. 4, pp. 332–339, Apr. 2005.

[3] D. A. Bowman and R. P. McMahan, "Virtual reality: how much immersion is enough?", *Computer*, vol. 40, no. 7, pp. 36–43, Jul. 2007.

[4] J. J. Cummings and J. N. Bailenson, "How immersive is enough? a meta-analysis of the effect of immersive technology on user presence", *Media Psychology*, vol. 19, no. 2, pp. 272–309, Apr. 2, 2016.

[5] W. Wirth, T. Hartmann, S. Böcking, *et al.*, "A process model of the formation of spatial presence experiences", *Media Psychology*, vol. 9, no. 3, pp. 493–525, May 15, 2007.

[6] J. O. Bailey and J. N. Bailenson, "Chapter 9 - immersive virtual reality and the developing child", in *Cognitive Development in Digital Contexts*, F. C. Blumberg and P. J. Brooks, Eds., San Diego: Academic Press, Jan. 1, 2017, pp. 181–200.

[7] C. A. Thornson, B. F. Goldiez, and H. Le, "Predicting presence: constructing the tendency toward presence inventory", *International Journal of Human-Computer Studies*, vol. 67, no. 1, pp. 62–78, Jan. 1, 2009.

[8] P. Haggard and V. Chambon, "Sense of agency", *Current Biology*, vol. 22, no. 10, R390–R392, May 22, 2012.

[9] P. Haggard, "Sense of agency in the human brain", *Nature Reviews Neuroscience*, vol. 18, no. 4, pp. 196–207, Apr. 2017.

[10] N. Braun, S. Debener, N. Spychala, *et al.*, "The senses of agency and ownership: a review", *Front Psychol*, vol. 9, Apr. 16, 2018.

[11] N. David, A. Newen, and K. Vogeley, "The "sense of agency" and its underlying cognitive and neural mechanisms", *Consciousness and Cognition*, Social Cognition, Emotion, and Self-Consciousness, vol. 17, no. 2, pp. 523–534, Jun. 1, 2008.

[12] K. Kilteni, R. Groten, and M. Slater, "The sense of embodiment in virtual reality", *Presence*, vol. 21, no. 4, pp. 373–387, Nov. 2012.

[13] G. Rognini, A. Sengül, J. E. Aspell, *et al.*, "Visuo-tactile integration and body ownership during self-generated action", *European Journal of Neuroscience*, vol. 37, no. 7, pp. 1120–1129, 2013.

[14] A. Sato and A. Yasuda, "Illusion of sense of self-agency: discrepancy between the predicted and actual sensory consequences of actions modulates the sense of self-agency, but not the sense of self-ownership", *Cognition*, vol. 94, no. 3, pp. 241–255, Jan. 1, 2005.

[15] R. Zopf, V. Polito, and J. Moore, "Revisiting the link between body and agency: visual movement congruency enhances intentional binding but is not body-specific", *Sci Rep*, vol. 8, no. 1, p. 196, 2018.

[16] J. A. Granek, D. J. Gorbet, and L. E. Sergio, "Extensive video-game experience alters cortical networks for complex visuomotor transformations", *Cortex*, vol. 46, no. 9, pp. 1165–1177, Oct. 1, 2010.

[17] D. G. Gozli, D. Bavelier, and J. Pratt, "The effect of action video game playing on sensorimotor learning: evidence from a movement tracking task", *Human Movement Science*, vol. 38, pp. 152–162, Dec. 1, 2014.

[18] M. Mihelj, D. Novak, and S. Samo Beguš, *Virtual Reality Technology and Applications*, ser. Intelligent Systems, Control and Automation: Science and Engineering. Springer, 2014, vol. 68.

[19] Oculus. (Mar. 19, 2014). Oculus rift DK2 hands-on and first-impressions, SlashGear, [Online]. Available: https://www.slashgear.com/oculus-rift-dk2-hands-on-and-first-impressions-19321282/ (visited on 01/02/2019).

[20] C. Cruz-Neira, D. J. Sandin, T. A. DeFanti, *et al.*, "The CAVE audio visual experience automatic virtual environment", *Commun ACM*, vol. 35, no. 6, pp. 65–72, Jun. 1, 1992.

[21] J. J. Laviola, "A discussion of cybersickness in virtual environments", *SIGCHI Bulletin*, 2000.

[22] P. Kozulin, S. L. Ames, and N. A. McBrien, "Effects of a head-mounted display on the oculomotor system of children", *Optom Vis Sci*, vol. 86, no. 7, pp. 845–856, Jul. 2009.

[23] A. Burkins and R. Kopper, "Wayfinding by auditory cues in virtual environments", in *2015 IEEE Virtual Reality (VR)*, Mar. 2015, pp. 155–156.

[24] G. García-Valle, M. Ferre, J. Breñosa, and D. Vargas, "Evaluation of presence in virtual environments: haptic vest and user's haptic skills", *IEEE Access*, vol. 6, pp. 7224–7233, 2018.

[25] K. J. Kuchenbecker, J. Fiene, and G. Niemeyer, "Improving contact realism through event-based haptic feedback", *IEEE Transactions on Visualization and Computer Graphics*, vol. 12, no. 2, pp. 219–230, Mar. 2006.

[26] J. K. Koehn and K. J. Kuchenbecker, "Surgeons and non-surgeons prefer haptic feedback of instrument vibrations during robotic surgery", *Surg Endosc*, vol. 29, no. 10, pp. 2970–2983, Oct. 2015.

[27] P. Kapur, M. Jensen, L. J. Buxbaum, *et al.*, "Spatially distributed tactile feedback for kinesthetic motion guidance", Departmental Papers (MEAM), 2010.

[28] I. Bortone, D. Leonardis, N. Mastronicola, *et al.*, "Wearable haptics and immersive virtual reality rehabilitation training in children with neuromotor impairments", *IEEE Transactions on Neural Systems and Rehabilitation Engineering*, vol. 26, no. 7, pp. 1469–1478, Jul. 2018.

[29] R. Riener, M. Frey, T. Proll, *et al.*, "Phantom-based multimodal interactions for medical education and training: the munich knee joint simulator", *IEEE Transactions on Information Technology in Biomedicine*, vol. 8, no. 2, pp. 208–216, Jun. 2004.

[30] M. Frey, J. Hoogen, R. Burgkart, and R. Riener, "Physical interaction with a virtual knee joint - the 9 DOF haptic display of the munich knee joint simulator", *Presence*, vol. 15, no. 5, pp. 570–587, Oct. 2006.

[31] A. Baheti, S. Seshadri, A. Kumar, *et al.*, "RoSS: virtual reality robotic surgical simulator for the da vinci surgical system", in *2008 Symposium on Haptic Interfaces for Virtual Environment and Teleoperator Systems*, Mar. 2008, pp. 479–480.

[32] R. Hinchet, V. Vechev, H. R. Shea, and O. Hilliges, "DextrES: wearable haptic feedback for grasping in VR via a thin form-factor electrostatic brake", in *UIST*, 2018.

[33] TechCrunch, *HaptX is bringing touch to VR with a pair of scary-looking gloves and a pneumatic suitcase*, http://social.techcrunch.com/2018/10/03/haptx-is-bringing-touch-to-vr-with-a-pair-of-scary-looking-gloves-and-a-pneumatic-suitcase/.

[34] P. Pita. (). Full list of glove controllers for vr, [Online]. Available: https://virtualrealitytimes.com/2017/03/14/full-list-of-glove-controllers-for-vr/ (visited on 01/22/2019).

[35] R. P. Khurshid and K. J. Kuchenbecker, "Data-driven motion mappings improve transparency in teleoperation", *Presence: Teleoperators and Virtual Environments*, vol. 24, no. 2, pp. 132–154, May 1, 2015.

[36] C. Passenberg, A. Peer, and M. Buss, "A survey of environment-, operator-, and task-adapted controllers for teleoperation systems", *Mechatronics*, Special Issue on Design and Control Methodologies in Telerobotics, vol. 20, no. 7, pp. 787–801, Oct. 2010.

[37] J. V. Draper and L. M. Blair, "Workload, flow, and telepresence during teleoperation", in *Proceedings of IEEE International Conference on Robotics and Automation*, vol. 2, Apr. 1996, 1030–1035 vol.2.

[38] J. M. Oscillada, *List of virtual reality controllers*, https://virtualrealitytimes.com/2016/07/12/list-vr-controllers/.

[39] S. Park, Y. Jung, and J. Bae, "A tele-operation interface with a motion capture system and a haptic glove", in *2016 13th International Conference on Ubiquitous Robots and Ambient Intelligence (URAI)*, Aug. 2016, pp. 544–549.

[40] M. Casadio, R. Ranganathan, and F. A. Mussa-Ivaldi, "The body-machine interface: a new perspective on an old theme", *J Mot Behav*, vol. 44, no. 6, pp. 419–433, Nov. 2012.

[41] D. Kranzlmuller, B. Reitinger, I. Hackl, and J. Volkert, "Voice controlled virtual reality and its perspectives for everyday life", *Itg Fachbericht*, pp. 101–108, 2001.

[42] K. Craig. (Oct. 24, 2016). How to implement speech interactions in virtual reality, Medium, [Online]. Available: https://medium.com/@craigjk/how-to-implement-speech-interactions-in-virtual-reality-1556d776ac8 (visited on 01/22/2019).

[43] *Amazon alexa*, https://developer.amazon.com/fr/alexa.

[44] *Siri, apple*, https://www.apple.com/fr/siri/.

[45] R. Leeb and G. Pfurtscheller, "Walking through a virtual city by thought", in *The 26th Annual International Conference of the IEEE Engineering in Medicine and Biology Society*, vol. 2, Sep. 2004, pp. 4503–4506.

[46] J. Chun, B. Bae, and S. Jo, "BCI based hybrid interface for 3d object control in virtual reality", in *2016 4th International Winter Conference on Brain-Computer Interface (BCI)*, Feb. 2016, pp. 1–4.

[47] A. Choo and A. May, "Virtual mindfulness meditation: virtual reality and electroencephalography for health gamification", in *2014 IEEE Games Media Entertainment*, Oct. 2014, pp. 1–3.

[48] T. Carlson, L. Tonin, S. Perdikis, *et al.*, "A hybrid BCI for enhanced control of a telepresence robot", in *2013 35th Annual International Conference of the IEEE Engineering in Medicine and Biology Society (EMBC)*, Jul. 2013, pp. 3097–3100.

[49] R. Leeb, D. Friedman, G. R. Müller-Putz, *et al.*, "Self-paced (asynchronous) BCI control of a wheelchair in virtual environments: a case study with a tetraplegic", *Comput Intell Neurosci*, vol. 2007, 2007.

[50] K. LaFleur, K. Cassady, A. Doud, *et al.*, "Quadcopter control in three-dimensional space using a noninvasive motor imagery-based brain–computer interface", *J. Neural Eng.*, vol. 10, no. 4, p. 046 003, 2013.

[51] J. R. Wolpaw, N. Birbaumer, D. J. McFarland, *et al.*, "Brain–computer interfaces for communication and control", *Clinical Neurophysiology*, vol. 113, no. 6, pp. 767–791, Jun. 1, 2002.

[52] (Jul. 30, 2017). The top 15 virtual reality experiences you should definitely check out, TheWrap, [Online]. Available: https://www.thewrap.com/15-best-virtual-reality-experiences-so-far/ (visited on 01/19/2019).

[53] P. Labbé. (Feb. 16, 2017). Everest VR : partez à l'assaut du toit du monde en réalité virtuelle, Réalité-Virtuelle.com, [Online]. Available: https://www.realite-virtuelle.com/everest-vr-simulation-escalade-1602 (visited on 01/19/2019).

[54] *Titans of space®, oculus go / gear VR*, http://www.titansofspacevr.com/.

[55] (Apr. 11, 2016). NASA is using virtual reality to train astronauts, Unimersiv, [Online]. Available: https://unimersiv.com/how-nasa-is-using-virtual-and-augmented-reality-to-train-astronauts-37/ (visited on 01/22/2019).

[56] U. Army, *DSTS: first immersive virtual training system fielded*, www.army.mil, https://www.army.mil/article/84728/dsts_first_immersive_virtual_training_system_fielded.

[57] ——, *Stand-to!*, www.army.mil, http://www.army.mil/standto/archive_2014-05-19.

[58] P. Hajeswaran, N. Hung, T. Kesavadas, *et al.*, "AirwayVR: learning endotracheal intubation in virtual reality", in *2018 IEEE Conference on Virtual Reality and 3D User Interfaces (VR)*, Mar. 2018, pp. 669–670.

[59] S. Haque and S. Srinivasan, "A meta-analysis of the training effectiveness of virtual reality surgical simulators", *IEEE Transactions on Information Technology in Biomedicine*, vol. 10, no. 1, pp. 51–58, Jan. 2006.

[60] L. Morelli, S. Guadagni, G. Di Franco, *et al.*, "Da vinci single site© surgical platform in clinical practice: a systematic review", *Int J Med Robotics Comput Assist Surg*, vol. 12, no. 4, pp. 724–734, Dec. 1, 2016.

[61] K. Stepan, J. Zeiger, S. Hanchuk, *et al.*, "Immersive virtual reality as a teaching tool for neuroanatomy", *Int Forum Allergy Rhinol*, vol. 7, no. 10, pp. 1006–1013, 2017.

[62] C. news, *Stanford studies virtual reality, kids, and the effects of make-believe*, VHIL, http://vhil.stanford.edu/news/2015/stanford-studies-virtual-reality-kids-and-the-effects-of-make-believe/.

[63] D. Jack, R. Boian, A. S. Merians, *et al.*, "Virtual reality-enhanced stroke rehabilitation", *IEEE Transactions on Neural Systems and Rehabilitation Engineering*, vol. 9, no. 3, pp. 308–318, Sep. 2001.

[64] J. Messier, S. Adamovich, D. Jack, *et al.*, "Visuomotor learning in immersive 3d virtual reality in parkinson's disease and in aging", *Exp Brain Res*, vol. 179, no. 3, pp. 457–474, May 1, 2007.

[65] D. Perez-Marcos, O. Chevalley, T. Schmidlin, *et al.*, "Increasing upper limb training intensity in chronic stroke using embodied virtual reality: a pilot study", *J Neuroeng Rehabil*, vol. 14, Nov. 17, 2017.

[66] Y. Mao, P. Chen, L. Li, and D. Huang, "Virtual reality training improves balance function", *Neural Regen Res*, vol. 9, no. 17, pp. 1628–1634, Sep. 1, 2014.

[67] M. I. Khan, A. Prado, and S. K. Agrawal, "Effects of virtual reality training with trunk support trainer (TruST) on postural kinematics", *IEEE Robotics and Automation Letters*, vol. 2, no. 4, pp. 2240–2247, Oct. 2017.

[68] S. E. Kober, G. Wood, D. Hofer, *et al.*, "Virtual reality in neurologic rehabilitation of spatial disorientation", *J Neuroeng Rehabil*, vol. 10, p. 17, Feb. 8, 2013.

[69] G. J. Barton, M. B. Hawken, R. J. Foster, *et al.*, "The effects of virtual reality game training on trunk to pelvis coupling in a child with cerebral palsy", *Journal of NeuroEngineering and Rehabilitation*, vol. 10, p. 15, 2013.

[70] E. Monge Pereira, F. Molina Rueda, I. M. Alguacil Diego, *et al.*, "Use of virtual reality systems as proprioception method in cerebral palsy: clinical practice guideline", *Neurologia*, vol. 29, no. 9, pp. 550–559, Nov. 1, 2014.

[71] C. Gagliardi, A. C. Turconi, E. Biffi, *et al.*, "Immersive virtual reality to improve walking abilities in cerebral palsy: a pilot study", *Ann Biomed Eng*, vol. 46, no. 9, pp. 1376–1384, Sep. 2018.

[72] Y. Cai, N. K. H. Chia, D. Thalmann, *et al.*, "Design and development of a virtual dolphinarium for children with autism", *IEEE Transactions on Neural Systems and Rehabilitation Engineering*, vol. 21, no. 2, pp. 208–217, Mar. 2013.

[73] M. Wang and D. Reid, "Virtual reality in pediatric neurorehabilitation: attention deficit hyperactivity disorder, autism and cerebral palsy", *NED*, vol. 36, no. 1, pp. 2–18, 2011.

[74] S. R. Sharar, G. J. Carrougher, D. Nakamura, *et al.*, "Factors influencing the efficacy of virtual reality distraction analgesia during postburn physical therapy: preliminary results from 3 ongoing studies", *Archives of Physical Medicine and Rehabilitation*, The NIDRR Burn Injury Rehabilitation Model System Program: Selected Findings, vol. 88, no. 12, S43–S49, Dec. 1, 2007.

[75] A. S. Won, J. Bailey, J. Bailenson, *et al.*, "Immersive virtual reality for pediatric pain", *Children (Basel)*, vol. 4, no. 7, Jun. 23, 2017.

[76] M. Krijn, P. M. G. Emmelkamp, R. Biemond, *et al.*, "Treatment of acrophobia in virtual reality: the role of immersion and presence", *Behaviour Research and Therapy*, vol. 42, no. 2, pp. 229–239, Feb. 1, 2004.

[77] T. D. Parsons and A. A. Rizzo, "Affective outcomes of virtual reality exposure therapy for anxiety and specific phobias: a meta-analysis", *Journal of Behavior Therapy and Experimental Psychiatry*, vol. 39, no. 3, pp. 250–261, Sep. 1, 2008.

[78] D. Freeman, S. Reeve, A. Robinson, *et al.*, "Virtual reality in the assessment, understanding, and treatment of mental health disorders", *Psychol Med*, vol. 47, no. 14, pp. 2393–2400, Oct. 2017.

[79] C. Botella, J. Fernández-Álvarez, V. Guillén, *et al.*, "Recent progress in virtual reality exposure therapy for phobias: a systematic review", *Curr Psychiatry Rep*, vol. 19, no. 7, p. 42, Jul. 2017.

[80] S. L. CNN, *The very real health dangers of virtual reality*, CNN, https://www.cnn.com/2017/12/13/health/virtual-reality-vr-dangers-safety/index.html.

[81] S. VHIL, *Immersive virtual reality influences children's inhibitory control and social behavior*, https://vhil.stanford.edu/pubs/2017/immersive-virtual-reality-influences-childrens-inhibitory-control-and-social-behavior/.

[82] M. T. Schultheis, P. D, B. O. Rothbaum, and P. D, "Ethical issues for the use of virtual reality in the psychological sciences", in *In S. Bush & M. Drexler (Eds.), Ethical issues in clinical neuropsychology (pp. 243–280). Lisse, NL: Swets & Zeitlinger*, 2002.

[83] J. O. Bailey and J. N. Bailenson, "Considering virtual reality in children's lives", *Journal of Children and Media*, vol. 11, no. 1, pp. 107–113, Jan. 2, 2017.

[84] E. Southgate, S. P. Smith, and J. Scevak, "Asking ethical questions in research using immersive virtual and augmented reality technologies with children and youth", in *2017 IEEE Virtual Reality (VR)*, Mar. 2017, pp. 12–18.

[85] K. Y. Segovia and J. N. Bailenson, "Virtually true: children's acquisition of false memories in virtual reality", *Media Psychology*, vol. 12, no. 4, pp. 371–393, Nov. 23, 2009.

[86] T. Baumgartner, D. Speck, D. Wettstein, *et al.*, "Feeling present in arousing virtual reality worlds: prefrontal brain regions differentially orchestrate presence experience in adults and children", *Front. Hum. Neurosci.*, vol. 2, 2008.

[87] L. Jäncke, M. Cheetham, and T. Baumgartner, "Virtual reality and the role of the prefrontal cortex in adults and children.", *Front. Neurosci.*, vol. 3, 2009.

[88] B. E. Stein, T. R. Stanford, and B. A. Rowland, "The neural basis of multisensory integration in the midbrain: its organization and maturation", *Hear Res*, vol. 258, no. 1, pp. 4–15, Dec. 2009.

[89] E. Dionne-Dostie, N. Paquette, M. Lassonde, and A. Gallagher, "Multisensory integration and child neurodevelopment", *Brain Sci*, vol. 5, no. 1, pp. 32–57, Feb. 11, 2015.

[90] C. Kayser and L. Shams, "Multisensory causal inference in the brain", *PLOS Biology*, vol. 13, no. 2, e1002075, Feb. 24, 2015.

[91] M. O. Ernst and M. S. Banks, "Humans integrate visual and haptic information in a statistically optimal fashion", *Nature*, vol. 415, no. 6870, pp. 429–433, Jan. 24, 2002.

[92] M. Botvinick and J. Cohen, "Rubber hands 'feel' touch that eyes see", *Nature*, vol. 391, no. 6669, p. 756, Feb. 1998.

[93] K. Takakusaki, M. Takahashi, K. Obara, and R. Chiba, “Neural substrates involved in the control of posture”, *Advanced Robotics*, vol. 31, no. 1, pp. 2–23, Jan. 17, 2017.

[94] H. O. Karnath, D. Sievering, and M. Fetter, “The interactive contribution of neck muscle proprioception and vestibular stimulation to subjective "straight ahead"orientation in man”, *Exp Brain Res*, vol. 101, no. 1, pp. 140–146, 1994.

[95] K. Takakusaki, “Functional neuroanatomy for posture and gait control”, *Journal of Movement Disorders*, vol. 10, no. 1, pp. 1–17, Jan. 18, 2017.

[96] M. O. Ernst, “Multisensory integration: a late bloomer”, *Current Biology*, vol. 18, no. 12, R519–R521, Jun. 24, 2008.

[97] D. Burr and M. Gori, “Multisensory integration develops late in humans”, in *The Neural Bases of Multisensory Processes*, ser. Frontiers in Neuroscience, M. M. Murray and M. T. Wallace, Eds., Boca Raton (FL): CRC Press/Taylor & Francis, 2012.

[98] M. Gori, M. Del Viva, G. Sandini, and D. C. Burr, “Young children do not integrate visual and haptic form information”, *Current Biology*, vol. 18, no. 9, pp. 694–698, May 6, 2008.

[99] M. Nardini, P. Jones, R. Bedford, and O. Braddick, “Development of cue integration in human navigation”, *Current Biology*, vol. 18, no. 9, pp. 689–693, May 6, 2008.

[100] J. Negen, B. Chere, L. Bird, *et al.*, “Sensory cue combination in children under 10 years of age”, *BioRxiv*, p. 501 585, Dec. 20, 2018.

[101] N. Gouleme, M. D. Ezane, S. Wiener-Vacher, and M. P. Bucci, “Spatial and temporal postural analysis: a developmental study in healthy children”, *International Journal of Developmental Neuroscience*, vol. 38, pp. 169–177, Nov. 1, 2014.

[102] P. J. Sparto, M. S. Redfern, J. G. Jasko, *et al.*, “The influence of dynamic visual cues for postural control in children aged 7-12 years”, *Exp Brain Res*, vol. 168, no. 4, pp. 505–516, Jan. 2006.

[103] I. Flatters, F. Mushtaq, L. J. B. Hill, *et al.*, “Children’s head movements and postural stability as a function of task”, *Exp Brain Res*, vol. 232, no. 6, pp. 1953–1970, Jun. 1, 2014.

[104] J. M. Haddad, S. Rietdyk, L. J. Claxton, and J. Huber, “Task-dependent postural control throughout the lifespan”, *Exerc Sport Sci Rev*, vol. 41, no. 2, pp. 123–132, Apr. 2013.

[105] W. R. Corliss and E. G. Johnsen, “Teleoperator controls an AEC-NASA technology survey”, Dec. 1, 1968.

[106] R. Bogue, “Robots in the nuclear industry: a review of technologies and applications”, *Industrial Robot*, vol. 38, no. 2, pp. 113–118, Mar. 8, 2011.

[107] L. Briones, P. Bustamante, and M. A. Serna, “Wall-climbing robot for inspection in nuclear power plants”, in *Proceedings of the 1994 IEEE International Conference on Robotics and Automation*, May 1994, 1409–1414 vol.2.

[108] R. Murphy, "Human-robot interaction in rescue robotics", *IEEE Transactions on Systems, Man, and Cybernetics, Part C: Applications and Reviews*, vol. 34, no. 2, pp. 138–153, May 2004.

[109] J. L. Burke and R. R. Murphy, "Human-robot interaction in USAR technical search: two heads are better than one", in *RO-MAN 2004. 13th IEEE International Workshop on Robot and Human Interactive Communication (IEEE Catalog No.04TH8759)*, Sep. 2004, pp. 307–312.

[110] J. Casper and R. R. Murphy, "Human-robot interactions during the robot-assisted urban search and rescue response at the world trade center", *IEEE Transactions on Systems, Man, and Cybernetics, Part B (Cybernetics)*, vol. 33, no. 3, pp. 367–385, Jun. 2003.

[111] A. Bolopion and S. Régnier, "A review of haptic feedback teleoperation systems for micromanipulation and microassembly", *IEEE Transactions on Automation Science and Engineering*, vol. 10, no. 3, pp. 496–502, Jul. 2013.

[112] B. Rebsamen, E. Burdet, C. Guan, *et al.*, "A brain-controlled wheelchair based on p300 and path guidance", in *The First IEEE/RAS-EMBS International Conference on Biomedical Robotics and Biomechatronics, 2006. BioRob 2006.*, Feb. 2006, pp. 1101–1106.

[113] L. Tonin, T. Carlson, R. Leeb, and J. d. R. Millán, "Brain-controlled telepresence robot by motor-disabled people", in *2011 Annual International Conference of the IEEE Engineering in Medicine and Biology Society*, Aug. 2011, pp. 4227–4230.

[114] S. Jain, A. Farshchiansadegh, A. Broad, *et al.*, "Assistive robotic manipulation through shared autonomy and a body-machine interface", in *2015 IEEE International Conference on Rehabilitation Robotics (ICORR)*, Aug. 2015, pp. 526–531.

[115] J. Y. C. Chen, E. C. Haas, and M. J. Barnes, "Human performance issues and user interface design for teleoperated robots", *IEEE Transactions on Systems, Man, and Cybernetics, Part C (Applications and Reviews)*, vol. 37, no. 6, pp. 1231–1245, Nov. 2007.

[116] M. Alimardani, S. Nishio, and H. Ishiguro, "Removal of proprioception by BCI raises a stronger body ownership illusion in control of a humanlike robot", *Scientific Reports*, vol. 6, p. 33 514, Sep. 22, 2016.

[117] B. H. Kim, M. Kim, and S. Jo, "Quadcopter flight control using a low-cost hybrid interface with EEG-based classification and eye tracking", *Computers in Biology and Medicine*, vol. 51, pp. 82–92, Aug. 1, 2014.

[118] X. Song, K. Mann, E. Allison, *et al.*, "A quadcopter controlled by brain concentration and eye blink", presented at the IEEE Signal Processing in Medicine and Biology Symposium, Philadelphia, 2016.

[119] M. Casadio, A. Pressman, A. Fishbach, *et al.*, "Functional reorganization of upper-body movement after spinal cord injury", *Exp Brain Res*, vol. 207, no. 3, pp. 233–247, Dec. 1, 2010.

[120] C. Pierella, F. Abdollahi, A. Farshchiansadegh, *et al.*, "Remapping residual coordination for controlling assistive devices and recovering motor functions", *Neuropsychologia*, Special Issue: Sensory Motor Integration, vol. 79, Part B, pp. 364–376, Dec. 2015.

[121] I. Seanez-Gonzalez, C. Pierella, A. Farshchiansadegh, *et al.*, "Static vs. dynamic decoding algorithms in a non-invasive body-machine interface", *IEEE Transactions on Neural Systems and Rehabilitation Engineering*, vol. PP, no. 99, pp. 1–1, 2017.

[122] M. Waibel. (Jul. 2, 2011). Controlling a quadrotor using kinect, IEEE Spectrum: Technology, Engineering, and Science News, [Online]. Available: http://spectrum.ieee.org/automaton/robotics/robotics-software/quadrotor-interaction (visited on 06/06/2017).

[123] K. Pfeil, S. L. Koh, and J. LaViola, "Exploring 3d gesture metaphors for interaction with unmanned aerial vehicles", in *Proceedings of the 2013 International Conference on Intelligent User Interfaces*, ser. IUI '13, New York, NY, USA: ACM, 2013, pp. 257–266.

[124] R. A. S. Fernández, J. L. Sanchez-Lopez, C. Sampedro, *et al.*, "Natural user interfaces for human-drone multi-modal interaction", in *2016 International Conference on Unmanned Aircraft Systems (ICUAS)*, Jun. 2016, pp. 1013–1022.

[125] D. Floreano and R. J. Wood, "Science, technology and the future of small autonomous drones", *Nature*, vol. 521, no. 7553, pp. 460–466, May 28, 2015.

[126] K. Higuchi, K. Fujii, and J. Rekimoto, "Flying head: a head-synchronization mechanism for flying telepresence", in *2013 23rd International Conference on Artificial Reality and Telexistence (ICAT)*, Dec. 2013, pp. 28–34.

[127] C. Pittman and J. J. LaViola Jr., "Exploring head tracked head mounted displays for first person robot teleoperation", in *Proceedings of the 19th International Conference on Intelligent User Interfaces*, ser. IUI '14, New York, NY, USA: ACM, 2014, pp. 323–328.

[128] K. Miyoshi, R. Konomura, and K. Hori, "Above your hand: direct and natural interaction with aerial robot", in *ACM SIGGRAPH 2014 Emerging Technologies*, ser. SIGGRAPH '14, New York, NY, USA: ACM, 2014, 8:1–8:1.

[129] A. Sarkar, K. A. Patel, R. K. G. Ram, and G. K. Capoor, "Gesture control of drone using a motion controller", in *2016 International Conference on Industrial Informatics and Computer Systems (CIICS)*, Mar. 2016, pp. 1–5.

[130] G. Jones, N. Berthouze, R. Bielski, and S. Julier, "Towards a situated, multimodal interface for multiple UAV control", in *2010 IEEE International Conference on Robotics and Automation*, May 2010, pp. 1739–1744.

[131] K. Ikeuchi, T. Otsuka, A. Yoshii, *et al.*, "KinecDrone: enhancing somatic sensation to fly in the sky with kinect and AR.drone", in *Proceedings of the 5th Augmented Human International Conference*, ser. AH '14, New York, NY, USA: ACM, 2014, 53:1–53:2.

[132] J. R. Cauchard, J. L. E, K. Y. Zhai, and J. A. Landay, "Drone & me: an exploration into natural human-drone interaction", in *Proceedings of the 2015 ACM International Joint Conference on Pervasive and Ubiquitous Computing*, ser. UbiComp '15, New York, NY, USA: ACM, 2015, pp. 361–365.

[133] M. Monajjemi, S. Mohaimenianpour, and R. Vaughan, "UAV, come to me: end-to-end, multi-scale situated HRI with an uninstrumented human and a distant UAV", in *2016 IEEE/RSJ International Conference on Intelligent Robots and Systems (IROS)*, Oct. 2016, pp. 4410–4417.

[134] E. Peshkova, M. Hitz, and D. Ahlström, "Exploring user-defined gestures and voice commands to control an unmanned aerial vehicle", in *Intelligent Technologies for Interactive Entertainment*, Springer, Cham, Jun. 28, 2016, pp. 47–62.

[135] A. Sanna, F. Lamberti, G. Paravati, and F. Manuri, "A kinect-based natural interface for quadrotor control", *Entertainment Computing*, vol. 4, no. 3, pp. 179–186, Aug. 2013.

[136] B. G. Witmer and M. J. Singer, "Measuring presence in virtual environments: a presence questionnaire", *Presence*, vol. 7, no. 3, pp. 225–240, Jun. 1998.

[137] S. Lupashin, M. Hehn, M. W. Mueller, *et al.*, "A platform for aerial robotics research and demonstration: the flying machine arena", *Mechatronics*, vol. 24, no. 1, pp. 41–54, Feb. 1, 2014.

[138] M. Burke and J. Lasenby, "Pantomimic gestures for human-robot interaction", *IEEE Transactions on Robotics*, vol. 31, no. 5, pp. 1225–1237, Oct. 2015.

[139] VICON, *Plug-in gait model details*, http://www.vicon.com/downloads/documentation/vicon-documentation/plug-in-gait-model-details.

[140] H. J. Hermens, B. Freriks, C. Disselhorst-Klug, and G. Rau, "Development of recommendations for SEMG sensors and sensor placement procedures", *Journal of Electromyography and Kinesiology*, vol. 10, no. 5, pp. 361–374, Oct. 2000.

[141] P. de Leva, "Joint center longitudinal positions computed from a selected subset of chandler's data", *J Biomech*, vol. 29, no. 9, pp. 1231–1233, Sep. 1996.

[142] P. d. Leva, "Adjustments to zatsiorsky-seluyanov's segment inertia parameters", *Journal of Biomechanics*, vol. 29, no. 9, pp. 1223–1230, Sep. 1, 1996.

[143] C. Anglin and U. P. Wyss, "Review of arm motion analyses", *Proc Inst Mech Eng H*, vol. 214, no. 5, pp. 541–555, 2000.

[144] G. Wu, F. C. T. van der Helm, H. E. J. D. Veeger, *et al.*, "ISB recommendation on definitions of joint coordinate systems of various joints for the reporting of human joint motion–part II: shoulder, elbow, wrist and hand", *J Biomech*, vol. 38, no. 5, pp. 981–992, May 2005.

[145] E. Pirondini, M. Coscia, S. Marcheschi, *et al.*, "Evaluation of the effects of the arm light exoskeleton on movement execution and muscle activities: a pilot study on healthy subjects", *J Neuroeng Rehabil*, vol. 13, Jan. 23, 2016.

[146] F. Artoni, A. Gemignani, L. Sebastiani, *et al.*, "ErpICASSO : a tool for reliability estimates of independent components in EEG event-related analysis", *Conf Proc IEEE Eng Med Biol Soc*, vol. 2012, pp. 368–371, 2012.

[147] F. Artoni, D. Menicucci, A. Delorme, *et al.*, "RELICA: a method for estimating the reliability of independent components", *Neuroimage*, vol. 103, pp. 391–400, Dec. 2014.

[148] D. Martelli, F. Artoni, V. Monaco, *et al.*, "Pre-impact fall detection: optimal sensor positioning based on a machine learning paradigm", *PLOS ONE*, vol. 9, no. 3, e92037, 2014.

[149] J. Himberg, A. Hyvärinen, and F. Esposito, "Validating the independent components of neuroimaging time series via clustering and visualization", *Neuroimage*, vol. 22, no. 3, pp. 1214–1222, Jul. 2004.

[150] R. Zass and A. Shashua, "Nonnegative sparse PCA", *Advances in Neural Information Processing Systems*, vol. 19, p. 1561, 2007.

[151] A. J. Flügge, "Non-negative PCA for EEG-data analysis", Bachelor Thesis, University College London, 2009.

[152] B. Siciliano and O. Khatib, *Springer Handbook of Robotics*. Springer, Jul. 27, 2016, 2259 pp., Google-Books-ID: RTvADAAAQBAJ.

[153] J. W. Frane, "A method of biased coin randomization, its implementation, and its validation", *Drug Information Journal*, vol. 32, no. 2, pp. 423–432, Apr. 1, 1998.

[154] A. Cherpillod, S. Mintchev, and D. Floreano, "Embodied flight with a drone", *ARXIV:1707.01788 [cs]*, Jul. 6, 2017. arXiv: 1707.01788.

[155] F. E. Ritter and L. J. Schooler, "Learning curve, the", in *International Encyclopedia of the Social & Behavioral Sciences*, N. J. Smelser and P. B. Baltes, Eds., Oxford: Pergamon, 2001, pp. 8602–8605.

[156] J. Gordon, M. F. Ghilardi, and C. Ghez, "Accuracy of planar reaching movements. i. independence of direction and extent variability", *Exp Brain Res*, vol. 99, no. 1, pp. 97–111, 1994.

[157] M. F. Ghilardi, J. Gordon, and C. Ghez, "Learning a visuomotor transformation in a local area of work space produces directional biases in other areas", *Journal of Neurophysiology*, vol. 73, no. 6, pp. 2535–2539, Jun. 1, 1995.

[158] R. M. Pierce and K. J. Kuchenbecker, "A data-driven method for determining natural human-robot motion mappings in teleoperation", in *2012 4th IEEE RAS EMBS International Conference on Biomedical Robotics and Biomechatronics (BioRob)*, Jun. 2012, pp. 169–176.

[159] C. Assaiante, S. Mallau, S. Viel, *et al.*, "Development of postural control in healthy children: a functional approach", *Neural Plast*, vol. 12, no. 2, pp. 109–118, 2005.

[160] J. A. Ashton-Miller, K. M. McGlashen, and A. B. Schultz, "Trunk positioning accuracy in children 7-18 years old", *Journal of Orthopaedic Research*, vol. 10, no. 2, pp. 217–225, Mar. 1, 1992.

[161] M. d. Onis, "WHO motor development study: windows of achievement for six gross motor development milestones", *Acta Paediatrica*, vol. 95, pp. 86–95, S450 2006.

[162] S. Mallau, M. Vaugoyeau, and C. Assaiante, "Postural strategies and sensory integration: no turning point between childhood and adolescence", *PLOS ONE*, vol. 5, no. 9, e13078, Sep. 29, 2010.

[163] S. S. Yeo, S. H. Jang, and S. M. Son, "The different maturation of the corticospinal tract and corticoreticular pathway in normal brain development: diffusion tensor imaging study", *Front Hum Neurosci*, vol. 8, Aug. 4, 2014.

[164] K. E. Adolph and J. M. Franchak, "The development of motor behavior", *Wiley Interdiscip Rev Cogn Sci*, vol. 8, no. 1, Jan. 2017.

[165] C. Simon-Martinez, G. L. d. Santos, E. Jaspers, *et al.*, "Age-related changes in upper limb motion during typical development", *PLOS ONE*, vol. 13, no. 6, e0198524, Jun. 6, 2018.

[166] J. C. van der Heide, B. Otten, L. A. van Eykern, and M. Hadders-Algra, "Development of postural adjustments during reaching in sitting children", *Exp Brain Res*, vol. 151, no. 1, pp. 32–45, Jul. 2003.

[167] C. Assaiante and B. Amblard, "Ontogenesis of head stabilization in space during locomotion in children: influence of visual cues", *Exp Brain Res*, vol. 93, no. 3, pp. 499–515, 1993.

[168] ——, "An ontogenetic model for the sensorimotor organization of balance control in humans", *Human Movement Science*, vol. 14, no. 1, pp. 13–43, Jun. 1, 1995.

[169] N. A. Bernstein, *The co-ordination and regulation of movements*. Pergamon Press, 1967, 226 pp.

[170] O. Sporns and G. M. Edelman, "Solving bernstein's problem: a proposal for the development of coordinated movement by selection", *Child Development*, vol. 64, no. 4, pp. 960–981, 1993.

[171] M. N. Roncesvalles, C. Schmitz, M. Zedka, *et al.*, "From egocentric to exocentric spatial orientation: development of posture control in bimanual and trunk inclination tasks", *J Mot Behav*, vol. 37, no. 5, pp. 404–416, Sep. 2005.

[172] H. Sveistrup, S. Schneiberg, P. A. McKinley, *et al.*, "Head, arm and trunk coordination during reaching in children", *Exp Brain Res*, vol. 188, no. 2, pp. 237–247, Jun. 1, 2008.

[173] R. Grasso, C. Assaiante, P. Prévost, and A. Berthoz, "Development of anticipatory orienting strategies during locomotor tasks in children", *Neuroscience & Biobehavioral Reviews*, vol. 22, no. 4, pp. 533–539, Mar. 4, 1998.

[174] S. Viel, M. Vaugoyeau, and C. Assaiante, "Adolescence: a transient period of proprioceptive neglect in sensory integration of postural control", *Motor Control*, vol. 13, no. 1, pp. 25–42, Jan. 2009.

[175] C. Chambers, T. Sokhey, D. Gaebler-Spira, and K. P. Kording, "The integration of probabilistic information during sensorimotor estimation is unimpaired in children with cerebral palsy", *PLOS One*, vol. 12, no. 11, Nov. 29, 2017.

[176] C. Chambers, T. Sokhey, D. Gaebler-Spira, and K. P. Kording, "The development of bayesian integration in sensorimotor estimation", *J Vis*, vol. 18, no. 12, Nov. 15, 2018.

[177] J. L. Contreras-Vidal, "Development of forward models for hand localization and movement control in 6- to 10-year-old children", *Human Movement Science*, Advances in Graphonomics: Studies on Fine Motor Control, Its Development and Disorders, vol. 25, no. 4, pp. 634–645, Oct. 1, 2006.

[178] M. Nardini, T. Dekker, and K. Petrini, "Crossmodal integration: a glimpse into the development of sensory remapping", *Curr. Biol.*, vol. 24, no. 11, R532–534, Jun. 2, 2014.

[179] S. Greffou, A. Bertone, J.-M. Hanssens, and J. Faubert, "Development of visually driven postural reactivity: a fully immersive virtual reality study", *Journal of Vision*, vol. 8, no. 11, pp. 15–15, Aug. 5, 2008.

[180] A. Shumway-Cook and M. H. Woollacott, "The growth of stability", *Journal of Motor Behavior*, vol. 17, no. 2, pp. 131–147, Jun. 1, 1985.

[181] K. Petrini, A. Caradonna, C. Foster, *et al.*, "How vision and self-motion combine or compete during path reproduction changes with age", *Sci Rep*, vol. 6, Jul. 6, 2016.

[182] S.-i. Hirabayashi and Y. Iwasaki, "Developmental perspective of sensory organization on postural control", *Brain and Development*, vol. 17, no. 2, pp. 111–113, Mar. 1, 1995.

[183] G. M. Redding, Y. Rossetti, and B. Wallace, "Applications of prism adaptation: a tutorial in theory and method", *Neurosci Biobehav Rev*, vol. 29, no. 3, pp. 431–444, May 2005.

[184] T. Mergner, C. Siebold, G. Schweigart, and W. Becker, "Human perception of horizontal trunk and head rotation in space during vestibular and neck stimulation", *Exp Brain Res*, vol. 85, no. 2, pp. 389–404, 1991.

[185] V. E. Pettorossi and M. Schieppati, "Neck proprioception shapes body orientation and perception of motion", *Front Hum Neurosci*, vol. 8, Nov. 4, 2014.

[186] J. Thang, *VR headset specs compared: PSVR, HTC vive, oculus rift, and more*, GameSpot, https://www.gamespot.com/articles/vr-headset-specs-compared-psvr-htc-vive-oculus-rif/1100-6456697/.

[187] K. F. Hew and W. S. Cheung, "Use of three-dimensional (3-d) immersive virtual worlds in k-12 and higher education settings: a review of the research", *British Journal of Educational Technology*, vol. 41, no. 1, pp. 33–55, 2010.

[188] T. A. Mikropoulos and A. Natsis, "Educational virtual environments: a ten-year review of empirical research (1999–2009)", *Computers & Education*, vol. 56, no. 3, pp. 769–780, Apr. 1, 2011.

[189] Z. Merchant, E. T. Goetz, L. Cifuentes, *et al.*, "Effectiveness of virtual reality-based instruction on students' learning outcomes in k-12 and higher education: a meta-analysis", *Computers & Education*, vol. 70, pp. 29–40, Jan. 1, 2014.

[190] G. Makransky, T. S. Terkildsen, and R. E. Mayer, "Adding immersive virtual reality to a science lab simulation causes more presence but less learning", *Learning and Instruction*, Dec. 26, 2017.

[191] B. A. Morrongiello, M. Corbett, M. Milanovic, and J. Beer, "Using a virtual environment to examine how children cross streets: advancing our understanding of how injury risk arises", *J Pediatr Psychol*, vol. 41, no. 2, pp. 265–275, Mar. 1, 2016.

[192] E. Biffi, E. Beretta, A. Cesareo, *et al.*, "An immersive virtual reality platform to enhance walking ability of children with acquired brain injuries", *Methods Inf Med*, vol. 56, no. 2, pp. 119–126, Mar. 23, 2017.

[193] T. Massetti, T. D. da Silva, T. B. Crocetta, *et al.*, "The clinical utility of virtual reality in neurorehabilitation: a systematic review", *J Cent Nerv Syst Dis*, vol. 10, Nov. 27, 2018.

[194] H. Adams, G. Narasimham, J. Rieser, *et al.*, "Locomotive recalibration and prism adaptation of children and teens in immersive virtual environments", *IEEE Transactions on Visualization and Computer Graphics*, vol. 24, no. 4, pp. 1408–1417, Apr. 2018.

[195] J. Miehlbradt, A. Cherpillod, S. Mintchev, *et al.*, "Data-driven body–machine interface for the accurate control of drones", *PNAS*, vol. 115, no. 31, pp. 7913–7918, Jul. 31, 2018.

[196] E. Catmull and R. Rom, "A class of local interpolating splines", in *Computer Aided Geometric Design*, New York: Academic Press, 1974, pp. 317–326.

[197] B. Rohrer, S. Fasoli, H. I. Krebs, *et al.*, "Movement smoothness changes during stroke recovery", *J. Neurosci.*, vol. 22, no. 18, pp. 8297–8304, Sep. 15, 2002.

[198] L. Dipietro, H. I. Krebs, B. T. Volpe, *et al.*, "Learning, not adaptation, characterizes stroke motor recovery: evidence from kinematic changes induced by robot-assisted therapy in trained and untrained task in the same workspace", *IEEE Transactions on Neural Systems and Rehabilitation Engineering*, vol. 20, no. 1, pp. 48–57, Jan. 2012.

[199] D. J. Berndt and J. Clifford, "Using dynamic time warping to find patterns in time series", presented at the KDD workshop, vol. 10, Seattle, WA: AAAI, 1994, pp. 359–370.

[200] G. A. ten Holt, M. J. T. Reinders, and E. A. Hendriks, "Multi-dimensional dynamic time warping for gesture recognition", presented at the Thirteenth annual conference of the Advanced School for Computing and Imaging, vol. 300, 2007.

[201] S. Balasubramanian, A. Melendez-Calderon, and E. Burdet, "A robust and sensitive metric for quantifying movement smoothness", *IEEE Transactions on Biomedical Engineering*, vol. 59, no. 8, pp. 2126–2136, Aug. 2012.

[202] P. Gulde and J. Hermsdörfer, "Smoothness metrics in complex movement tasks", *Front. Neurol.*, vol. 9, 2018.

[203] D. L. Davies and D. W. Bouldin, "A cluster separation measure", *IEEE Transactions on Pattern Analysis and Machine Intelligence*, vol. PAMI-1, no. 2, pp. 224–227, Apr. 1979.

[204] N. Shirai, T. Seno, and S. Morohashi, "More rapid and stronger vection in elementary school children compared with adults", *Perception*, vol. 41, no. 11, pp. 1399–1402, 2012.

[205] N. Shirai, T. Imura, R. Tamura, and T. Seno, "Stronger vection in junior high school children than in adults", *Front. Psychol.*, vol. 5, 2014.

[206] R. O. Gilmore, A. L. Thomas, and J. Fesi, "Children's brain responses to optic flow vary by pattern type and motion speed", *PLOS ONE*, vol. 11, no. 6, e0157911, Jun. 21, 2016.

[207] M. Krüger and G. Jahn, "Children's spatial representations: 3- and 4-year-olds are affected by irrelevant peripheral references", *Front Psychol*, vol. 6, Nov. 10, 2015.

[208] E. Freud and M. Behrmann, "The life-span trajectory of visual perception of 3d objects", *Sci Rep*, vol. 7, Sep. 8, 2017.

[209] I. Kovács, P. Kozma, Á. Fehér, and G. Benedek, "Late maturation of visual spatial integration in humans", *Proc Natl Acad Sci U S A*, vol. 96, no. 21, pp. 12 204–12 209, Oct. 12, 1999.

[210] R. Grasso, S. Glasauer, Y. Takei, and A. Berthoz, "The predictive brain: anticipatory control of head direction for the steering of locomotion", *Neuroreport*, vol. 7, no. 6, pp. 1170–1174, Apr. 26, 1996.

[211] C. von Hofsten and B. Rösblad, "The integration of sensory information in the development of precise manual pointing", *Neuropsychologia*, vol. 26, no. 6, pp. 805–821, Jan. 1, 1988.

[212] K. Wu, Y. Taki, K. Sato, *et al.*, "Topological organization of functional brain networks in healthy children: differences in relation to age, sex, and intelligence", *PLOS ONE*, vol. 8, no. 2, e55347, Feb. 4, 2013.

[213] J. B. Hellige, "Hemispheric asymmetry for visual information processing", *Acta Neurobiol Exp (Wars)*, vol. 56, no. 1, pp. 485–497, 1996.

[214] D. M. Wolpert and J. R. Flanagan, "Q&a: robotics as a tool to understand the brain", *BMC Biol.*, vol. 8, p. 92, Jul. 23, 2010.

[215] D. Bombari, M. Schmid Mast, E. Canadas, and M. Bachmann, "Studying social interactions through immersive virtual environment technology: virtues, pitfalls, and future challenges", *Front. Psychol.*, vol. 6, 2015.

[216] P. Hagmann, O. Sporns, N. Madan, *et al.*, "White matter maturation reshapes structural connectivity in the late developing human brain", *PNAS*, vol. 107, no. 44, pp. 19 067–19 072, Nov. 2, 2010.

[217] E. L. Dennis, N. Jahanshad, K. L. McMahon, *et al.*, "Development of brain structural connectivity between ages 12 and 30: a 4-tesla diffusion imaging study in 439 adolescents and adults", *Neuroimage*, vol. 64, pp. 671–684, Jan. 1, 2013.

Jenifer **Miehlbradt**

PhD Candidate · Human-machine Interactions

Place des Augustins 11, 1205 Geneva, Switzerland

(+41) 78 637 39 77 | jenifer.miehlbradt@epfl.ch · jenifer.miehlbradt@gmail.com | jenifer-miehlbradt | jmiehlbradt

Education

EPFL *Lausanne, Switzerland*

PhD *Dec. 2014 - present*

- Thesis: Neural correlates of gestural interactions with virtual environments

ETHZ *Zurich, Switzerland*

MSc. Biomedical Engineering *Sept.2011 - Dec. 2013*

- Master Thesis: Development and control of an actuated backrest for posture control during neurorehabilitation of paralyzed rats
- Semester project : Ligament Implementation for a Lumbar Spine Finite Element Model

EPFL *Lausanne, Switzerland*

BSc. Life Sciences *Sept. 2008 - June 2011*

- Bachelor Thesis: Measurement of Internal-External rotation in Prosthetic Knee

Skills

Neurophysiology	Acquisition and processing of kinematic (Vicon, IMUs), EMG and EEG data
Programming	Basic knowledge of C++ and Python
Engineering software	Matlab, Simulink, R, Latex
Graphic design	Adobe Illustrator, Adobe InDesign, Adobe Photoshop, Unity
Languages	French - mother tongue, German - mother tongue, English - fluent, Spanish - conversational

Experience

Bertarelli Foundation chair in Translational Neural Engineering (TNE), EPFL *Lausanne, Switzerland*

PhD candidate *Dec. 2014 - April 2019*

Investigated different neurophysiological aspects during human-machine interactions.

- Developed an intuitive Body-Machine interface for the immersive control of real and simulated drones
- Assessed the development of interjoint coordination across childhood during a virtual piloting task using a Body-Machine Interface
- Extracted and analyzed correlates of brain connectivity associated with performance levels in a virtual reaching task with altered visual feedback

Bertarelli Foundation chair in Translational Neural Engineering (TNE), EPFL *Lausanne, Switzerland*

Research assistant *Feb. 2014 - Nov. 2014*

Investigated the effect of trunk orientation and perturbations at the trunk level during locomotor training of spinal cord injured rodents.

- Developed a controllable mechanical system to adapt and optimize the trunk position
- Implemented the real-time control algorithms to optimize the upper-body position based on kinematic parameters
- Performed gait analyses
- Prepared histological samples for microscopy observation

Brain Research Institute (Hifo), University of Zurich *Zurich, Switzerland*

Research Assistant *Sept. 2012 - May 2013*

Participated in a study on motor recovery after corticospinal tract lesions in rodents

- Extracted kinematic parameters from video recordings of behavioural experiments
- Prepared histological samples for microscopy observation

Laboratory for Cognitive Neuroscience (LNCO),EPFL *Lausanne, Switzerland*

Intern *July 2010 - Sept. 2010*

Expanded a python/OpenGL virtual reality environment for a body perception experiment

Teaching & Project supervision

Teaching activities

2015 - 2017 **Fundamentals in Neuroengineering,** Exercise sessions for first-year Master students, *EPFL*

2012 - 2013 **Laboratory course in Biomechanics,** Practical sessions for third-year Bachelor students, *ETHZ*

Supervised student projects

Sept. 2017 - March 2018 **Master Thesis,** Development of visuomotor integration during a gesture-based piloting task in immersive virtual reality, *Davide Esposito, Scuola Superiore Sant'Anna*

April 2017 - Oct. 2017 **Master Thesis,** Upper-limb rehabilitation of post-stroke patients based on a modular IMU motion capture system using video games, *Alessia Rapalino, Politecnico di Torino*

Sept. 2017 – Jan. 2018 **Semester project,** Traditional versus robot-assisted rehabilitation for post-stroke patients: an EEG study, *Elena Beanato, EPFL*

Jan.2017 - June 2017 **Bachelor thesis,** Extensions to a human-to-machine interface for the control of flying robots, *Wissam Houria Taibi, EPFL*

Publications

Peer-reviewed articles

Miehlbradt, J., Cuturi, L., Gori, M., and Micera, S. "Development of head-trunk coordination during interactions with virtual reality". In: *In preparation* (2019).

Esposito, D., Miehlbradt, J., Tonelli, A., and Gori, M. "Get Out of the Body! Virtual Reality Displays Link Between Visual-Body Coordination and Egocentric Reference Developments". In: *In preparation* (2019).

Miehlbradt, J., Cherpillod, A., Mintchev, S., Coscia, M., Artoni, F., Floreano*, D., and Micera*, S. "Data-driven body–machine interface for the accurate control of drones". In: *PNAS* 115.31 (2018), pp. 7913–7918.

Martin Moraud*, E., von Zitzewitz*, J., Miehlbradt, J., Wurth, S., Formento, E., DiGiovanna, J., Capogrosso, M., Courtine, G., and Micera, S. "Closed-loop control of trunk posture improves locomotion through the regulation of leg proprioceptive feedback after spinal cord injury". In: *Sci Rep* 8 (2018).

Mosberger, A., Miehlbradt, J., Bjelopoljak, N., Schneider, M., Wahl, A.-S., Ineichen, B. V., Gullo, M., and Schwab, M. E. "Axotomized Corticospinal Neurons Increase Supra-Lesional Innervation and Remain Crucial for Skilled Reaching after Bilateral Pyramidotomy". In: *Cereb Cortex* (2017), pp. 1–19.

Arami, A., Miehlbradt, J., and Aminian, K. "Accurate internal–external rotation measurement in total knee prostheses: A magnetic solution". In: *Journal of Biomechanics* 45.11 (2012), pp. 2023–2027.

Poster presentations

Miehlbradt, J., Pierella, C., Giang, C., Kinany, N., Pirondini, E., Coscia, M., and Micera, S. "Modulation of the task-related functional connectivity during motor adaptation - an exploratory study". Poster presented at the annual meeting of the Society of Neuroscience (SfN), San Diego, CA. 2018.

Miehlbradt, J., Pierella, C., Giang, C., Kinany, N., Coscia, M., Pirondini, E., Vissano, M., Mazzoni, A., Magnin, C., Nicolo, P., Guggisberg, A. G., and Micera, S. "Evolution of Cortical Asymmetry with Post-stroke Rehabilitation:A Pilot Study". Poster presented at the International Conference for Neurorehabilitation (ICNR), Pisa, Italy. 2018.

Miehlbradt*, J., Wurth*, S., Martin Moraud, E., von Zitzewitz, J., Courtine, G., and Micera, S. "Closed-loop control of dynamic trunk posture improves gait patterns during locomotor training after spinal cord injury". Poster presented at the annual meeting of the Society of Neuroscience (SfN), Washington, MD. 2014.

**Ce document a été imprimé au Centre d'impression EPFL,
imprimerie climatiquement neutre, certifiée myClimate.**